THE SYNTHESES OF BIS-GUANIDIUM SALTS AND THEIR APPLICATIONS IN ASYMMETRIC MUKAIYAMA TYPE S_N2 ALKYLATION REACTIONS

DONG SHENG

(BSc., Zhejiang University)

A THESIS SUBMITTED

FOR THE DEGREE OF MASTER OF SCIENCE
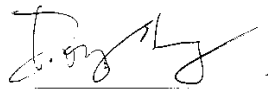
DEPARTMENT OF CHEMISTRY

NATIONAL UNIVERSITY OF SINGAPORE

2014

DECLARATION

I hereby declare that this thesis is my original work and it has been written by me in its entirety. I have duly acknowledged all the sources of information which have been used in the thesis.

This thesis has also not been submitted for any degree in any university previously.

Dong Sheng

16 July 2014

To my family

for their love, support, and encouragement

Acknowledgements

It is hard for me to express myself in English, but I know I have to. This is the only and the best chance for me to show all my gratitude, to everyone and everything appeared in my past three years.

Firstly, I need to thank all my families in China for everything they did in the past 27 years. They built my world with their hands, their hearts and their love. I wouldn't be the happiest guy in this world if any of them is absent for even a single second. They would never know about this, because none of them knows English very well and I won't translate this part to them. LOL.

Secondly, I need to thank my beloved Ms. Jiang Xiang'er for her love and understanding in last year and endless time in future. I will take her to a French restaurant when I get my degree if she pays the bill.

Thirdly, I want to thank my supervisor, Associate Professor Tan Choon Hong. He brought me to Singapore, and taught me a lot of things about chemistry and life which may help me to be survived on this island.

Last but not the least, I want to thank all my friends, in Singapore and any other places. I won't list their names, since that list would be too long. But you will always be there, in my heart.

Content

2

Summary

In this study, we designed and successfully synthesized a new type of phase-transfer catalysts with full alkylated guanidiums as functional centers and applied these catalysts in asymmetric catalysis of 1,4-dicarbonyl compounds via Mukaiyama type S_N2 alkylation reactions.

Firstly, a series of bis-guanidium salts were synthesized from commercially available and cheap chiral sources in 4 to 5 steps. For most of the derivatives, the overall yields were good. Synthetic problems were met when the catalysts were highly sterically hindered or strong electron withdrawing.

Then, these chiral bis-guanidium salts were tested in asymmetric Mukaiyama type S_N2 alkylation reactions as phase-transfer catalysts. Up to 86% ee was obtained, and for most of the substrates, the yields were good. Two catalytic systems were studied, and each of them had their advantages and disadvantages.

At the last of this work, suggestions to further improvement were proposed and detailed experimental procedures were provided.

List of Tables

List of Figures

List of Schemes

6

List of Abbreviations

AcOH	acetic acid
$[\alpha]$	optical rotation
aq.	aqueous
Bn	benzyl
t-Bu	*tert*-butyl
^{o}C	degrees (Celcius)
δ	chemical shift in parts per million
DCM	dichloromethane
DMAP	4-dimethylaminopyridine
DMF	dimethylformamide
DMSO	dimethyl sulfoxide
dd	doublet of doublet
d	day(s)
ee	enantiomeric excess
ESI	electro spray ionization
Et	ethyl
EtOH	ethanol
g	grams
hr	hour(s)

equiv.	equivalent
HPLC	high pressure liquid chromatography
HRMS	high resolution mass spectroscopy
Hz	hertz
IPA	isopropanol
J	coupling constant
KHMDS	potassium bis(trimethylsilyl)amide
LHMDS	lithium bis(trimethylsilyl)amide
Me	methyl
MeCN	acetonitrile
MeOH	methanol
mg	milligram
MHz	megahertz
min.	minute(s)
mL	milliliter
μL	microliter
mmol	millimole
MS	mass spectroscopy
NMR	nulcear magnetic resonance
n.d.	Not determined
n.p.	No product

n.r.	No reaction
Ph	Phenyl
*i*Pr	isopropyl
ppm	parts per million
PTC	Phase-transfer catalyst
TMS	Trimethyl silyl
TES	Triethyl silyl
TBS	Di(methyl)*tert*-butyl silyl
r.t.	room temperature
THF	tetrahydrofuran
TLC	thin layer chromatography
TBAB	*tetra*-n-Butylammonium bromide
TBAF	*tetra*-n-Butylammonium fluoride
TBME	*tert*-Butyl methyl ether
TFA	trifluoroacetic acid
TMAB	tetramethyl ammonium bromide
TMAF	tetramethyl ammonium fluoride
Boc	*tert*-Butyloxycarbonyl
M	mol·L^{-1}
mM	mmol·L^{-1}

Chapter 1

The Syntheses of Various Bis-Guanidium Salts

1.1 Introduction to Asymmetric Phase-Transfer Catalysis

1.1.1 General Introduction

Phase-transfer catalysts (PTCs) are chemical agents that facilitate the transfer of a molecule or ion from one reaction phase to another and in doing so can greatly accelerate the rate of heterogeneous (polyphasic) reaction processes.[1-3] As the concept declares, phase-transfer catalysts can help to transfer a reagent or ion from one phase to the other and enhance the reactivity.

In the middle to late 1960s, Starks, Makosza and Brandstorm discovered and built the foundation of phase transfer reactions.[4,5] Based on their own research data and phenomena, Starks and Makosza proposed different mechanisms both of which are generally accepted nowadays. Makosza proposed the interfacial mechanism (Figure 1.1), which means the exchange of the counter ions happen at the interface of two immiscible phases, and PTCs cannot enter the aqueous phase.
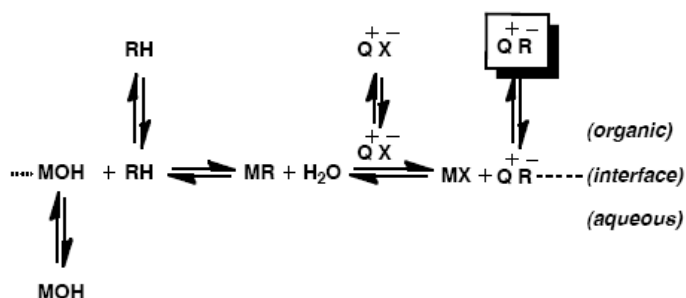
Figure 1.1. Interfacial Mechanism of Phase-Transfer Catalysis Proposed by Makosza. Starks proposed a different mechanism which is known as extraction mechanism. For example, in 1971, Starks did the S_N2 reaction of 1-chlorooctane (starting material and organic phase) with NaCN aqueous solution catalyzed by

hexadecyltributylphosphonium bromide (Scheme 1.1). The catalyst could distribute in

both organic and aqueous layers, and exchanged the anions in the aqueous phase and

took them back to the organic phase. Without the phosphosium salt as the catalyst,

there was no reaction even in a prolonged reaction time. In this case, the term of

"phase-transfer catalysis" was first introduced to explain the reaction phenomenon

and the important role of ammonium or phosphonium salts in this heterogeneous

system.[4]
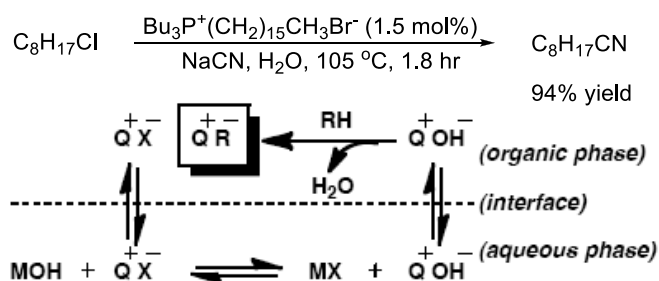
Scheme1.1. Extraction Mechanism of Phase-Transfer Catalysis Proposed by Starks.

Both of these two mechanisms can be true due to different reaction conditions.[6]

Because of the bulkiness of asymmetric PTCs, almost all the catalysts undergo the

Makosza pathway.

Compared with homogeneous reactions, phase-transfer catalysis has several unique

advantages in application:[7]

✧ The anion reactivities of both Q^+R^- and Q^+OH^- (in Starks pathway) are increased

due to larger separation of charges and reduced number of hydration, which

results in higher reaction rate than that of homogeneous media.

✧ Phase-transfer catalysis usually show better selectivity than homogeneous

reactions due to the milder conditions applied and controllable delivery of

reactive reagent to the target phase, even sometimes show different chemoselectivity.

✧ The workup procedures of phase-transfer catalysis are generally much easier than homogeneous reactions, due to many of the byproducts and reagents may be in aqueous phase, which may also be easier to recover starting materials and make it more applicable to industry.

Due to the advantages mentioned above, phase-transfer catalysis has been widely applied in organic syntheses for the last 30 years,[1-3] and has been recognized as an important branch of "green chemistry", which is sure the future direction of modern organic chemistry development.

1.1.2 Previous Reports with Different Types of Chiral PTCs

The first example of enantioselective phase-transfer reactions was reported by Tamejiro Hiyama and his coworkers in 1974.[8] The catalysts were synthesized from chiral ephedrine, and after several steps, a series of chiral PTCs were obtained which are shown in Scheme 1.2 and Scheme 1.3. They applied these catalysts to Corey-Chaykovsky epoxidation reaction. As shown in Scheme 1.3, ee values obtained from different catalysts were greatly different, and the hydroxyl group on benzyl position was important for high ee induction.
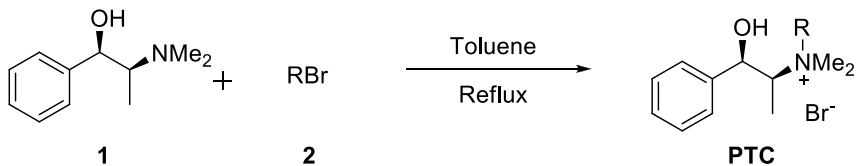
Scheme 1.2. Preparation of Ephedrine Derived Chiral Phase-Transfer Catalyst.
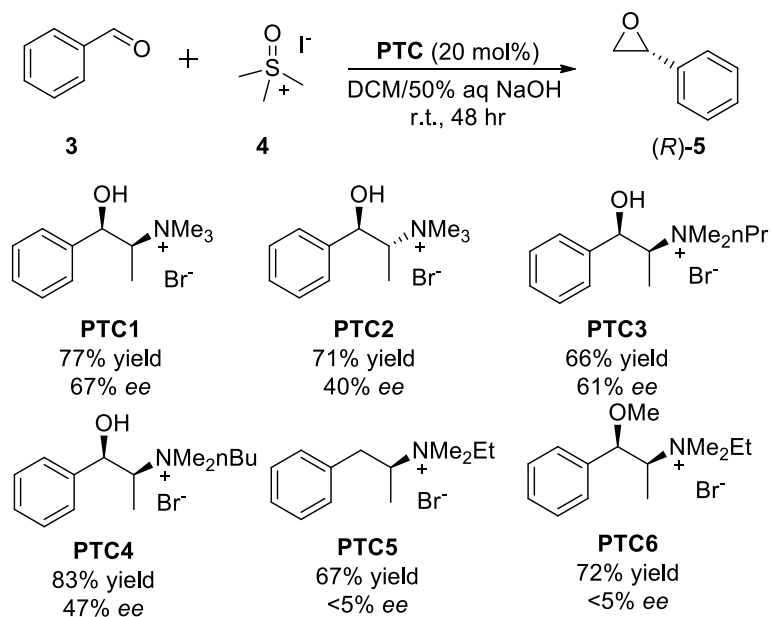
Scheme 1.3. Corey-Chaykovsky Reaction Catalyzed by Ephedrine Derived PTC.

According to the author's proposed mechanism, the chiral induction should be related

to the zwitterionic species **6** and **7** formed in organic layer (Figure 1.2). The

dipole-dipole interaction between **4** and the catalyst could form a strong chiral

complex so that the ylide attacked will prefer one of the enantiotopic faces of **3**.
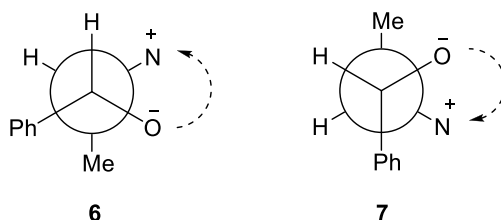
Figure 1.2. The Dipole-Dipole Interaction of the Zwitterionic Species with
Dimethylsulfonium Methylide.

Solvent effect was studied then. They found that **PTC1** in polar solvents like THF (66%

yield, 9% ee) and MeCN (48% yield, 0% ee) could not provide the results as good as

those in nonpolar solvents due to the larger polarity of solvents might destroy the

dipole-dipole interaction between the substrate and the catalyst. Further optimization

showed that the enantiomeric excess could be improved to 97% by using benzene as the solvent and **PTC2** as the catalyst. Also the catalyst loading might affect the ee value greatly. Optimized results are presented in Scheme 1.4.
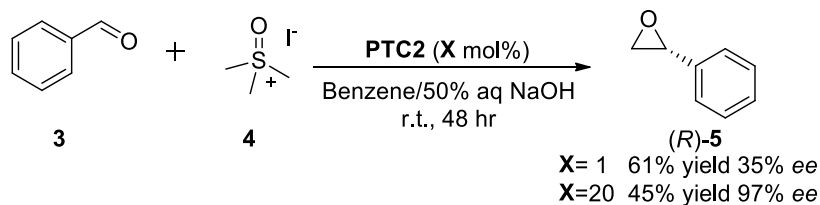
Scheme 1.4. Ephedrine Derived PTC Catalyzed Highly Enantioselective Epoxidation of Aldehyde.

Using the same type catalyst as **PTC1**, Fiaud finished the alkylation reaction of ethyl 2-oxocyclohexanecarboxylate in 1975.[9] The precise ee values were not presented, due to the lack of chiral HPLC analysis at that time and the lack of optically pure products for optical rotation measurements. But based on the ^{1}H NMR spectroscopy of the mixture of compound **10b** and a chiral shift reagent Eu(tfacCam)$_3$, around 5%-6% ee can be evaluated. Optimization showed that a higher catalyst loading could not increase the enantiomeric excess. More reaction results are presented in Scheme 1.5 below.
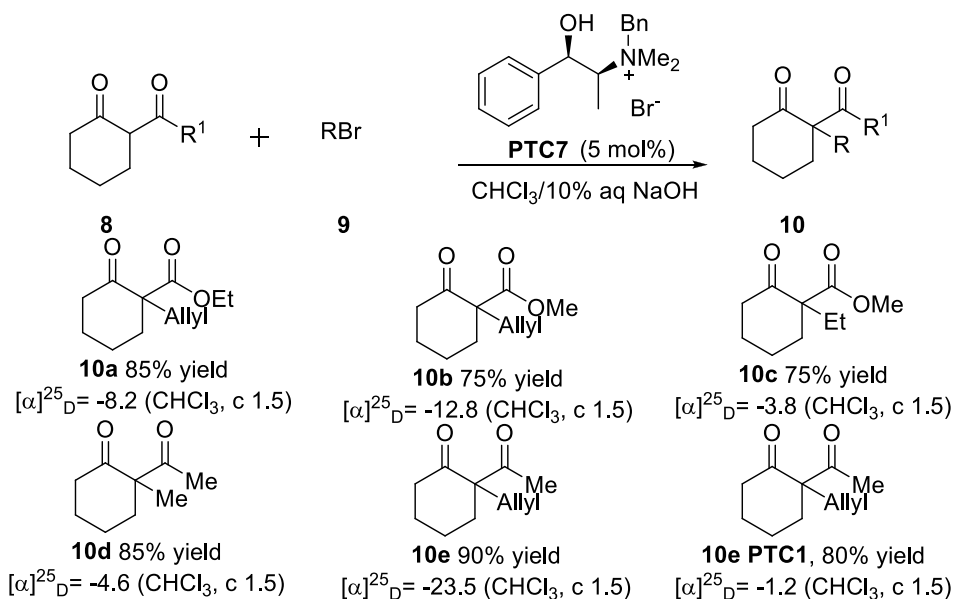
Scheme 1.5. Alkylation Reactions Catalyzed by Ephedrine Derived PTC.

In 1984, Dolling and his coworkers refluxed cinchona alkaloid with benzyl halide, and synthesized the first cinchona alkaloids derived chiral PTC, the family of which turned out to be the most successful PTCs in this research area (Scheme 1.6).[10] The catalyst then was tested on the alkylation reaction of substituted indanone. Excellent ee value and yield were obtained. Further application studies transformed the compound **16** into a bioactive molecule, (+)-indacrinone (Scheme 1.7).
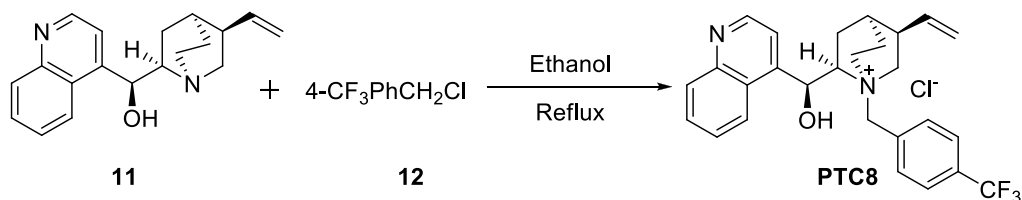
Scheme 1.6. N-Alkylation Reaction to Synthesize Alkaloid Derived PTC.

Detailed studies showed that the ee value could be higher in nonpolar solvents, such as toluene and benzene, than relative polar solvents like DCM and TBME. Dilution might help to increase the ee value, too. Different concentrations of NaOH solutions

were screened and 50% NaOH (aq.) gave the best results. Different catalyst loadings

might result in different reaction rates, but showed no direct relation with ee value of

the product.
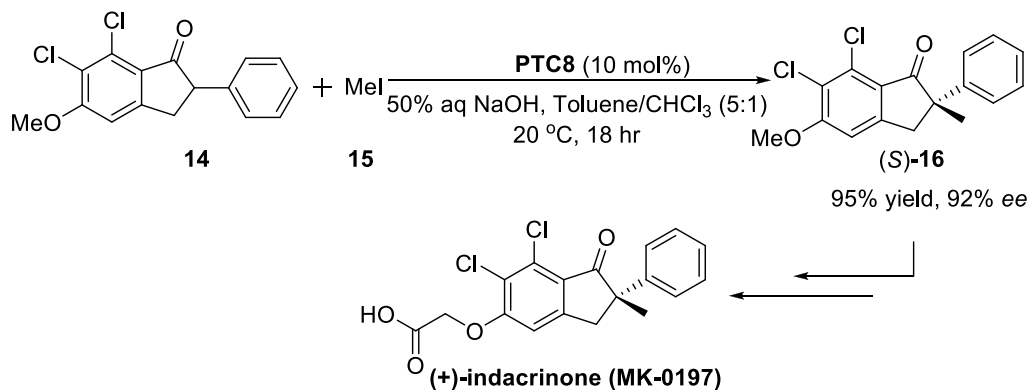
Scheme 1.7. Alkylation of Indanone Catalyzed by Alkaloid Derived PTC.

In 1989, inspired by Dolling's previous result, Donnell modified the cinchona

alkaloid and got the chiral **PTC9**, and applied it in the enantioselective synthesis of

amino acid **20** (Scheme 1.8).[11]

It was easier to obtain (*R*)-**19** in good yield and moderate ee, and with **PTC 10**, the

enantiomer of **PTC 9**, (*S*)-**19** can also be synthesized. Although the ee values of the

product were not high enough to be used directly, the ee could be simply increased

to >99% by a single recrystalization with 50% overall yield. Further optimization

showed that if the hydroxyl group was protected with allyl group, the ee value could

be further increased to 81%.
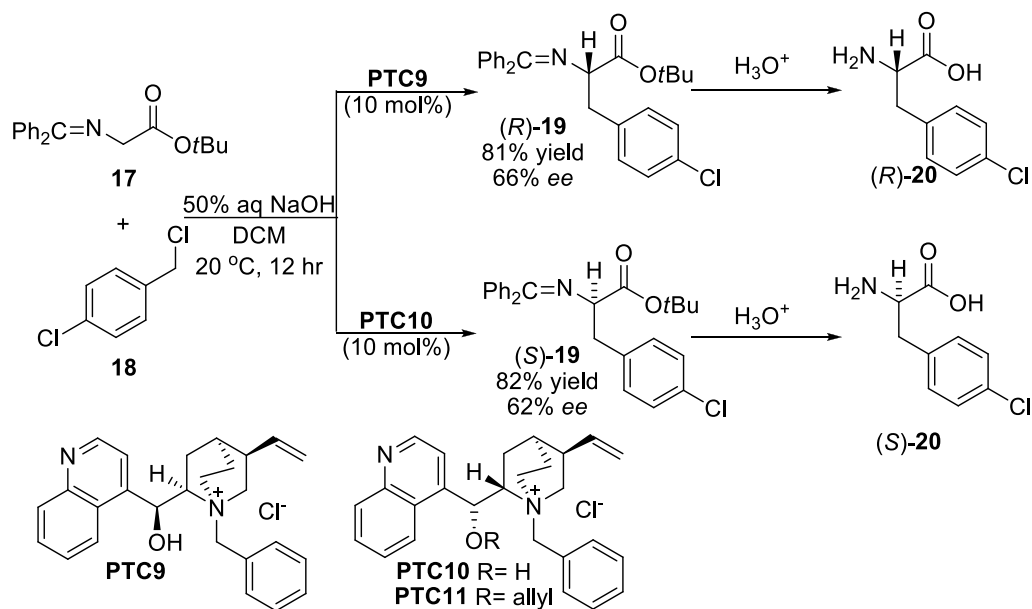
Scheme 1.8. Asymmetric Monoalkylation of **17** Catalyzed by Alkaloid Derived PTC.

It had been 8 years until the next masterpiece in the area of phase-transfer catalysis came out. In 1997, Lygo and Corey did the independent research on the asymmetric alkylation of Schiff base **17**, while got the same results.[12] N-anthracenylmethyl ammonium salt could be a better catalyst to the reaction than Donnell's catalysts (Scheme 1.9).

Corey suggested that the reason why 9-anthracenylmethyl group could enhance the enantioselectivity was its huge steric hindrance that could block one face of R_4N^+, and fix the 3D structure of functional positions. He suggested the catalyst could be easily tuned by attaching different R groups on the hydroxyl group to meet different substrates.
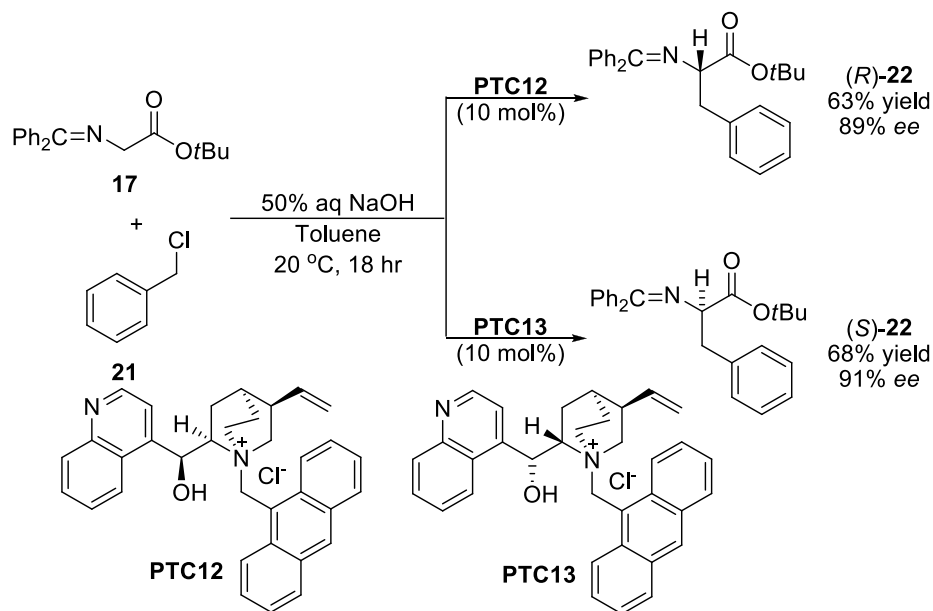
Scheme 1.9. Professor Lygo's PTC Catalyzed Alkylation of **17**.

To exam this analysis, Corey synthesized **PTC 14** and used it in the monoalkylation of schiff base **17** (Scheme 1.10). Excellent results were obtained with different electrophiles.

R = Me, Et, nHex, allyl, Bn, 2-Meallyl
71%-91% yield, 92%-99.5% *ee*
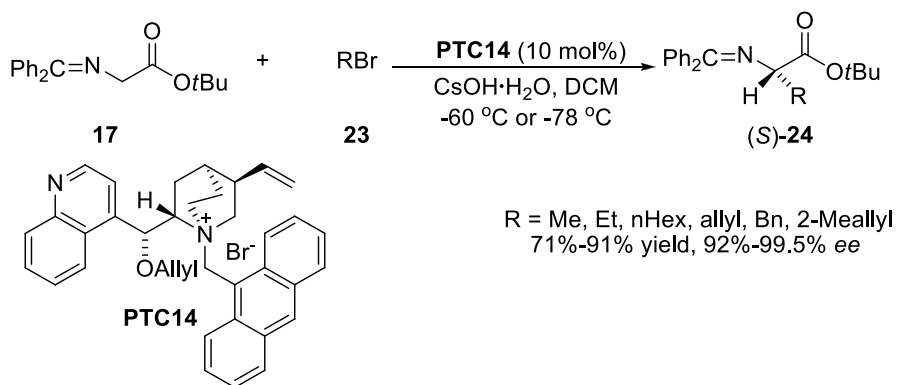
Scheme 1.10. Corey's Alkaloid Derived PTC Catalyzed Monoalkylation of **17**

Starting from the commercially available chiral 1,1'-bi-2-naphthol, Maruoka and his coworkers successfully synthesized chiral spiroammonium salts **PTC 15** and **PTC 16** in 1999.[13a] These rigid C_2-symmetric catalysts showed great efficiency in the asymmetric alkylation of **17** (Scheme 1.11).
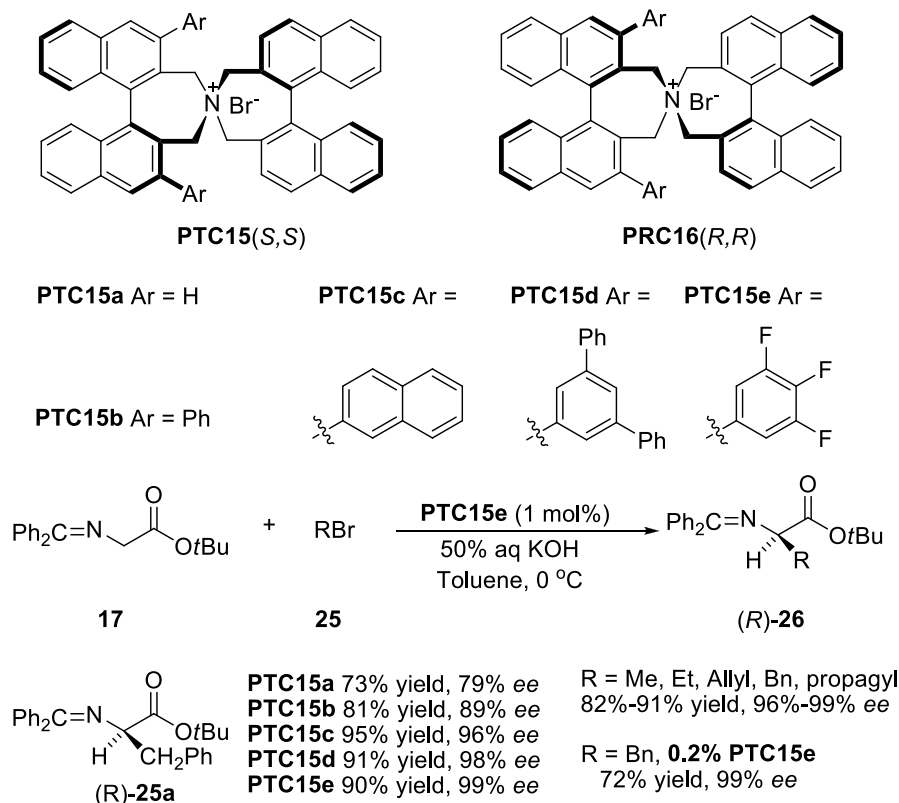
Scheme 1.11. Asymmtric Alkylation of **17** Catalyzed by Maruoka's Chiral Spiroammonium Salts Type of PTC.

After screening several catalysts in this family, the author found that when Ar group on the catalyst was 3,4,5-trifluorophenyl group (**PTC 15e**), they could get highest ee. While compared with **PTC 15b**, **PTC 15e** showed almost no different in steric effect. So the author suggested that the electron withdrawing effect might affect the enantioselectivity significantly. Further optimization showed that the catalyst loading could be reduced to 0.2 mol% without erosing its enantioselectivity. This was a great breakthrough compared with previous high loading PTCs, because the cost of the catalyst would be much easier to be accepted by industry. After this work, more reactions have been developed using this family of chiral catalysts, such as aldol

reactions, Mannich reactions, epoxidation reactions and made this family of catalysts as famous as cinchona alkaloids derived PTCs.[13b, 13c]

In 2002, Nagasawa reported enantioselective alkylation of Schiff base **17**, which was generally a standard reaction to exam the efficiency of new type of catalysts. The catalyst he used was a C_2-symmetric chiral cyclic guanidine (Scheme 1.12). Compared with cinchona alkaloids derived PTCs and Maruoka's chiral PTCs, this catalyst system was not so successful due to extremely long reaction time, moderate yield and higher catalyst loading.
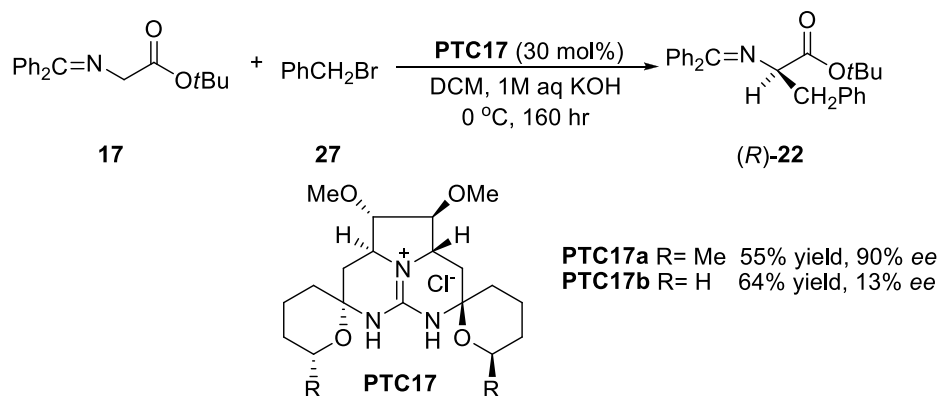
Scheme 1.12. Asymmetric Alkylation of **17** Catalyzed by Chiral Guanidium Type of PTC.

In 2003, Takabe and Mase designed and prepared a new type of chiral PTC, **PTC 19**.[15] Tested on the model benzylation reaction, the catalyst could only provided moderate yield and ee. But there were some innovations in the catalyst design, one was the usage C_3-symmetric structure rather than that of C_2-symmetric; the other innovation was the great flexibility of the catalyst. Bifunctional character of the catalyst was the key to ee induction (Scheme 1.13).
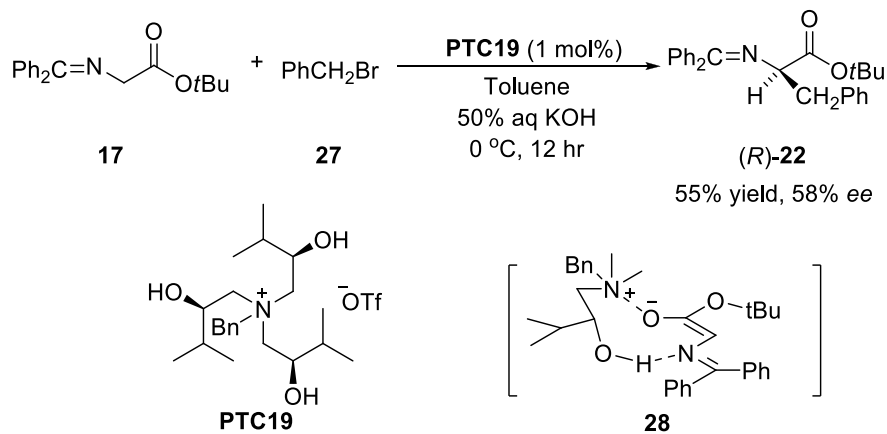
Scheme 1.13. Asymmetric Alkylation of **17** Catalyzed by Flexible C$_3$-Symmetric Chiral PTC.

In 2003, Sasai developed a new chiral bis-spiroammonium salt **PTC 20** and achieved excellent ee and yield with the model reaction (Scheme 1.14).[16]
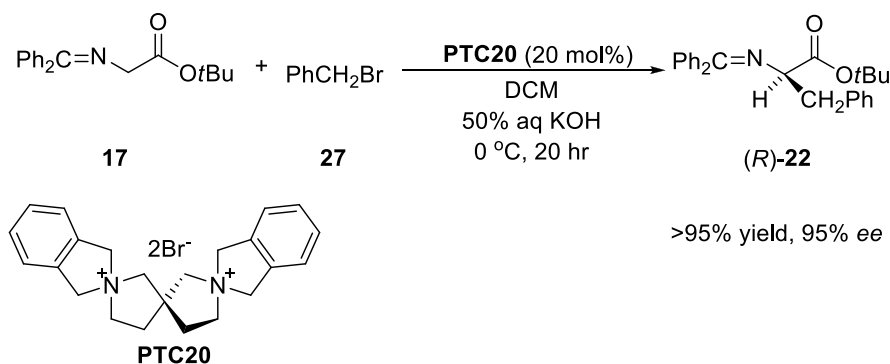
Scheme 1.14. Asymmetric Alkylation of **17** Catalyzed by Chiral Bis(spiroammonium) Salt as a Phase-Transfer Catalyst.

Shibasaki also designed and synthesized a new chiral bis-ammonium catalyst with flexible structure **PTC21** derived from tartrate, which is a quite cheaper chiral source. The author obtained excellent results in the model alkylation reaction.[17] The author found that changing the counteranion of the catalyst from I$^-$ to BF$_4^-$ could increase both ee and yield a little bit, which could be an evidence of counterion effect (Scheme

1.15).

Scheme 1.15. Tartrate-Derived Linear Chiral PTC Catalyzed Alkylation of **17**.

Inspired by the work of Shibasaki, MacFarland also prepared a new tartrate derived

bis-ammonium **PTC 22**, bearing 2, 5-dimethylpyrroline motieties.[18] They tested it on

the model asymmetric alkylation reaction, but only low yield and low ee were

obtained (Scheme 1.16).

Scheme 1.16. Tartrate-Derived Cyclic Chiral PTC Catalyzed Alkylation of **17**.

Besides ammonium PTCs, crown ether is also a famous catalyst used in

phase-transfer catalysis for its selective coordination with specific cations. Some

attempts were made to synthesize chiral crown ethers.

In 1981, Cram develop a chiral crown ether PTC, and used it in an asymmetric Michael addition reaction shown in Scheme 1.17.[19] Although the substrate scope was limited, for some specific substrates, they could obtain excellent results. While there is another great problem of chiral crown ethers that the synthesis of these catalysts are high cost and low yield till now.
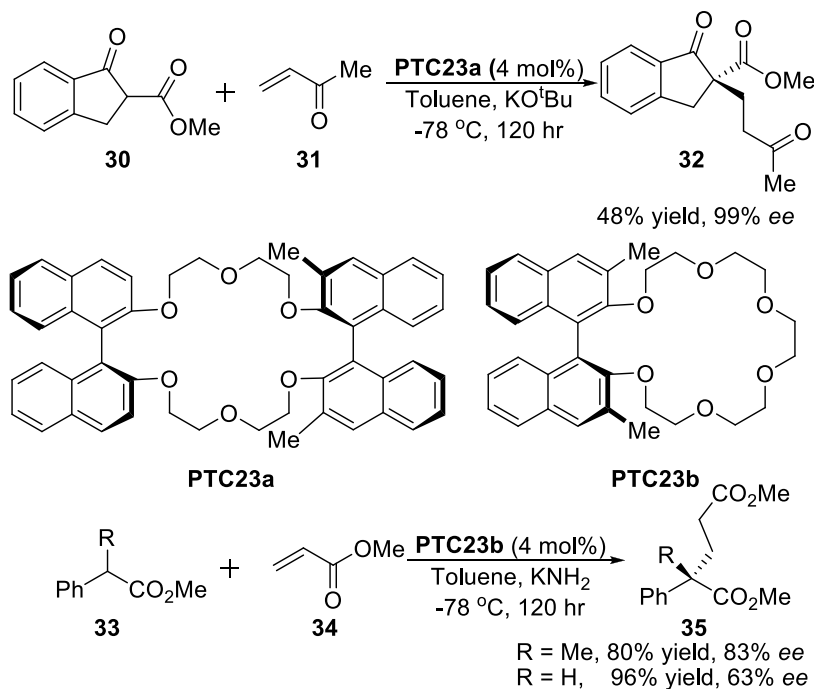
Scheme 1.17. Michael Addition to Acrylates Catalyzed by Chiral Crown Complexes.

Till now, there have been many families of PTCs developed now. Most of them are sp^3 quaternary ammonium salts. Professor Nagasawa did an interesting attempt on the development of sp^2 guanidine PTC. Although the result was not as good as those of cinchona alkaloids derived catalysts or Maruoka's rigid spiroammonium PTCs, his pioneering work proved that sp^2 guanidine moieties could also be ultilized as the active part of phase-transfer catalysts, but still need to be further modified.

Since our group's long term interest in developing Brønsted base catalysts modified

from guanidine moieties, we tried to increase the basicity by extending three nitrogen conjugations to five nitrogen conjugations to break through the pKa barrier (Figure 1.3). So compound **37** with different R groups were synthesized and tested. But the results did not consist with our hypothesis. The basicity tended to be weaker with more conjugated nitrogen atoms and enantioselectivity of these catalysts were not good. We proposed that the lack of sterical hindrance was the main reason for this failure. With bulkier R groups, full alkylatedcompound **38** could be a better catalyst, not as a Brønsted base catalyst, but as a phase-transfer catalyst.

Although over several decades, there have been many families of PTCs developed, many of them were given up after several attempts for different reasons. Only two families of PTCs are still robust now which are cinchona alkaloids derived PTCs and Maruoka's rigid spiroammonium catalysts. But because of the nature of chemistry, no catalyst scaffold can be suitable to all substrates or all extreme reaction conditions, such as oxidation conditions and strong basic and high temperature conditions. Also the costs of Maruoka's catalysts actually are still too high to be accepted by industry. So it is still necessary for us to develop a third type of PTCs as alternatives, especially when the costs are relatively lower.

Before our work, all the guanidine based PTCs' active parts were acid forms of guanidine (protonated guanidines), which could be surely deprotonated under basic conditions. Then the real bases that deprotonated the starting materials could be the base form of guanidines, which are weaker than inorganic bases like NaOH. So we assumed that our full alkylated pentanidium salts should at least show better reaction rates than previous guanidine based PTCs. Then we started to investigate these

pentanidium salts and their applications.
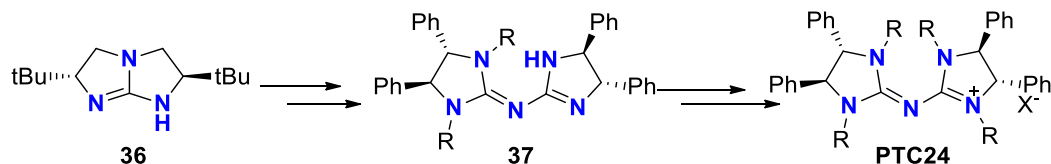
Figure 1.3. From Guanidine to Pentanidine and Pentanidium Salt.
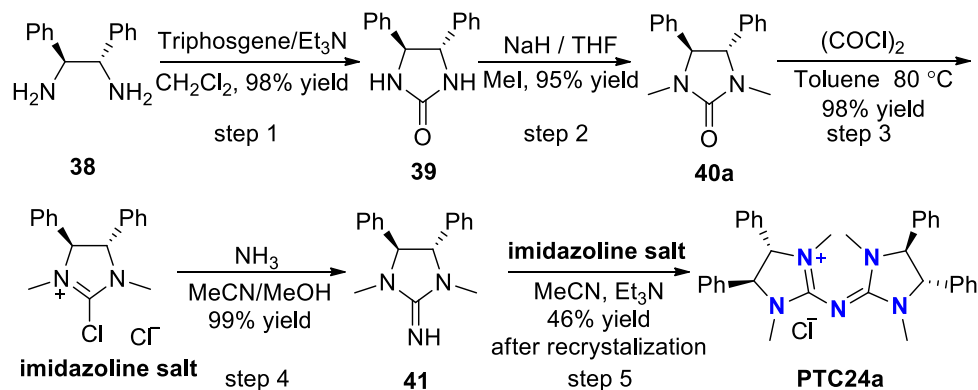
Scheme 1.18. Synthesis of Full Methylated Pentanidium Salt.

As shown above (Scheme 1.18), full methylation pentanidium **PTC 24a** could be easily synthesized from commercial available, cheap chiral amine **38** (2000 SGD/Kg) with high overall yield.

43a R = 4-H, Cl, OMe, NO$_2$
83%-91% yield, 87%-92% *ee*
99:1 dr

43b R = 4-F, Br, Ph, OMe, Cl
88%-98% yield, 85%-94% *ee*
99:1 dr

43c R = Me, Et, nBu, OEt, OBn
71%-97% yield, 91%-97% ee
43c5, R = OBn, 0.03% **PTC24a**
75%yield, 91% *ee*
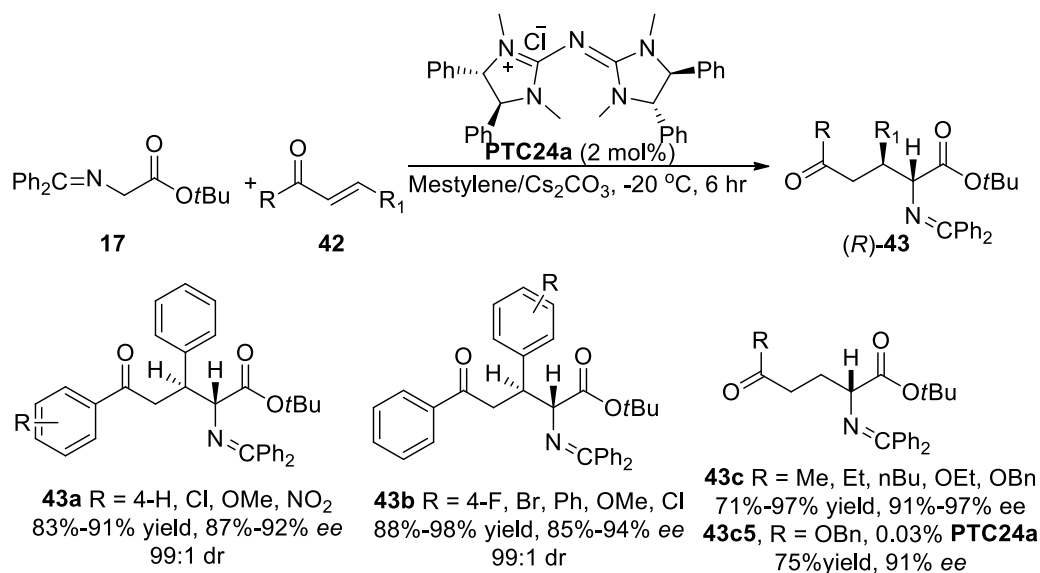
Scheme 1.19. Pentanidium-Catalyzed Conjugate Addition of Schiff Base **17** to **42**.

In 2011, it was successfully used in enantioselective Michael addition reaction of Schiff base **17** with acrylates and chalcones (Scheme1.19). Excellent results were obtained, and reaction rate were very fast as our hypothesis. Tested on one example of **43c5**, the catalyst loading could be lowered to 0.03 mol% without obvious erosion of ee value, which was a very important factor to potential industry applications.

Meanwhile, our group continued to synthesize a serie of pentanidium salts with different R groups, built the catalyst library and systematically studied the properties of this catalyst family.

In 2012, we used modified pentanidium salt **PTC 24b** to solve the asymmetric α-hydroxylation reaction of oxindoles with air (Scheme 1.20). Mechanistically, the reaction contained 2 parts: enantioselective oxidation with O_2 to form chiral peroxide intermediates, and kenetic resolution reduction of peroxides with oxindole enolates. Both ee and yield were excellent. Interestingly, during the optimization, we found that when both R_1 and R_2 were 3, 5-di(*t*-Bu)$C_6H_3CH_2$ group, enantioselectivity were the best, slightly better than **PTC 24b**, but the reaction rate would be lowered a lot.
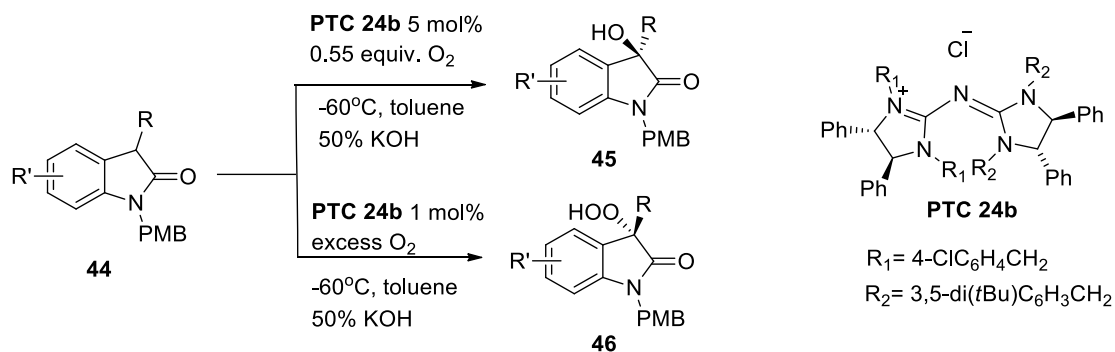
Scheme 1.20. Pentanidium-Catalyzed Asymmetric α-Hydroxylation Reaction of **44**.

In 2013, inspired by our group's pioneering work, Hii prepared another type of sp^2 quarternary nitrogen PTCs, and tried on the asymmetric conjugate addition of **17** with different Michael acceptors (Scheme 1.21).[20]
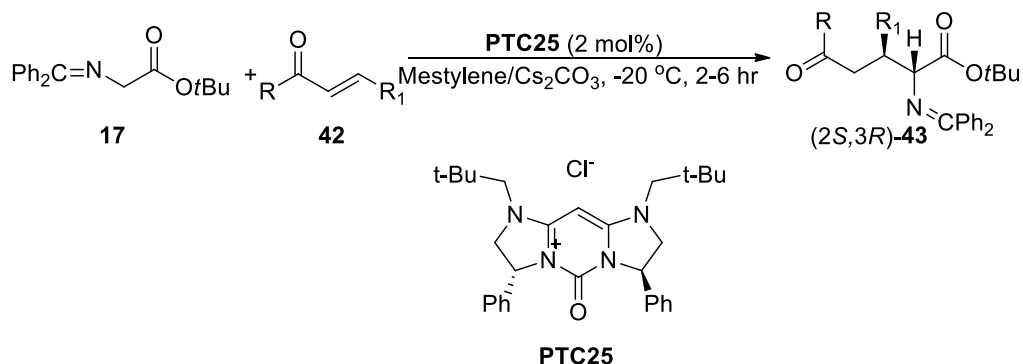
Scheme 1.21. Asymmetric Conjugate Addition Reactions Catalyzed by **PTC 25**.

Based on our own research results and previous literatures, we found that both steric and electronic effects of the R groups attached to the nitrogens had great influence on the enantioselectivity. Furthermore, the five conjugated nitrogens of our catalysts were not necessary to get excellent enantiomeric excesses in some cases. Full alkylated guanidines might be already good enough for catalysis and easier to be synthesized. We also got a hint from some of the previous literatures that they used bis-ammonium salts as phase transfer catalyst and obtained good results,[16,17,18] so we decided to try to develop a new type of catalysts: full alkylated bis-guanidium PTCs (Figure 1.4).
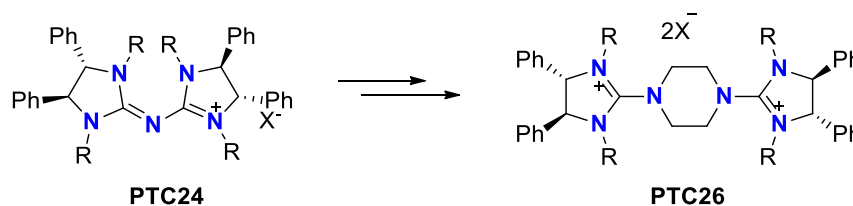
Figure 1.4. From Pentanidium Salts to Bis-Guanidium Salts.

1.2 Syntheses of Various Bis-Guanidium Salts

Since the basic fragments of bis-guanidium salts are the same as those of pentanidium salts, the synthetic procedure is modified from that of pentanidium salts. Standard procedure is shown in Scheme 1.22. Urea **39** can be easily synthesized from commercial available chiral diamine **38** with triphosgen under basic conditions, and N-alkylated product **40** can be synthesized with quantitative yield. Different R groups on the nitrogen may lead to different procedure for the following steps. Methylated **40a** is active enough to react with $(COCl)_2$ to form the imdazoline intermediate. But ureas with other substituents on nitrogens (even if ethyl group) have to be further activated by transforming ureas to thioureas with Lawesson's reagent. Compound **48**, which was identified by LC-MS (ESI), was condensed with rotary evaporator and vacumn dried before being used in the next step. Column purification is not applicable due to its sensitivity of moisture. Finally, the simple reflux of **48** with 0.3 equivalent of piperazine in MeCN can provide the bis-guanidium salts with good overall yield in 4 to 5 steps.
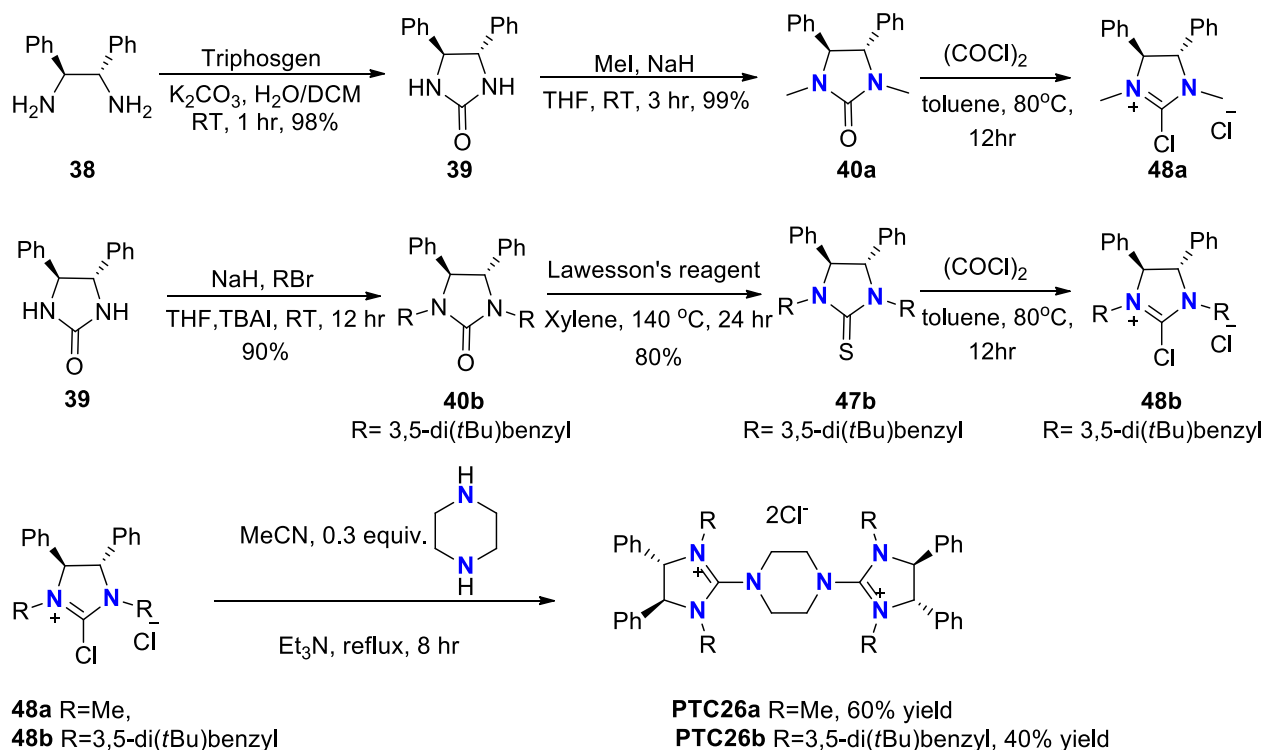
Scheme 1.22. Standrad Procedure of Bis-guanidium Salts Syntheses.

With the standard procedure, different modifications on chiral backbones, R groups and central linkers were carried out, and the successfully synthesized catalysts were presented in Table 1.1.

Table 1.1. Bis-Guanidium Salts Synthesized from Standard Procedure and Its Modified Versions.

Entry	Structure	Entry	Structure
Code：**PTC 26a** MW.^{a}: 655.70		Code：**PTC 26b** MW.^{a}: 1408.94	

Code：**PTC 26c**
MW.[a]: 1801.03
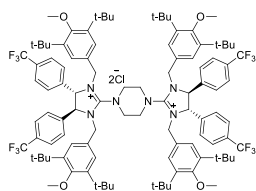
Code：**PTC 26d**
MW.[a]: 1160.32
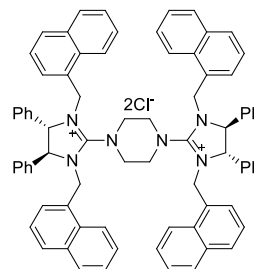
Code：**PTC 26e**
MW.[a]: 962.10
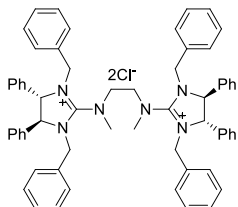
Code：**PTC 26f**
MW.[a]:1160.32
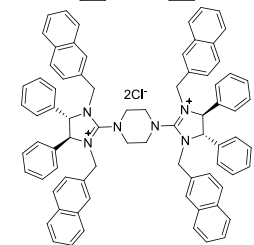
Code：**PTC 26g**
MW.[a]: 1724.52
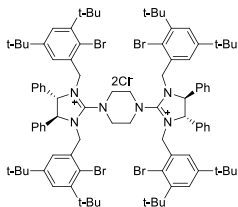
Code：**PTC 26h**
MW.[a]: 1320.40
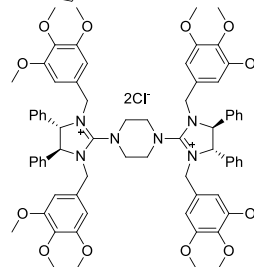
Code：**PTC 26i**
MW.[a]: 1184.51
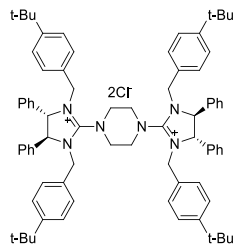
Code：**PTC 26j**
MW.[a]: 1240.62
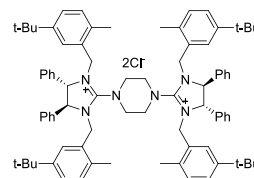
Code：**PTC 26k**
MW.[a]: 1529.04
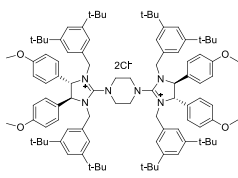
Code：**PTC 26l**
MW.[a]: 1546.72
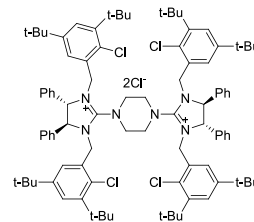
Code: **PTC26m**
MW.[a]: 1465.04
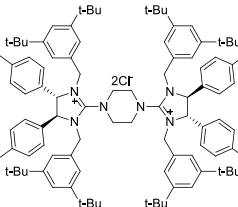
Code：**PTC 26n**
MW.[a]: 1432.96
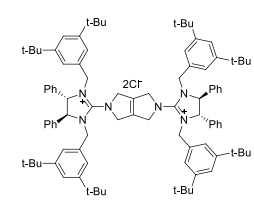
Code：**PTC 26o**
MW.[a]: 1609.17

Code：**PTC26p**
MW.[a]: 1537.54

Code: **PTC 26q** MW. [a]: 1633.36		Code: **PTC 26r** MW. [a]: 1436.99	
Code: **PTC 26s** MW. [a]: 1504.07		Code: **PTC 26t** MW. [a]: 1588.93	
Code: **PTC 26u** MW. [a]: 1680.93			
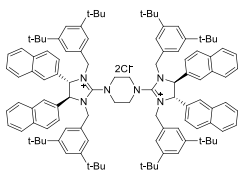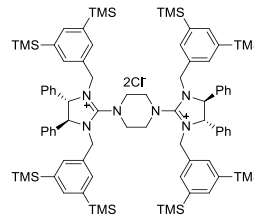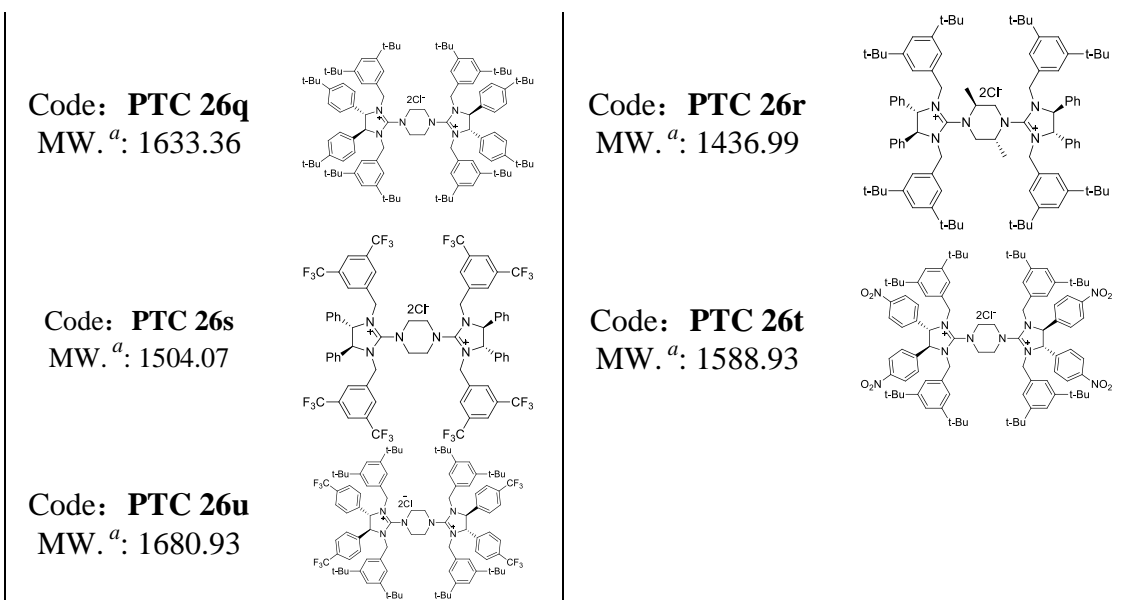
[a] The molecular weights shown in the table are calculated by ChemBioDraw Ultra 12.0

PTC 26a to **PTC 26n** could be easily synthesized according to the synthetic procedure with a range of 40 to 50% overall yield. But for those more sterically hindered bis-guanidiums (**PTC 26o** to **PTC 26r**), the last steps needed to be proceeded in sealed tubes at 110 ^{o}C in acetonitrile to obtained a reasonable yield (30 to 40% overall yield). For those bis-guanidiums bearing strong electron withdrawing substituents (**PTC 26s** to **PTC 26u**), the last steps should be carried out at 50 to 60 ^{o}C, since the structures of these bis-guanidiums were less stable to heat and only 20 to 30% overall yield could be achieved.

Besides these successful examples, many designs of bis-guanidium structures were failed to be synthesized even with all our efforts. In most cases, the problem appeared at the last step that compound **48** could not couple with the linker due to the too much steric hindrance. Some examples are presented in Figure 1.5.

48w

48x

48y

48z
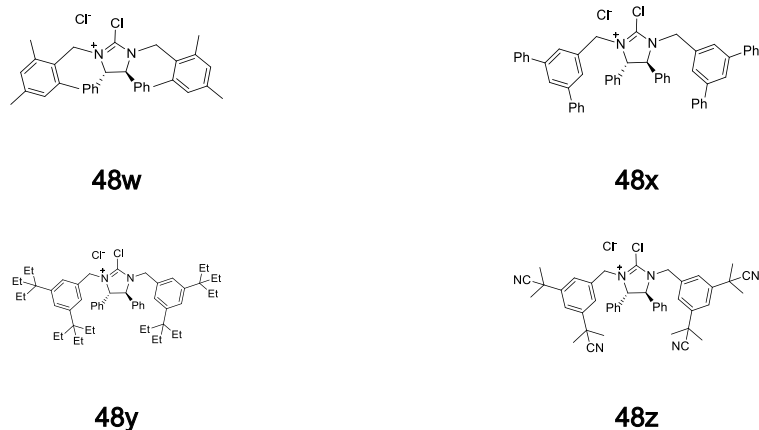
Figure 1.5. Imidazoline Salts of Highly Steric Hindrance which were failed to Couple with Piperizine.

There are also failed attempts due to the electronic effects, and a selected example is shown in Scheme 1.23. After the first coupling, the aromatic ring system transported part of the positive charge to the other conjugate nitrogen atoms and reduced its nucleophilicity so that only monoalkylated product was obtained.
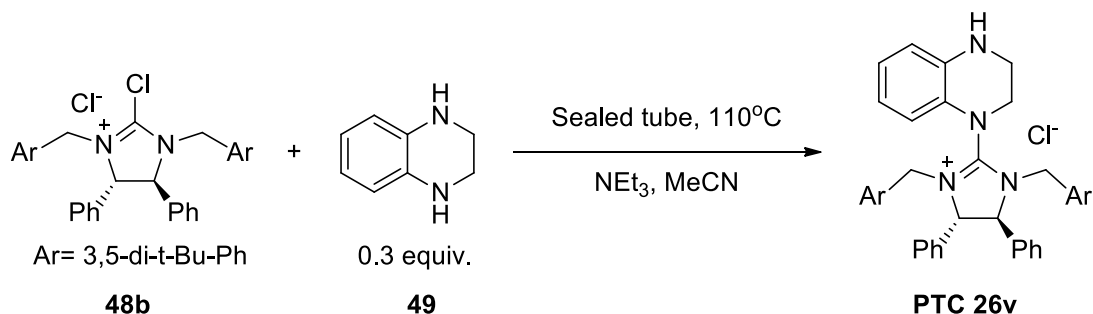
Scheme 1.23. Monocoupling of Imidazoline Salt **48b** with Linker **49** due to the Electronic Effect.

1.3 Summary

Over the years, many types of asymmetric phase-transfer catalysts have been

synthesized and studied. Hugh success has been achieved by now but problems such as high catalyst loading and long synthetic route were still significant. Our group recently developed a new type of bis-guanidium salts as phase-transfer catalysts. More than 20 catalysts of this family have been synthesized in 4 to 5 steps from cheap, commercial available chiral sources with good overall yields. Synthetic procedures for highly sterically hindered and strong electron withdrawing bis-guanidiums are still needed to be further optimized. As an extension of this work, these chiral bis-guanidium salts were used for reactions, which will be discussed in the next chapter.

References

1   (a) M. E.Halpern, Phase Transfer Catalysis, Mechanisms and Synthesis;American Chemical Society: Washington, DC, **1997**; (b)Handbook of Phase Transfer Catalysis, Sasson, Y., Neumann, R.Eds.; Blackie: London, **1997**; (c) C. M.Starks,C. L.Liotta,M. C. Halpern,Phase-Transfer Catalysis: Fundamentals,Applications, andIndustrial Perspectives; Chapman & Hall: New York, **1994**; (d) PhaseTransfer Catalysis; E. V.Dehmlow,S. S.Dehmlow, VCH:Weinheim, Germany, **1993**.

2   B. Lygo, Phase-Transfer Reactions. Rodd's Chemistry of CarbonCompounds, Vol. V: Asymmetric Catalysis; Elsevier ScienceLtd.: Oxford, U.K. **2001**, pp101−149.

3   R. A. Jones, Quaternary Ammonium Salts. Their Use in Phase-Transfer Catalysis; Academic Press: London, **2001**.

4   (a)M. Makosza, *Tetrahedron Lett.***1966**, *7*, 4621−4624;(b)M. Makosza,*Tetrahedron Lett.***1966**, *7*, 5489−5492;(c)M. Makosza, *Tetrahedron*

*Lett.***1969**, *10*, 673–676;(d)M. Makosza, *Tetrahedron Lett.***1969**, 10, 677–678;(e)A. Brndstrum, *Adv. Phys. Org. Chem.* **1977**, *15*, 267–330.

5   C. M. Starks, *J. Am. Chem. Soc.***1971**, *93*, 195–199.

6   (a)M. Makosza, *Pure Appl. Chem.***1975**, *43*, 439–462; (b)H.-M. Yang,H.-S. Wu, *Catal. Rev.***2003**, *45*, 463–540.

7   B. Lygo, B. Andrews,*Acc. Chem. Res.***2004,** *37*, 518–525

8   T. Hiyama,T. Mishima, H. Sawada, H. Nozaki,*J. Am. Chem. Soc.***1975,** *97,* 1626–1627

9   S. Usui, L. A.Paquette, *Tetrahedron Lett.***1975**, *40,*3495 – 3496.

10 U. Dolling, P. Davis, E. Grabowski,*J. Am. Chem. Soc.***1984,** *106,* 446–447.

11 M. J. O'Donnell,W. D. Bennett, S. Wu,*J.Am. Chem. Soc.***1989**,*111*.2353–2355.

12 (a) E. J. Corey, F. Xu, M. C. Noe,*J. Am. Chem. Soc.* **1997,** *119,* 12414–12415; (b) B. Lygo, P. G. Wainwright, *Tetrahedron Lett.***1997**,*38*, 8595–8598.

13 (a) T. Ooi, M. Kameda, K. Maruoka.*J.Am. Chem. Soc*. **2003**, 125, 5139–5151; (b) T. Ooi, K. Maruoka, *Angew. Chem. Int. Ed.* **2007***, 46,* 4222 – 4266; (c) T. Hashimoto, K. Maruoka, *Chem. Rev*. **2007**, *107*, 5656–5682.

14 T. Kita, A. Georgieva, Y. Hashimoto, T. Nakata, K. Nagasawa. *Angew. Chem. Int. Ed.***2002**, *41*, 2832–2834.

15 N. Mase, T. Ohno, N. Hoshikawa, K. Ohishi, H. Morimoto, H.Yoda, K. Takabe, *Tetrahedron Lett.***2003**, *44*, 4073– 4075.

16 H. Sasai (Jpn. Kokai Tokkyo Koho), JP2003335780, **2003**.

17 (a)T. Shibuguchi, Y. Fukuta, Y. Akachi, A. Sekine, T. Ohshima,M. Shibasaki,*Tetrahedron Lett.***2002**, *43*, 9539–9543; (b)T. Ohshima, T.Shibuguchi,

Y. Fukuta, M. Shibasaki, *Tetrahedron,***2004**, *60*, 7743–7754.

18 (a) W. E. Kowtoniuk, D. K. MacFarland, G. N. Grover, *TetrahedronLett.***2005**, *46*, 5703–5705;(b) M. E. Rueffer, L. K. Fort,D. K. MacFarland, *Tetrahedron: Asymmetry*, **2004**, *15*, 3297–3300.

19 D. J. Cram, G. D. Y. Sogah, *J. Chem. Soc. Chem. Commun.***1981**, 625–628.

20 A. E. Sheshenev, E. V. Boltukhina, A. J. P. White, K. K. Hii, *Angew. Chem. Int. Ed.* **2013***, 52,* 6988 – 6991.

Chapter 2

Bis-Guanidium Catalyzed Mukaiyama Type S_N2

Alkylation Reactions to Synthesize

1,4-Dicarbonyl Compounds

2.1 Introduction of Asymmetric Organocatalysis of Chiral Quaternary Ammonium Fluorides

2.1.1 General Introduction

Quaternary ammonium salts, which are known as one of the most important branches of phase-transfer catalysts, have different applications when bearing different counter ions. Compared with quaternary ammonium hydroxides, quaternary ammonium fluorides were less studied before, now have drawn many people's attention, due to its specific affinity to silicon atom and relatively strong basicity in aportic solvents.[1] The strong F-Si bond enables quaternary ammonium fluorides as a specific deprotecting reagent to silyl groups, which can generate nucleophiles from silicon protected compounds. The relatively strong basicity of fluoride anions in aprotic solvents allows direct deprotonation from substrates with lower pKa, and makes the fluoride anions an alternative to OH$^-$. Both of these two properties make quaternary ammonium fluorides a great reagent or catalyst in organic syntheses, especially in asymmetric versions. Therefore, I reviewed most of the previous literatures in this area, and presented them below.

2.1.2 Previous Reports with Chiral Quaternary Ammonium Fluorides

The first asymmetric example using chiral quaternary ammonium fluoride catalyst was a Michael addition reaction of nitromethane to chalcone done by Wynberg in 1978.[2] In his procedure, the chiral catalyst 2 and 4a with fluoride anions were in situ generated by conteranion exchange of catalyst 1 and 3a (10 mol%) with excess amount of KF (15 equiv.) in toluene at 20 ^{o}C (Scheme 2.1). Although the

enantioselectivity for both of these two catalysts was not satisfying, comparison of the experimental data could be enlightening. Regardless the structure difference of cations, the catalyst with bromide as counter anion showed lower yield than the catalyst with chloride counter anion. So besides the enantioselectivity, the efficiency of counter anion exchange should also be taken into consideration.
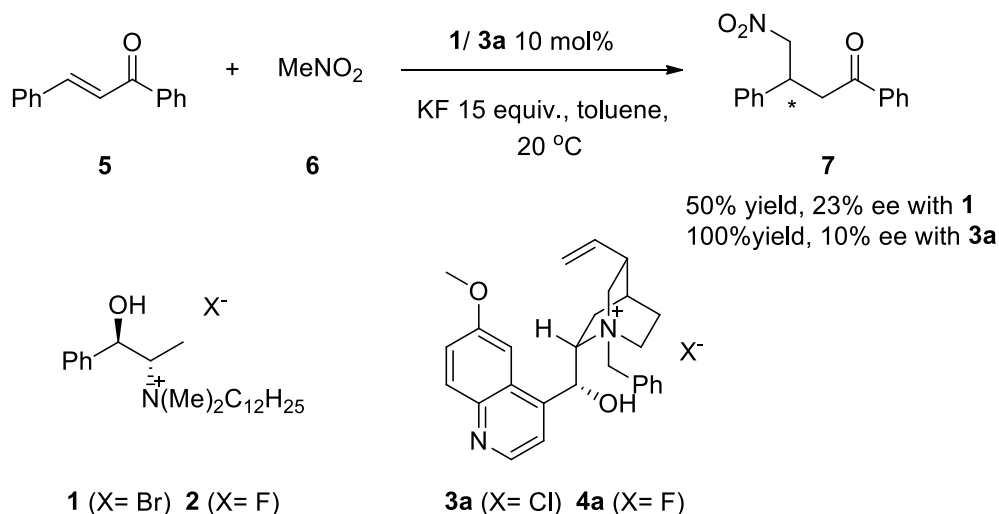
Scheme 2.1. Asymmetric Conjugate Addition of Nitromethane to Chalcone Catalyzed by In Situ Formed Chiral Quaternary Ammonium Fluorides.

Maruoka did a systematic study on this problem using Mukaiyama aldol reaction as a model.[3] The catalytic amount of fluoride anions were just the initiators to the reaction and the intermediate formed by nucleophilic addition of the enolate to benzaldehyde could further deprotect another molecule of silyl protected compound so that closed the catalytic cycle. Therefore, the counterion exchange basically only existed at the very beginning stage, and the whole process could hardly be regarded as phase-transfer catalysis for the mechanism we just mentioned above.
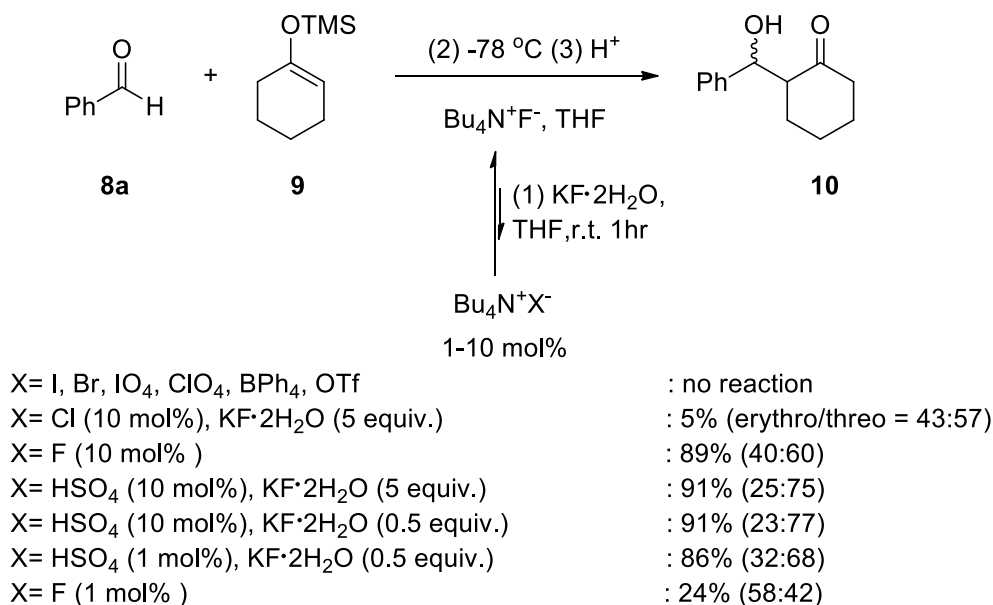
Scheme 2.2. Counterion Effect of the Catalyst in Mukaiyama Aldol Reaction.

From Scheme 2.2 we can see that, only when the counterion is HSO$_4^-$, the results could be comparable with those of directly using F$^-$ as the counterion. Some lipophilic anions even showed no catalytic effect. This phenomenon actually can be explained by different distribution rates of anions in a heterogeneous system (Table 2.1). Since the system is an organic/ solid heterogeneous system, anions with higher order of lipophilicitiy will be preferred in the exchange between catalysts in organic phase and solid salts.

Picrate$^-$ >> MnO$_4^-$ > ClO$_4^-$ > SCN$^-$ > I$^-$ (ClO$_3^-$, OTs$^-$) > NO$_3^-$ > Br$^-$ > (CN$^-$, BrO$_3^-$, PhCOO$^-$) > (NO$_2^-$, Cl$^-$) > HSO$_4^-$ > (HCO$_3^-$, OAc$^-$) > (F$^-$, OH$^-$) > SO$_4^{2-}$ > CO$_3^{2-}$ > PO$_4^{3-}$
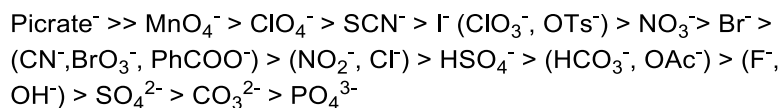
Table 2.1. Order of Lipophilicities of Anions.

Although there are many factors in a reaction system may affect the selectivity of anions, the most important two factors are sizes and the number of charges of the

anions. Anions with larger ratio of volume/ N(charge), will be more lipophilic theoretically. It is easier to be understood that some anions (Br$^-$, I$^-$, etc.) might poison the catalyst. The equilibrium between these anions and fluoride anion far more prefers the former fat ones, so the functional quaternary ammonium fluorides just own very little percentage in organic layer that bad reaction yields were obtained. Interestingly, when the counterion was HSO$_4^-$, which is obviously more lipophilic than F$^-$, and has similar lipophilicity to Cl$^-$, the reaction showed great improvement on yield (up to 91% isolated yield). It's because that the HSO$_4^-$ can be deprotonated in the reaction system by F$^-$, and eventually form SO$_4^{2-}$, which is less lipophilic than F$^-$ so that no catalyst poisoning effect could be observed.

After acquiring a better understanding of the reaction mechanism, Maruoka succeeded to develop its chiral version with his classical catalysts in 2001.[3] During the optimization, they found that the mixed solvent of THF and toluene showed better diastereo- and enantioselectivities. Excellent yields and good to excellent enantiomeric excesses were obtained (Scheme 2.3).

When optimizing the reaction, they found that the electron withdrawing Ar group was important since the chiral cation could form a tighter ion pair with fluoride anion and the following enolate generated from silyl enol ether.

8a R= Ph   **11a**: 90% yield (*erthro/threo* = 83:17), 84% ee (*S,S*)
8b R= a-Np   **11a**: 90% yield (*erthro/threo* = 94:6), 91% ee (*S,S*)

11a
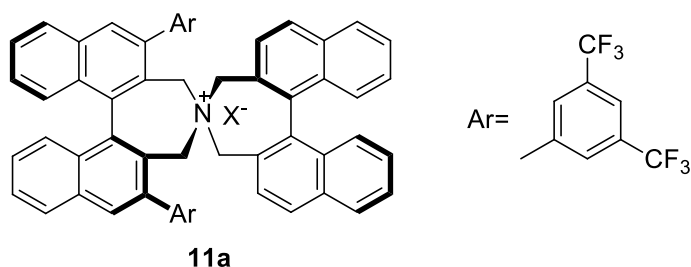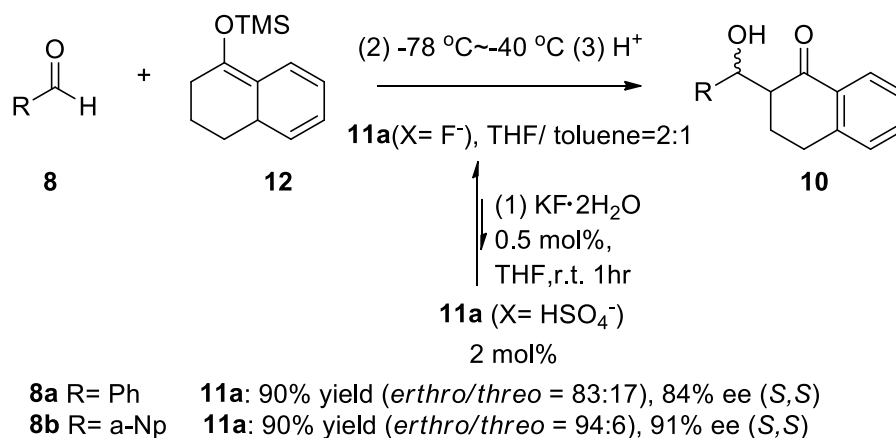
Scheme 2.3. Cyclic Type of Asymmetric Mukaiyama Aldol Reaction.

Another example achieved by Maruoka using his catalysts with HSO$_4^-$ as counterion is alkylative kenetic resolution of secondary alkyl halides.[4] One example shown below is preparation of 1-(naphthalene-1-yl)ethyl 3-phenylpropanoate using 3-phenylpropionic acid and excess amount of 1-(1-bromoethyl)naphthalene, moderate enantiomeric excess was obtained (Scheme 2.4).
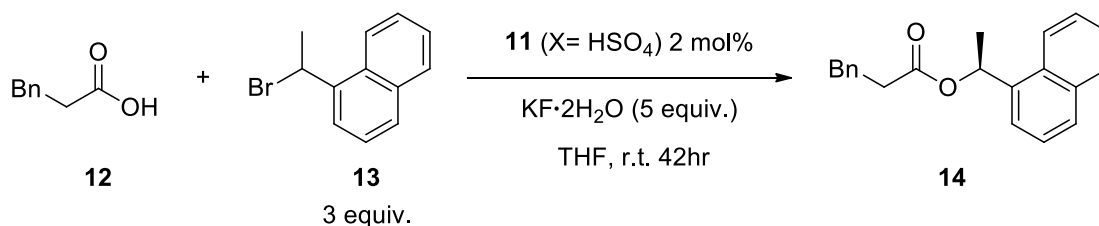
Scheme 2.4. Alkylative Kenetic Resolution of Secondary Alkyl Halides.

But no synthetic route now can directly synthesize catalysts bearing HSO$_4^-$ as counterion. Changing the counterion to F$^-$ sometimes can be more reasonable due to no extra fluoride source need to be added. Several counterion exchange methods were studied systematically by Shioiri and co-workers in 1993 to change the N-benzylcinchonium bromide **15a** to its fluoride salt (Scheme 2.5).[5] Following tests showed that the catalyst was stable under different methods of counterion exchange and the efficiencies of **15b** prepared from different methods were the same (tested with Mukaiyama aldol reaction).
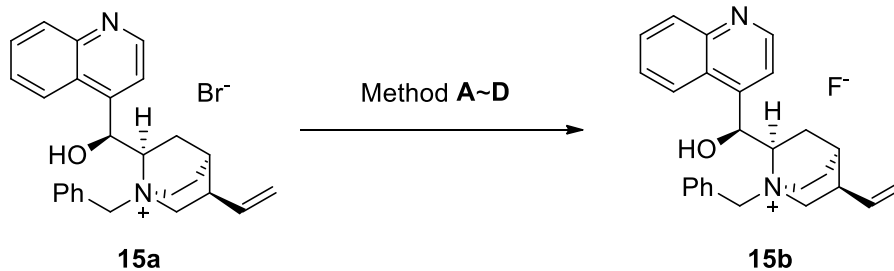
A 1) Amberlite IRA-410 F$^-$ form; 2) Evaporation
B 1) Amberlyst A-26 F$^-$ form; 2) Evaporation
C 1) Amberlyst A-26 OH$^-$ form; 2) 1N HF 3) Evaporation
D 1) AgF; 2) Filtration; 3) Evaporation

Scheme 2.5. Methods of Counterion Exchange from Bromide to Fluoride.

Furthermore, Shioiri did an asymmetric Mukaiyama aldol reaction with linear silyl enol ethers and benzaldehyde. Poor to moderate enantiomeric excesses were obtained using **15b** and its peudoenantiomer **15c** as catalysts (Scheme 2.6).[5]

16a R= Ph   **8a**

16b R= *t*-Bu

R= Ph: 76%, 39.5% ee (*S*), **11b**
        46%, 35.5% ee (*R*), **11c**
R=t-Bu: 62%, 62% ee (*S*), **11b**
        55%, 39% ee (*R*), **11c**

15c
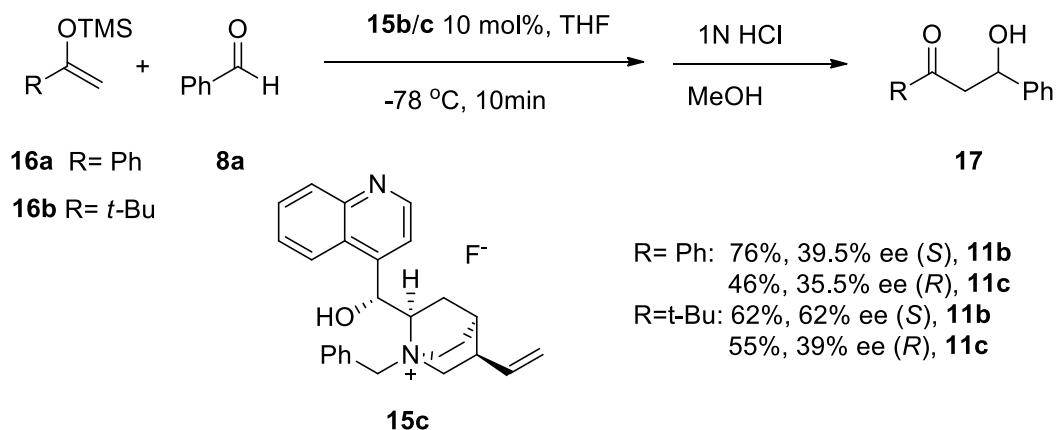
Scheme 2.6. Linear Type of Asymmetric Mukaiyama Aldol Reatcion.

In 2001, Campagne and Bluet reported asymmetric vinylogous Mukaiyama aldol reaction catalyzed by **15b** (Scheme 2.7).[6] 20% ee could be obtained at room temperature, and 30% ee at 0 °C.

18   **19**   **15b** 10 mol%, THF, 24h   **20**

20% ee, at r.t.
30% ee, at 0°C
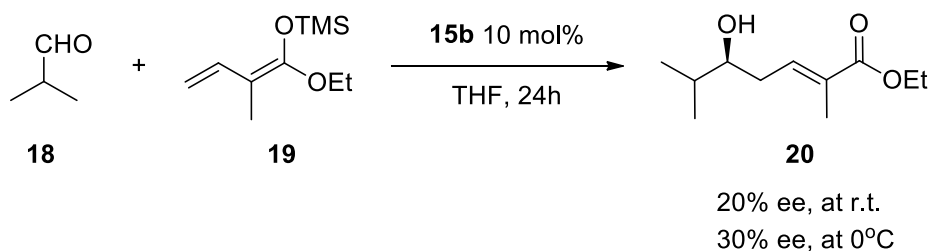
Scheme 2.7. Asymmetric Vinlogous Mukaiyama Aldol Reaction.

In 1994, Iseki, Nagai, and Kobayashi reported asymmetric aldol reaction of aromatic aldehyde/ ketones and TMSCF$_3$ initiated by fluoride anions. The catalysts **15d** and **15e** were prepared from corresponding bromides, and up to 51% ee was obtained (Scheme 2.8).[7]

R1	cat. (mol%)	% yield	% ee
H	**15d** (10)	>99	37(R)
H	**15e** (20)	>99	46(R)
Me	**15d** (20)	91	48(R)
i-Pr	**15d** (20)	87	51(R)

15d R$_2$= H, R$_3$= CF$_3$
15e R$_2$= R3= CF$_3$
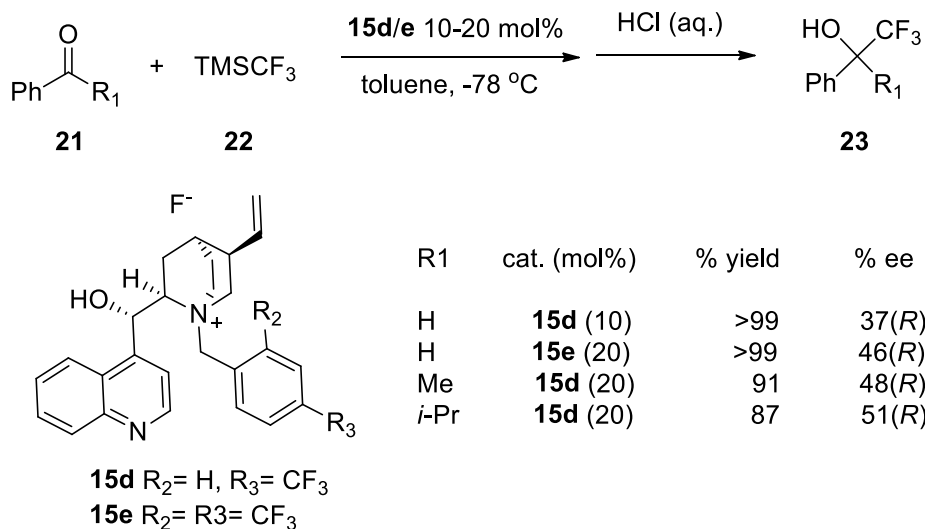
Scheme 2.8. Asymmetric Trifluoromethylation of Aromatic Aldehyde and Ketones.

In 1997, Lawrence reported asymmetric reduction of aromatic ketones using polymethylhydrosiloxane (PMHS) and other silanes as hydride source. Although PMHS might accelerate the reaction rate significantly, the enantiomeric excess was only 28%. Less reactive (TMSO)$_3$SiH could result in better enantioselectivity (65% ee) but longer reaction time (Scheme 2.9).[8]

R1	silane	% yield	% ee
Me	(MeO)$_3$SiH	>99	51
Et	(MeO)$_3$SiH	>99	65
Me	(TMSO)$_3$SiH	91	65
Me	PMHS	87	28
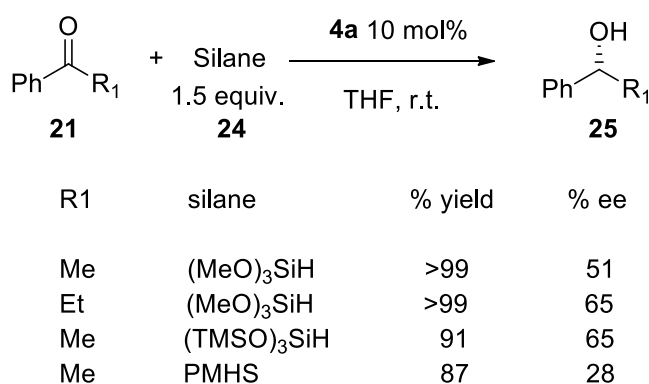
Scheme 2.9. Asymmetric Reduction of Ketones with Alkoxysilanes.

Since fluoride anion can form strong hydrogen bonds with protic compounds, in

nonpolar solvents $R_4N^+F^-$ generally exists as the adduct of hydrogen halides and water, $R_4N^+F^-(HY)_n$. This property can explain the hygroscopic nature of $R_4N^+F^-$. However, under strictly anhydrous conditions, Hoffman elimination may happen due to intramolecular deprotonation of fluoride anion so that the ammonium salt will degrade to trialkylamine, olefin and ammonium bifluoride salt (Figure 2.1).[1] The resulting ammonium bifluoride salt is more stable and easier to be handled than corresponding fluoride salt so that it can be an alternative to deprotection the silyl groups.

$$2\ R_4N^+F^- \longrightarrow R_4N^+HF_2^- + R_3N + R'CH=CH_2$$

Hoffman elimination mechanism
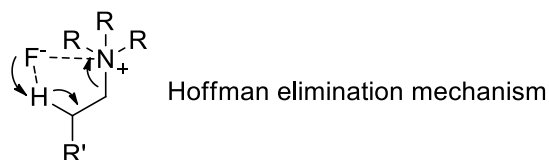
Figure 2.1. Hoffman Elimination of Tetraalkylammonium Fluoride Salt.

In 1999, Corey reported an asymmetric Mukaiyama aldol reaction of TMS protected Schiff base **26** and aldehydes catalyzed by cinchonidine derived bifluoride **15f**. Products of different diastereoselectivity could be formed under different reaction pathways. *Syn*-**28** was obtained as the major product. Good to excellent enantiomeric excesses were obtained under optimized reaction conditions (Scheme 2.10).[9]
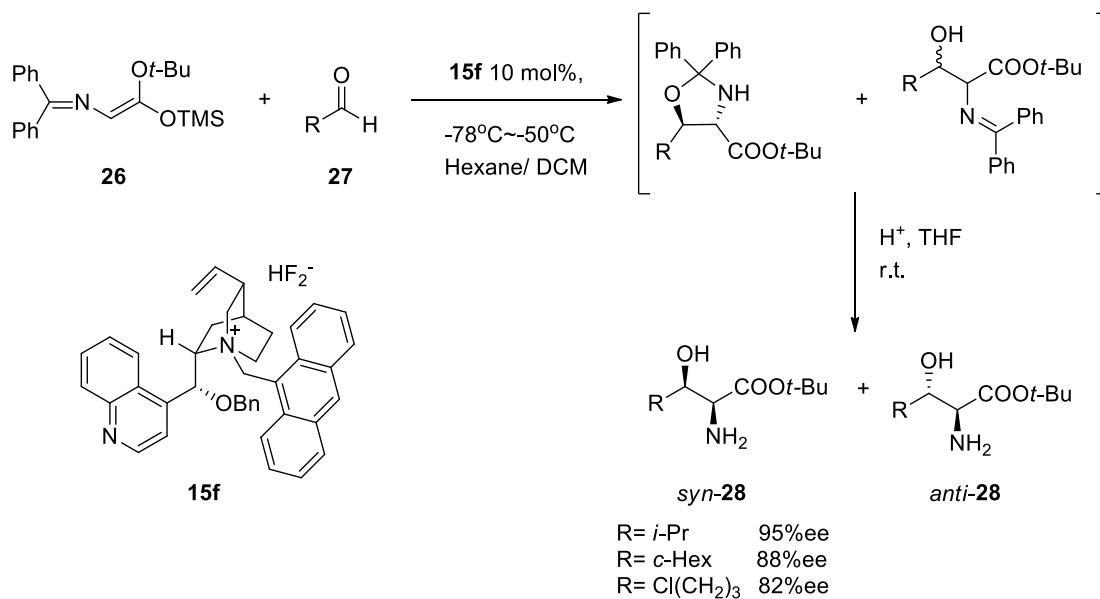
Scheme 2.10. Asymmetric Synthesis of α-Amino Acid via Mukaiyama Aldol Reaction.

In 2003, Maruoka used his designer chiral spiro ammonium bifluoride as catalyst, and finished the asymmetric version of Mukaiyama type nitroaldol reaction (Scheme 2.11).[10] During the optimization, they found that further increasing the steric effect of Ar groups on the catalyst from **11a** (X=HF$_2$) to **11b** could result in great improvement of diastereo- and enantioselectivity. *Anti*-nitroaldols were obtained as major products with excellent ee values.

R= Ph	92% yield, *anti/syn*= 92:8	95% ee
R= *p*-Me-C$_6$H$_4$	92% yield, *anti/syn*= 94:6	97% ee
R= *p*-F-C$_6$H$_4$	94% yield, *anti/syn*= 83:17	90% ee
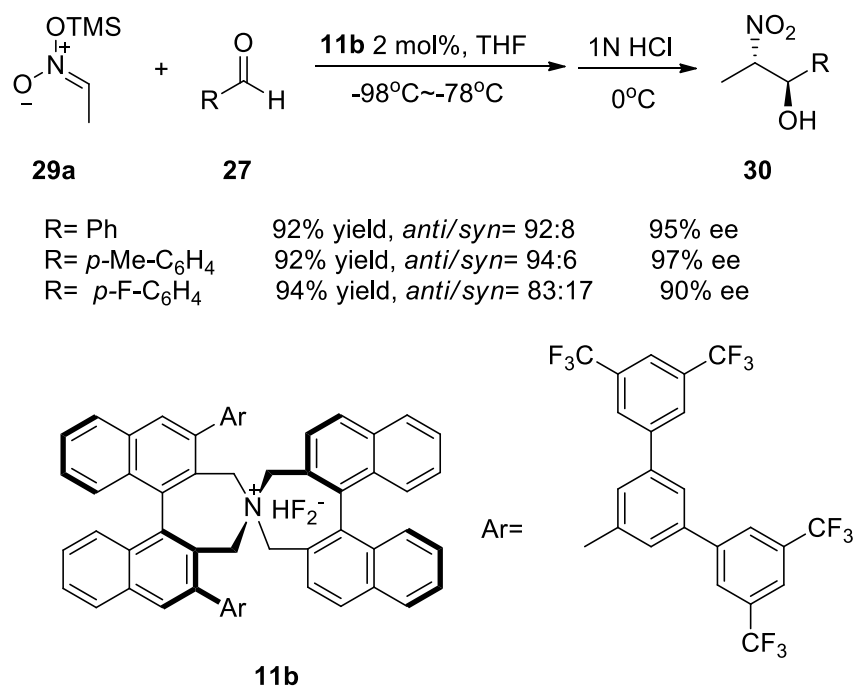
Scheme 2.11. Asymmetric Mukaiyama Type Nitroaldol Reaction.

When they extended the substrate scope from different substituted benzaldehydes to *trans*-cinnamaldehyde, 1,4-addition product *syn*-**32** was the major product, rather than nitroaldol product (with a ratio of 8:2). Interestingly, when the chiral catalyst was replaced by achiral catalyst TBAF, the ratio of Michael and nitroaldol type product was 1.1: 1 which indicated the in situ formation of ammonium nitronate salts (Scheme 2.12). Furthermore, Muruoka studied this reaction thoroughly and developed a larger substrate scope for this Mukaiyama type Michael addition reaction.[11]
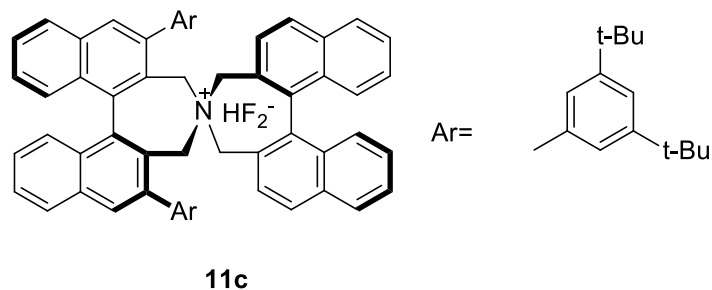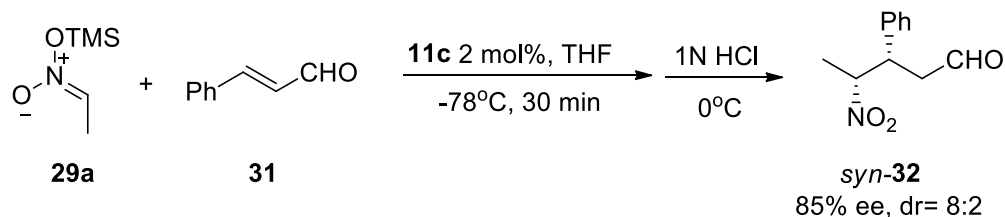
Scheme 2.12. Asymmetric Michael Addition of TMS-Protected Nitroethane to *Trans*-Cinnamaldehyde.

2.1.3 Conclusion

Asymmetric catalysis using ammonium fluoride salts as catalysts is still not fully developed now and it is lack of significant improvement recent years. Although Maruoka has done most of the pioneering works in this research area, the reactions mostly are limited to aldol and Michael addition reactions and enantioselectivity need to be further improved. Many other types of reactions have been solved using achiral ammonium fluorides as catalysts, so it is promising to develop their asymmetric versions. Also it is hopeful to improve the enantioselectivity by changing the chiral backbones of the catalysts and further tuning the reaction conditions.

2.2 Brief Introduction of Asymmetric Organocatalysis of 1,4-Dicarbonyl Compounds

2.2.1 Brief Introduction

1,4-dicarbonyl compounds are kinds of very important and fundamental fragments in organic syntheses not only for its universal existence in organic compounds, but also for its easy introduction of further two chiral centers by reduction. There have been numerous protocols introducing the syntheses of these valuable substrates, but only a few of them can construct 1,4-dicarbonyl structures enantioselectivily. Most of these published examples can be categorized into three families:

(1) Asymmetric reduction of dimethyl itaconate and its derivatives with H$_2$ catalyzed by chiral transition metal complexes.

(2) Asymmetric inter- and intramolecular Stetter reactions.

(3) Enantioselective α-enolation of aldehydes via MacMillan's SOMO catalysis. Transition metal (such as Rh^{2+}, Rh$^+$) catalyzed asymmetric hydrogenation of dimethyl itaconate and its derivatives have became a very successful method to synthesize chiral 1,4-diesters after several decades' study. Both excellent yield and enantioselectivity can be achieved simultaneously. One of the latest examples Shown in Scheme 2.13 reported by Leitner in 2013 indicated that industrial application is the direction to further optimizing this reaction system.[12] Continuous-flow process was applied in this work and supercritical CO$_2$ was used as mobile phase. Full conversion and enantiopure product were achieved and turnover number of the catalyst was larger

than 100000 which mean at least 100 kg product could be produced with only 1 g of rhodium catalyst.
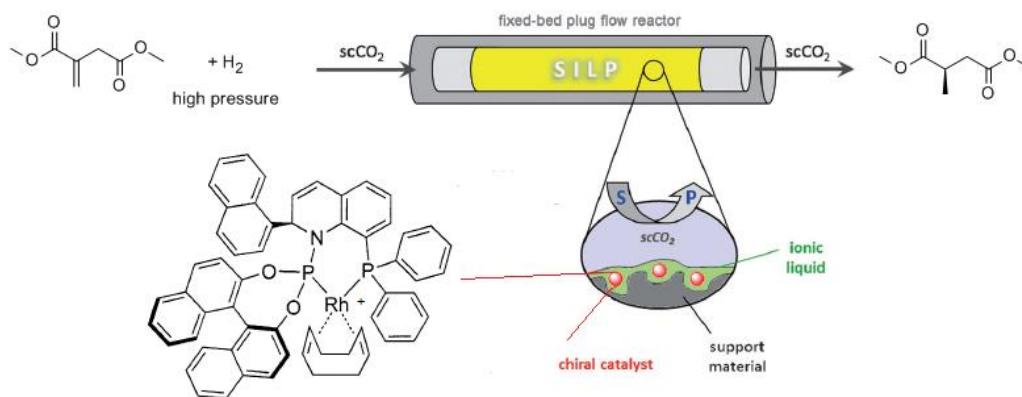
Scheme 2.13.[12] Concept of Asymmetric Hydrogenation of Dimethyl Itaconate with Flow Reactor.

In 2013, Bouteiller also applied supramolecular catalyst to the hydrogenation of dimethyl itaconate and achieved excellent results.[13] Since organometallic asymmetric catalysis is another branch of asymmetric catalysis and not extremely related to our topic asymmetric organocatalysis, further explanation won't be included in this chapter.

Stetter reaction was first discovered by Stetter in 1973 and consist of conjugate addition of acyl anion equivalents to α,β-unsaturated carbonyl compounds, which involved CN$^-$ or NHC carbenes as umpolung catalysts.[14] The first example of asymmetric intramolecular Stetter reactions was reported by Enders in 1996 (Scheme 2.14).[15] Although the enantiomeric excesses were just moderate, this pioneering work

inspired more groups to develop more efficient catalysts and suitable protocols and achieved excellent enantioselectivity.

33a	R= H	73% yield	60% ee
33b	R= 8-MeO	44% yield	68% ee
33c	R= 7-MeO	22% yield	71% ee
33d	R= 6-MeO	56% yield	61% ee
33e	R= Cl	50% yield	41% ee
33f	R= [5,6]-Ph	51% yield	65% ee
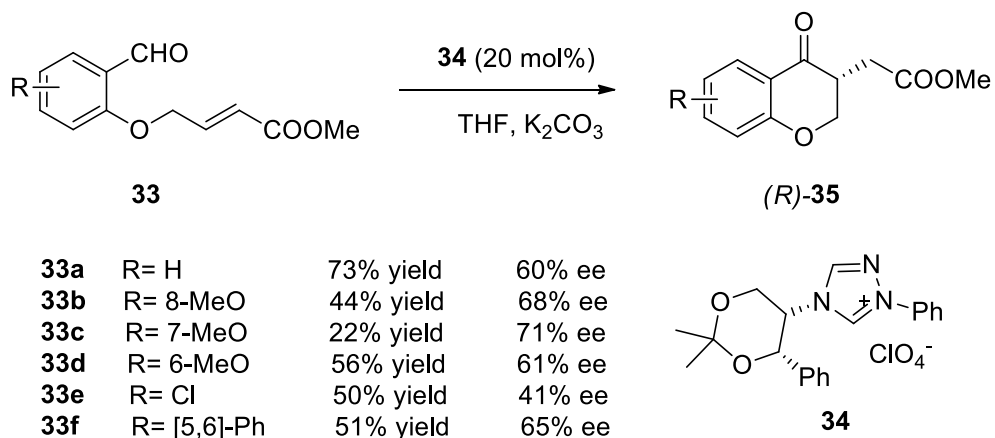
Scheme 2.14. First Asymmetric Intramolecular Stetter Reaction.

The disadvantages of intramolecular Stetter reactions are quite obvious. One is extra steps to synthesize the starting materials and the other is only cyclic products could be obtained. Development of intermolecular Stetter reactions could solve these problems. Enders' group reported the first asymmetric intermolecular Stetter reaction in 1993 with 4% yield and 39% ee.[16] With continuous study on NHC catalysts, they found that the reactivity of the catalysts depended on the substituents on nitrogen greatly. So after 15 years, they reported the first successful example of asymmetric intermolecular Stetter reaction with moderate to good yields and good enantiomeric excesses (Scheme 2.15).[17] They used the same catalyst and changed the Michael acceptors from substituted chalcones to arylidenemalonates and achieved moderate to good ees.
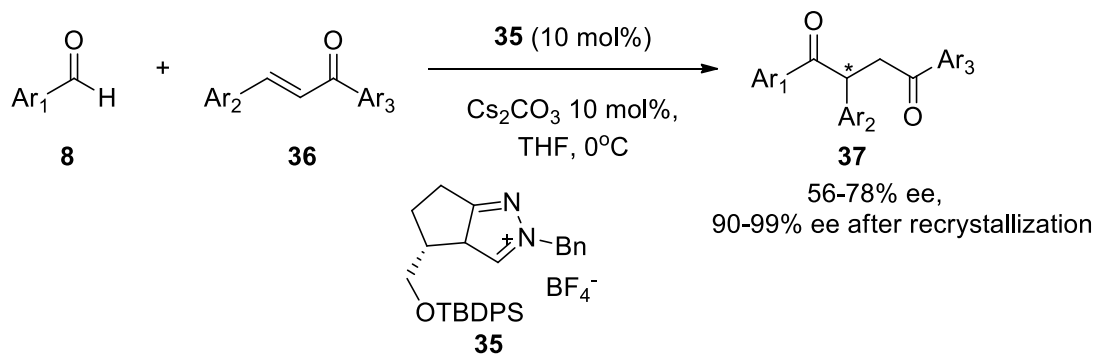
Scheme 2.15. Selected Example of First Successful Asymmetric Intermolecular Stetter Reaction.

Almost at the same time, Rovis independently published the asymmetric intermolecular Stetter reaction with good to excellent yields and enantioselectivities (**Scheme 2.16**).[18]
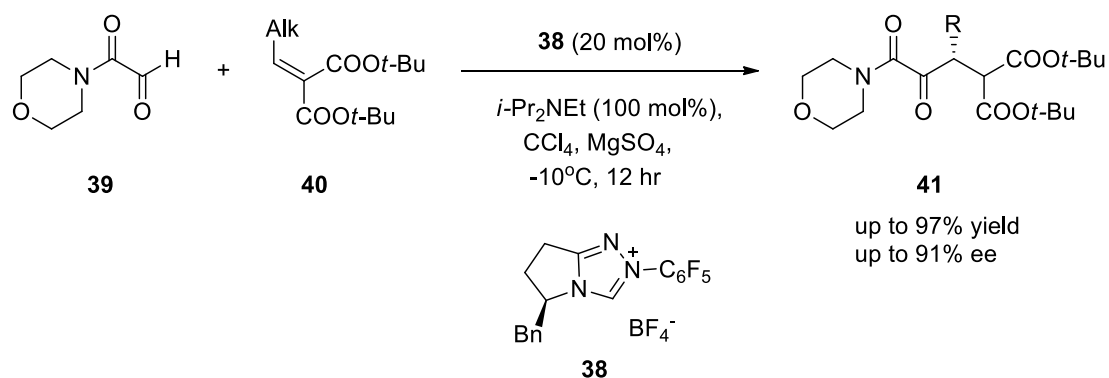
Scheme 2.16. First Asymmetric Intermolecular Stetter Reaction with Excellent Enantioselectivity.

In 2011, Glorius reported the highly enantioselective intermolecular Stetter reaction of benzaldehyde derivatives to N-acylamido acrylate which produced enantioenriched α-amino acid derivatives (Scheme 2.17).[19]
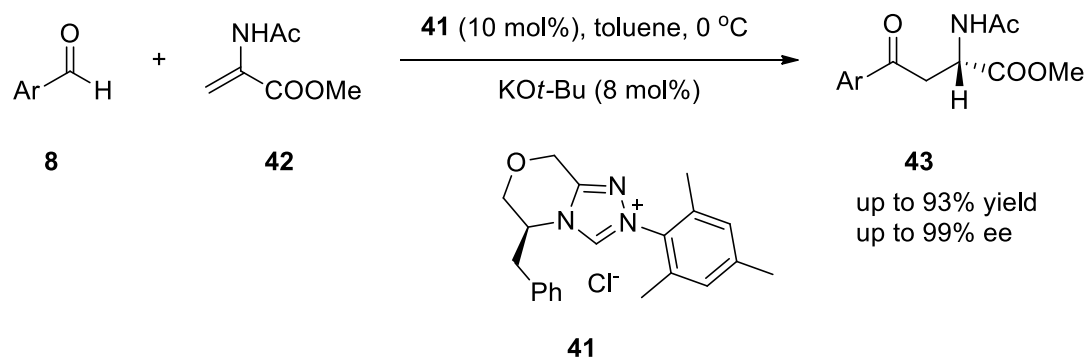
Scheme 2.17. Application of Asymmetric Intermolecular Stetter Reaction in the Synthesis of Enantioenriched α-Amino Acid Derivatives.

In 2011, Gravel reported the first highly enantioselective intermolecular Stetter reactions on β-aryl substituted acceptors. Excellent results were obtained and a selected example is presented in Scheme 2.18.[20]
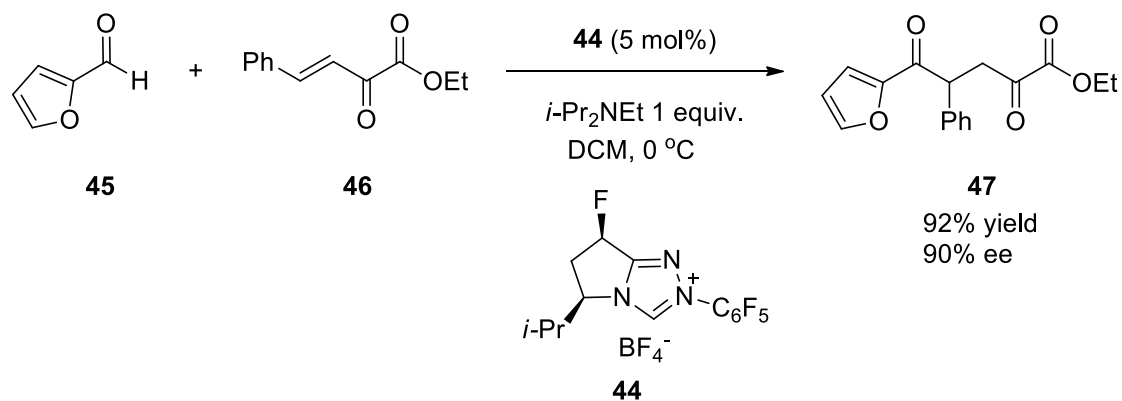
Scheme 2.18. Enantioselective Intermolecular Stetter Reactions on β-Aryl Substituted Acceptors.

Still in 2011, Chi reported highly enantioselective Stetter type conjugate addition of enals to modified chalcones catalyzed by NHC catalysts and obtained excellent results (Scheme 2.19).[21]
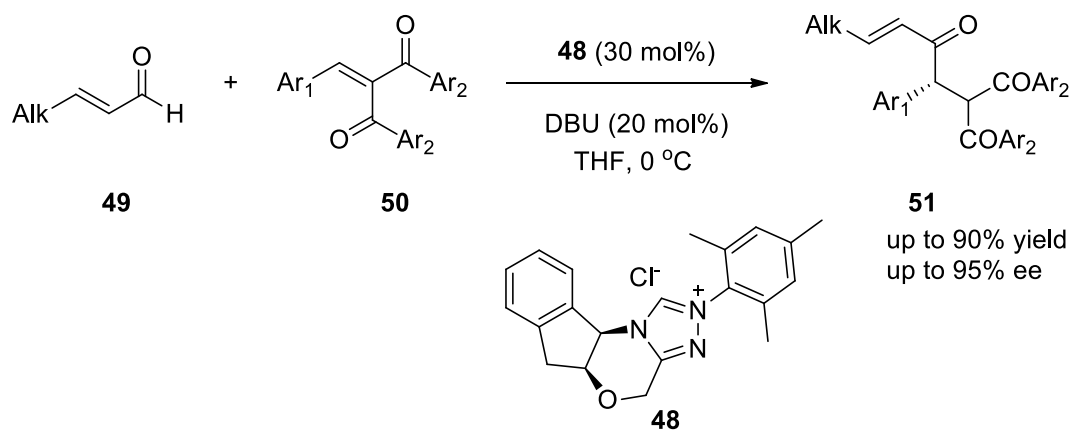
Scheme 2.19. Asymmetric Stetter type Michael addition of enals to modified chalcones.

Bearing a similar idea to Stetter reactions, in 2006, Johnson reported metallophosphite catalyzed asymmetric acylation of α,β-unsaturated amides with excellent enantioselectivities (after recrystallization) and moderate to good yields.[22]

Besides asymmetric intra- and intermolecular Stetter reactions, MacMillan's SOMO (singly occupied molecular orbital) catalysis is another mature and successful system to synthesize enantioenriched 1,4-dicarbonyl compounds. Mechanistically, the so-called SOMO catalysis is derived from enamine catalysis and further loses one electron via oxidation (Figure 2.2).[23]
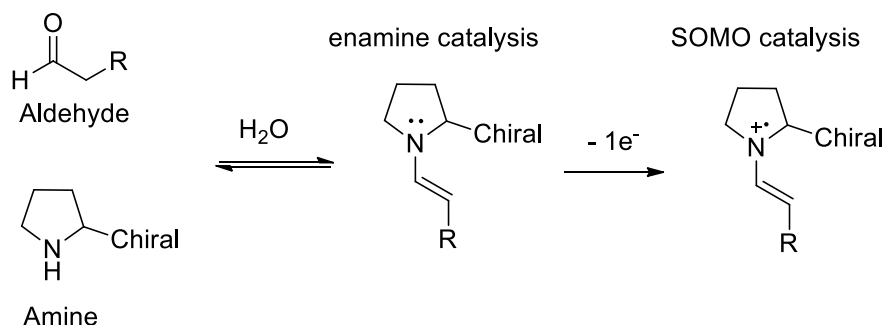
Figure 2.2. Concept of SOMO Catalysis.

This in situ formed electrophile is then attacked by nucleophiles existing in the reaction system and generates the desired product. MacMillan has used this reaction system in many reactions and achieved great success including enantioselective construction of 1,4-dicarbonyl compounds (Scheme 2.20). R groups on the substrates could be aliphatic and aromatic groups.
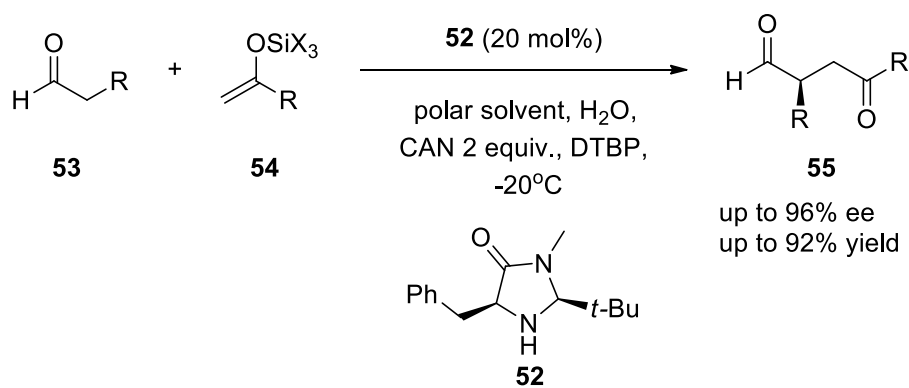
Scheme 2.20. Asymmetric SOMO Catalysis of 1,4-Dicarbonyl Compounds.

In 2008, MacMillan reported the photocatalysis version of SOMO catalysis. The former oxidant CAN was replaced by fluorescent light and photoredox catalysts (Scheme 2.21).[24] When **56** was α-bromocarbonyl compound, the product was 1,4-dicarbonyl compound.
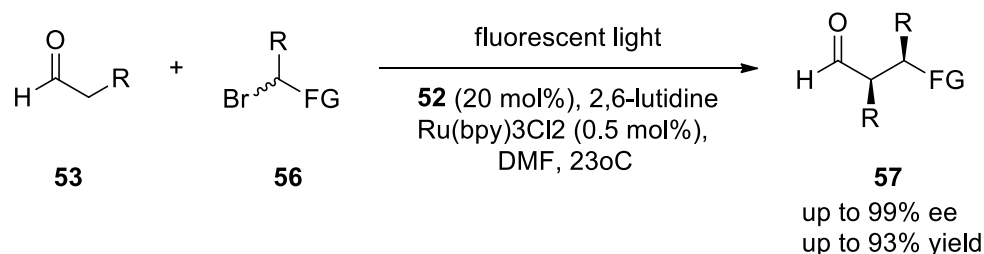
Scheme 2.21. Photocatalysis Version of SOMO catalysis.

There are some other publications of construction of 1,4-dicarbonyl compounds that cannot be categorized into these three catalytic families. For example, in 2010, Feng reported highly enantioselective aza-ene type reaction catalyzed by chiral N,N'-dioxide-nickel(II) complex (Scheme 2.22), and excellent results were obtained.[25]
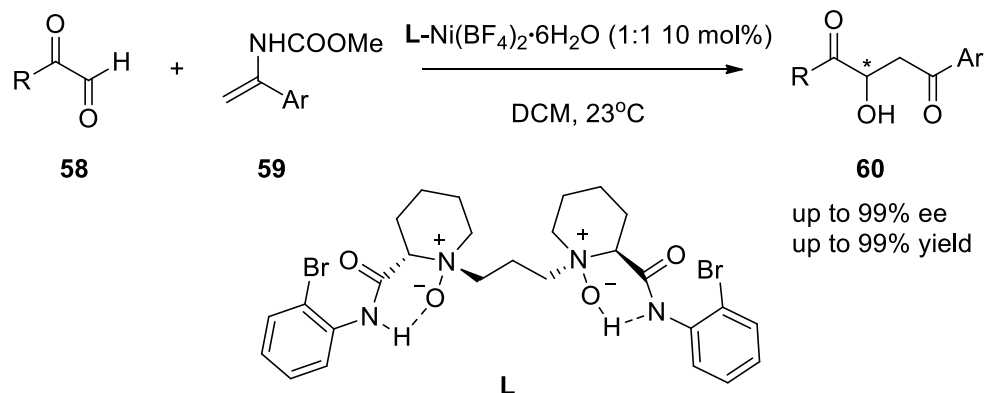
Scheme 2.22. Enantioselective Aza-Ene Type Reaction Catalyzed by Chiral N,N'-Dioxide-Nickel(II) Complex.

2.2.2 Conclusion

Enantioenriched 1,4-dicarbonyl compounds are kinds of very important and fundamental fragments in organic syntheses, and the synthesis of them is still an underdeveloped field. Oganocatalysis systems have been applied and achieved great success. Both of NHC catalysts and MacMillan's proline type catalysts can form covalent bonds with starting materials so that the further chiral induction is easy and robust. To my best knowledge, there is no example using phase-transfer catalysis system to synthesize enantioenriched 1,4-dicarbonyl compounds, which mechanistically should be possible and convenient.

2.3 Fluoride Anions Mediated Enantioselective Mukaiyama Type S$_N$2 Alkylation Reaction Catalyzed by Bis-Guanidium Salts.

2.3.1 Trigger of the Project

In 2009, our group reported a highly enantioselective conjugate addition reaction of 1,4-dicarbonyl but-2-enes to synthesize α-Stereogenic Amides and Ketones (**Scheme 2.23**). Both excellent yields and ees could be obtained using our classic guanidine catalyst.[26]
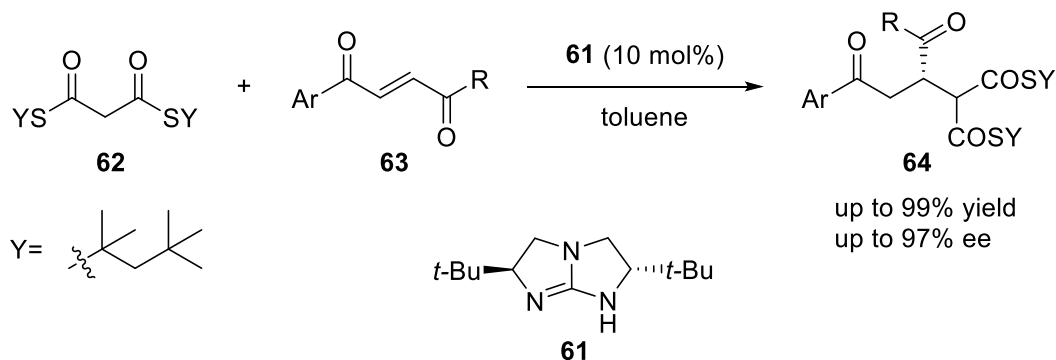
Scheme 2.23. Enantioselective Conjugate Addition Reaction of 1,4-Dicarbonyl But-2-Enes to Synthesize α-Stereogenic Amides and Ketones.

Although the results were perfect, the disadvantages were also obvious. The substrates were not easy to synthesize since more than one electron withdrawing groups were needed to lower the pKa of the starting materials. Some unusual auxiliaries were added to achieve high ees due to the difficulties in modifying the catalyst.

All these years, we have been seeking a method to solve these problems until we

started to study phase-transfer catalysis system and invented our easily modified phase-transfer catalysts introduced in Chapter 1. Catalytic properties of phase-transfer catalysts are heavily depended on the counter ions so that the basicity is tunable by changing the inorganic bases. Also many fragments of the catalysts can be easily modified to obtain appropriate steric and electronic effects so that extra auxiliary is not necessary to high enantioselectivity. Using retrosynthetic analysis, 1,4-dicarbonyl compounds can be easily obtained from propiophenone type substrates by reacting with α-bromoesters under basic conditions, and it is possible to achieve high enantioseletivity with a huge catalyst library in hand. At that moment, the basic idea of this project started to become clear.

2.3.2 Guanidium Salts Catalyzed Asymmetric S$_N$2 Alkylation Reaction

To prove the concept, propiophenone and methyl bromoacetate were the most straightforward choices to be the starting materials, and were tried in toluene-50% NaOH (aq.) bi-layer system. No desired product was obtained due to fast decomposition of methyl bromoacetate under strong basic condition. (*Z*)-1-phenylprop-1-en-1-yl acetate was also prepared and tried in this reaction which could generate enolates under weaker basic condition (10% NaOH aqueous solution). However unfortunately, this level of basicity was still too high to methyl bromoacetate (Scheme 2.24). Further studies showed that **66** could decompose even using Cs$_2$CO$_3$ solid as the base, which indicated that Brønsted base might not be suitable to this alkylation system.
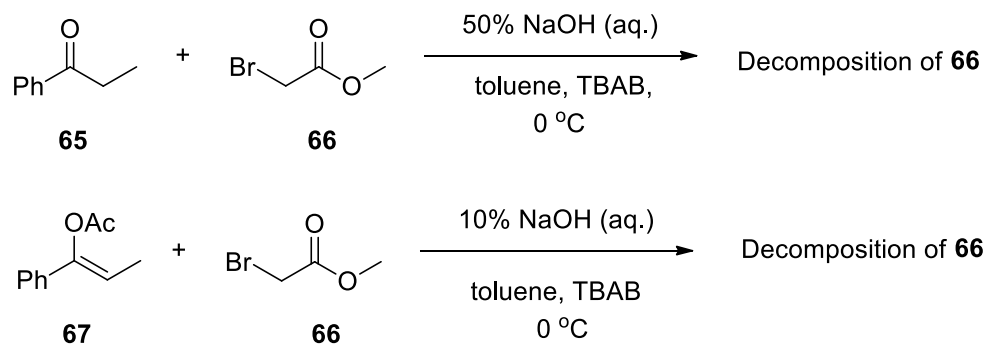
Scheme 2.24. Failed Attempts of OH$^-$ Mediated Alkylation Reactions.

Silyl enol ethers have been used as enolate precursors for more than half a century, and the specific affinity of fluoride anions to silicon can ensure the deprotection of silyl groups and tolerance of other sensitive parts at the same time. Pioneering works done by Maruoka in asymmetric Mukaiyama aldol reactions showed the possibility to solve our problem with chiral ammonium fluoride salts.

Model reaction was carried out using TMS protected propiophenone derived silyl enol ether and methyl bromoacetate as starting materials and stoichiometric amount of CsF solid as fluoride source (Scheme 2.25). The reaction couldn't finish in 5 days at room temperature and the yield was 52% when a lot of silyl enol ether still remained. The only significant byproduct was propiophenone formed by protonation of generated enolate. It was difficult to track back the proton source (compound **66** or water), since the reaction yield was extremely low when the system was critically unhydrous.
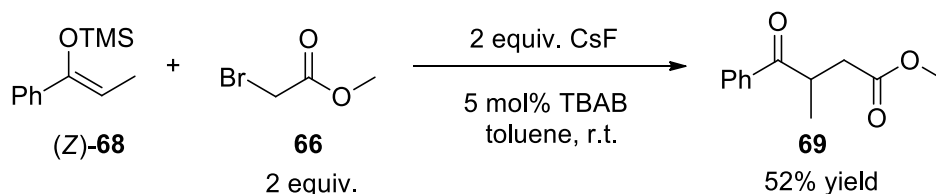
Scheme 2.25. Model Reaction of Mukaiyama Type S$_N$2 Alkylation Reaction.

With the racemic condition in hand, we started to screen the chiral PTCs in our library and some commercial available cinchonidine derived PTCs. The results of first round of catalyst screening are shown in Table 2.2. Since it's the preliminary screening of the catalysts, isolated yields were just calculated for the promising entries. Full catalyst list is presented in Table 2. 13 at the end of Section 2.3.2.

Table 2.2. First Round of Catalyst Screening Results of the Model Reaction.
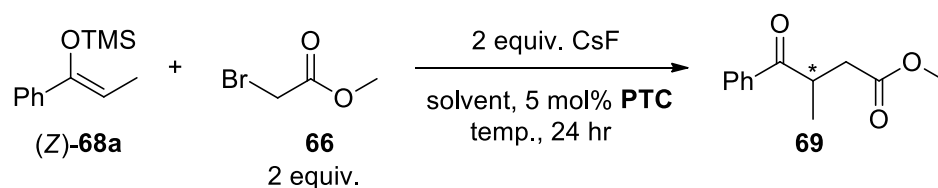
Entry[a]	Catalyst	Solvent	Temperature (°C)	Ee (%)[b]
1	**PTC 1**	TBME	0	25 (40% yield)[c]
2	**PTC 2**	TBME	25	10
3	**PTC 3**	TBME	25	7
4	**PTC 4**	TBME	25	15
5	**PTC 5**	TBME	25	5
6	**PTC 6**	TBME	25	12
7	**PTC 7**	TBME	25	5
8	**PTC 8**	TBME	25	0
9	**PTC 9**	TBME	25	n.p.
10	**PTC 10**	TBME	0	5
11	**PTC 11**	TBME	25	n.p.
12	**PTC 12**	Toluene	0	7
13	**PTC 13**	Toluene	0	0

14	**PTC 14**	Toluene	0	5
15	**PTC 15**	Toluene	0	6
16	**PTC 16a**	TBME	0	30 (50% yield)[c]
17	**PTC 16a**	Toluene	0	50 (55% yield)[c]
18	**PTC 16b**	TBME	0	7

[a] Reactions were carried out on a 0.02 mmol scale with 5 mol% PTC in 1.5 mL sealed vials with 150 μL solvents. [b] Determined by HPLC analysis. [c] Isolated yields.

During this round of catalyst screening, we tried all the pentanidiums in our catalyst library. Previously published full methylated pentanidium **PTC 1** showed 25% ee (optimized) and 40% yield in 24 hours. Any other pentanidium derivatives with larger steric effects and different distribution of the chiral centers showed lower enantioselectivity and activities of catalysis (Entry 2 to 8). No desired product was obtained when electron withdrawing R groups were attached to nitrogen (Entry 9). At this point, it was clear that the scaffold of pentanidium salts was not suitable in this reaction system. Three commercial available cinchonidine derived PTCs were tried in the model reaction. The reaction rates were faster than those of pentanidiums, but basically no reliable enantiomeric excess was obtained (Entry 13 to 15). **PTC 11** which had been proven to be effective in fluoride anion mediated Mukaiyama aldol reactions showed no catalytic activity in this S$_N$2 alkylation reaction.

However, highly sterically hindered bis-guanidium salt **PTC 16a** showed great match with the substrates. 50% ee was obtained when toluene was used as solvent, and the reaction rate was greatly higher than those of **PTC 1**. While full methylated bis-guanidium salt **PTC 16b** provided bad results, implying that the steric effect was

important in this case. Further studies proven that the bis-ammonium scaffold was necessary to the enantioselective control, since enantiomeric excesses of the mono-guanidium salts were not higher than 10% (Entry 10 and 12).

With an appropriate catalyst in hand, we began to optimize the reaction condition. Firstly, we screened solvents and inorganic fluoride salts (Table 2.3). The isolated yields were only calculated for promising entries.

Table 2.3. Preliminary Screening of Solvents and Fluoride salts.
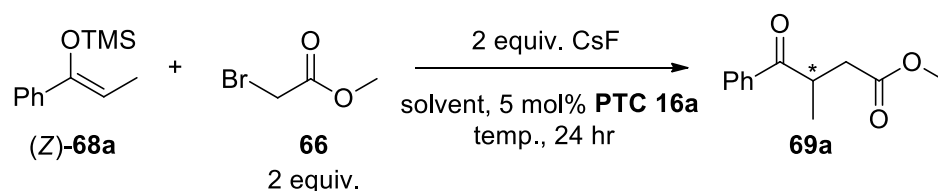
Entry[a]	Solvent	F$^-$ source	Temperature (^{o}C)	Conv. (%)[b]	Ee (%)[c]
1	Toluene	CsF	0	90 (55)[d]	50
2	Cyclohexane	CsF	0	50	27
3	Mesitylene	CsF	0	20	36
4	*o*-Xylene	CsF	0	80	42
5	*m*-Xylene	CsF	0	80	42
6	4-*t*-Bu-toluene	CsF	0	90 (70)[d]	55
7	Ethylbenzene	CsF	0	90	48
8	Anisole	CsF	0	100	31
9	DCM	CsF	0	100	0
10	TBME	CsF	0	90	30
11	4-*t*-Bu-toluene	CsF	-20	trace	n.d.
12[e]	Toluene	AgF	0	100(30)[d]	56
13[e]	*m*-Xylene	AgF	0	100(38)[d]	68

14 [e]	*o*-Xylene	AgF	0	100	63
15 [e]	4-*t*-Bu-toluene	AgF	0	100(50) [d]	71
16	Mesitylene	AgF	0	trace	67
17 [e]	TBME	AgF	0	100	40
18 [e]	DCM	AgF	0	100	0
19 [e]	Cyclohexane	AgF	0	100	45
20 [e]	Trifluorotoluene	AgF	0	100	18
21	Toluene	AgF	-20	trace	48
22	Toluene	AgF	25	100 (30) [d]	46

[a] Reactions were carried out on a 0.02 mmol scale with 5 mol% PTC in 1.5 mL sealed vials with 150 μL solvents, dark. [b] Conversion was based on **68a** determined by TLC. [c] Determined by HPLC analysis. [d] Isolated yields. [e] The reaction could be finished in 8 hours.

From the data presented in Table 2.3 we could see that toluene type solvents were more preferable than DCM, ether type and alkane type solvents no matter the fluoride salt was CsF or AgF. Further screening was carried out among toluene type solvents. Ethylbenzene showed little difference with toluene on aspects of ee and yield. *O*-xylene and *m*-xylene were tested which provided higher enantiomeric excesses than toluene when AgF was applied (Entry 13 and 14). *P*-xylene was not taken into consideration due to its higher melting point than 0 °C. Highly steric hindered mesitylene showed bad conversions under reaction conditions (Entry 3 and 16). More polar derivatives showed better reaction yield but far lower ees (Entry 8 and 20).

AgF showed better enantioselectivity and faster speed of starting material consumption than CsF, but lower yields due to strong side reactions induced by Ag$^+$ (dehalogenation and other effects). More propiophenone was produced and the spots

on TLC plates were messy. The situation could be improved by using 4-*t*-Bu-toluene as solvent, but the yield was still not satisfying. Dramatically, both CsF and AgF showed no activity when the temperature went down to -20 $^{\circ}$C, although at 0 $^{\circ}$C the reactions were still robust. It should be an important phenomenon, but we couldn't find a reasonable explanation. Silver fluoride salts of different purity levels (99% and $\leq$ 99.9% purchased from Sigma-Aldrich) were tested, and no obvious difference was observed. Different ratios of the two substrates (2:1, 1:1, 1:2) and the concentrations (0.06 M, 0.13 M, 0.25 M) for promising entries were also tested at this moment (not shown in the tables), yields and reaction rates could be affected, but enantioselectivity showed no obvious difference. At this preliminary stage, the best result was 71% ee and 50% isolated yield (Entry 15) temporarily, and further optimization was still needed.

Later more commercial available inorganic fluoride salts were screened, Namely NaF, KF, RbF, KHF_2, MgF_2, CaF_2, SrF_2, BaF_2, NH_4F, Na_3AlF_6, GaF_3, NH_4HF_2, TiF_3, VF_3, MnF_2, FeF_2, FeF_3, CoF_2, NiF_2, CuF_2, ZnF_2, AgF_2, SnF_4. However, none of them could activate the silyl compounds under standard condition. Hg_2F_2 was the most possible alternative to AgF since Hg$^+$ has similar properties to Ag$^+$. However its importation was forbidden by Singapore government so that we didn't obtain this data.

During the optimization, an interesting phenomenon came to us (Table 2.4). When the 1:1 mixtures of AgF and wet CsF (stored in open air) were used as fluoride source, 78% ee was obtained with lower reaction rate (Entry 3). The yield was not determined, since it depended on the amount of water contained by CsF. However, when we used dry CsF (freshly taken out of glovebox) and mixed it with AgF, both ee and yield were just the same as those of CsF (Entry 4).

**Table 2.4**. Screening of Fluoride Salts with the Model Reaction.
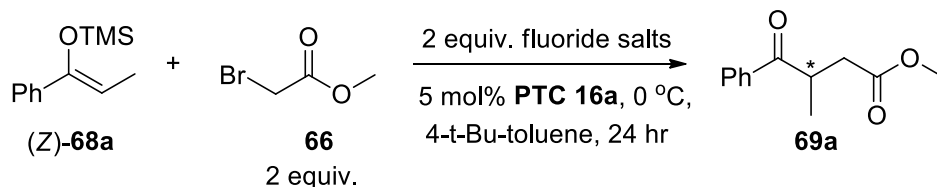
Entry[a]	F⁻ source	yield (%)	ee (%)[b]
1	CsF	70	50
2	AgF	50	71
3	AgF: CsF(wet)= 1:1	n.d.	78
4	AgF: CsF(dry)= 1:1	72	52

[a] Reactions were carried out on a 0.02 mmol scale with 5 mol% PTC in 1.5 mL sealed vials with 150 μL solvents, dark. [b] Determined by HPLC analysis.

From the data presented in Table 2.4, we proposed that the preferred fluoride source in the reaction system should be CsF due to the similar results of Entry 1 and 4. It could also be supported by HSAB theory (hard and soft acids and bases theory) and dehalogenation effect of silver cation, in which case Ag⁺ is soft, F⁻ is hard, and Cs⁺ is in between so that AgF prefers to exchange its anion with CsBr and precipitates out as AgBr. The existence of trace amount of free water may also help to dissolve the inorganic salts and accelerate the anion exchange. However due to some unknown reasons, stoichiometric amount of CsF is not good to achieve high enantiomeric excess so that a better way is to in situ generate CsF which means there will be only catalytic amount of CsF existing in the system throughout the reaction. The fluoride anions of wet CsF are fully bonded and deactivated by H$_2$O molecules so that the

anion exchange with AgF may generate catalytic amount of "active" CsF and further results in higher ee value of Entry 3.

To prove the existence of anion exchange in solid phase, we used CsF as fluoride source and added different sodium salts (whose anions cannot form strong competition with F$^-$) in to the system. Since NaF cannot activate the silyl compound under standard condition, if the exchange can really happen, there should be trace amount of product or even no product (Scheme 2.26). As we predicted, no reaction happened when 1 equivalent sodium salts were added so that our proposed mechanism was reasonable.
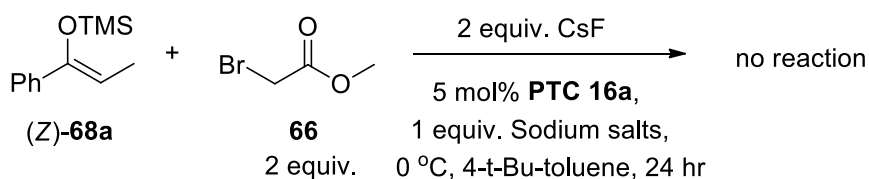
Sodium salts tried: NaCl, Na$_2$SO$_4$, Na$_2$CO$_3$.

Scheme 2.26. Proof of Anion Exchange in Solid Phase.

Then the most urgent thing we need to do was to find a suitable Cesium salt bearing a soft anion so that the anion exchange could happen with an appropriate rate. Several commercial available Cesium salts were tested and the results were presented in Table 2.5.

**Table 2.5**. Screening of Different Cesium Salts as Additives in the Model Reaction.
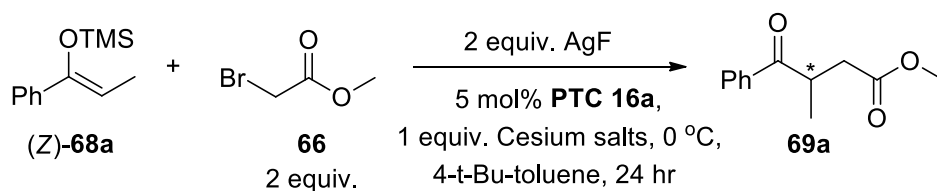
Entry[a]	Additives	Yield (%)	Ee (%)[b]
1	CsCl	65	79
2	CsOH·xH$_2$O	trace	n.d.
3	Cs$_2$CO$_3$	30	74
4	CsNO3	58	56
5	(COOCs)$_2$	67	75
6	CsOAc	69	84
7	HCOOCs	71	84
8[c]	AgOAc	52	50
9[c]	NaOAc	n.r.	--

[a] Reactions were carried out on a 0.02 mmol scale with 5 mol% PTC in 1.5 mL sealed vials with 150 μL solvents, dark. [b] Determined by HPLC analysis. [c] No cesium salt was added.

From the data in Table 2.5 we could see that cesium acetate and cesium formate provided the best results that increased enantiomeric excesses to 84% with roughly 70% yield (Entry 6 and 7). Changing cesium acetate to silver acetate showed no improvement on ee indicating that the enhancement of ee was not induced by addition of acetate anions (Entry 8). Data of Entry 9 could be explained by our proposed anion exchange mechanism. Since sodium fluoride couldn't mediate the reaction, no reaction happened when we changed cesium acetate to sodium acetate.

Different ratios of AgF and CsOAc were tested and the results were presented in Table 2.6.

Table 2.6. Testing of Different Loadings of CsOAc in the Model Reaction.
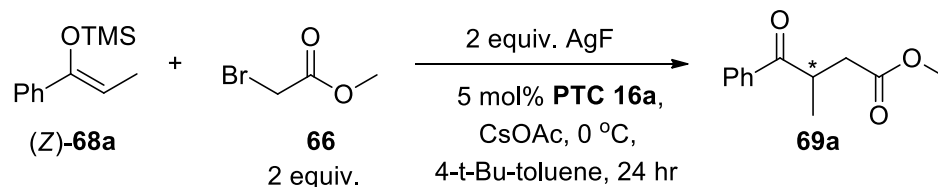
Entry[a]	Equiv. of CsOAc	Yield (%)[b]	Ee (%)[c]
1	1	69	84
2	2	54	83
3	0.5	68	83
4	0.1	55	69

[a] Reactions were carried out on a 0.02 mmol scale with 5 mol% PTC in 1.5 mL sealed vials with 150 μL solvents, dark.[b] Isolated yields.[c] Determined by HPLC analysis.

During the optimization, we found that when the loading of CsOAc was between 0.5 equivalents to 2 equivalents, the ee was independent to CsOAc. But more CsOAc was added, slower the reaction became due to the anion competition of F⁻ and OAc⁻ so that we didn't try loadings higher than 2 equivalents. When only 10 mol% CsOAc was added, the result was much similar to that of AgF alone. We also succeed to lower the loading of AgF to 1 equivalent since silver was expensive and heavy metal, and no difference in yield and ee was observed. But in the following optimization, we still used 2 equivalents of AgF due to easy weighing with balance.

With this mature reaction condition in hand, we started to tune the structure of bis-guanidium catalyst, and the data of this round of tuning is presented in Table 2.7. Full catalyst list is presented in Table 2. 13 at the end of Section 2.3.2.

Table 2.7. Catalyst Screening of Bis-Guanidium Salts with the Model Reaction.
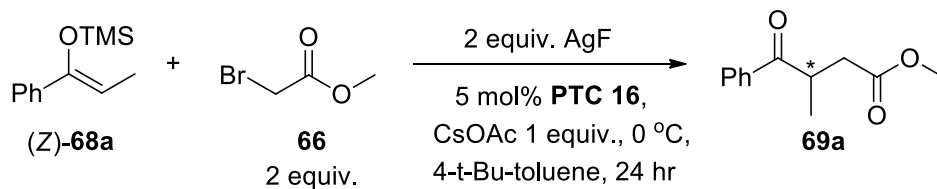
Entry[a]	Catalyst	Conv. (%)[b]	Ee (%)[c]
1	**PTC 16a**	90	86
2	**PTC 16b**	80	9
3	**PTC 16c**	80	0
4	**PTC 16d**	90	0
5	**PTC 16e**	80	3
6	**PTC 16f**	80	-10
7	**PTC 16g**	n.p.	--
8	**PTC 16h**	90	-13
9	**PTC 16i**	90	20
10	**PTC 16j**	80	17
11	**PTC 16k**	60	20
12	**PTC 16l**	n.p.	--
13	**PTC 16m**	90	74
14	**PTC 16n**	80	12
15	**PTC 16o**	30	34
16	**PTC 16p**	80	48
17	**PTC 16q**	n.p.	--
18	**PTC 16r**	60	33
19	**PTC 16s**	90	30
20	**PTC 16t**	90	15

[a]Reactions were carried out on a 0.02 mmol scale with 5 mol% PTC in 1.5 mL sealed vials with 150 μL solvents, dark.[b] Conversion was based on **68a** determined by TLC.[c] Determined by HPLC analysis.

Before the screening, honestly we were quite optimistic that this round of catalyst screening could push the ee value to 90%, since we had only tried two bis-guanidium salts, and there were still a lot of positions on the catalyst scaffold could be modified. But the results were not as good as our prediction. The model catalyst **PTC 16a** showed the best ee among the 20 bis-guanidiums we screened. R groups on nitrogen were the easiest place to modify. From the data we could see that, 3,5-disubstitutions on phenyl rings of the R groups were very important for enantioselectivity. The only one catalyst that showed comparable ee value with **PTC 16a** was **PTC 16m**, whose R groups on nitrogen were 3,5-di(TMS)-benzyl groups. Extra substituent on position 2 of the phenyl ring provided low ee (Entry 6 and 14). Strong electron withdrawing or strong electron donating groups substituted bis-guanidiums couldn't catalyze the reaction under the standard condition (Entry 7 and 12). Further modification was made on chiral backbones. Phenyl rings attached to the chiral centers were modified with steric (*para*-methyl phenyl, *para*- *t*-butyl phenyl, β-naphthyl phenyl groups), electron withdrawing (*para*-trifluoromethyl phenyl groups) and electron donating groups (*para*-methoxyl phenyl groups). But none of them showed acceptable result regarding to ee value.

The third and the last type modification we could think of was done on the central linker. Beside piperazine, we also tried 1,2,3,4,5,6-hexahydropyrrolo[3,4-c]pyrrole (Entry 20), N^1,N^2-dimethylethane-1,2-diamine (Entry 4) and

(2*S*,5*R*)-2,5-dimethylpiperazine (Entry 11) as the linker, but still the ee dropped dramatically.

With a series of setback in catalyst modification, we turned our focus to the tuning of two starting materials. Theoretically, we would only tune the protecting groups, leaving groups and ester groups which wouldn't narrow down the substrate scope and keep the methodology universal.

Firstly, we tried TES and TBS groups to replace TMS group. The new silyl protected enolate precursors were more stable than original TMS protected starting material, and could be isolated by silica column. But when we used them in the model reaction, no reaction happened in 24 hours and all silyl compounds were recovered. Further tuning of silyl groups would be meaningless, since TES was the most sensitive silyl group to fluoride anions except for TMS group. So using the mixture of AgF and CsOAc as the fluoride source, the only available silyl protecting group was TMS group.

As to the ester part, actually there are lots of strategies could be used. Scheme 2.27 showed different modifications we had tried and their results.

X= OEt	65% yield	83% ee
X= OBn	59% yield	79% ee
X= O*i*-Pr	trace	n.d.
X= O*t*-Bu	n.p.	—
X= OCH$_2$CF$_3$	n.p.	--
X= O*a*-Nap	54% yield	40% ee
X= S*t*-Bu	n.p.	—
X=N(CH$_2$)$_4$	trace	n.d.
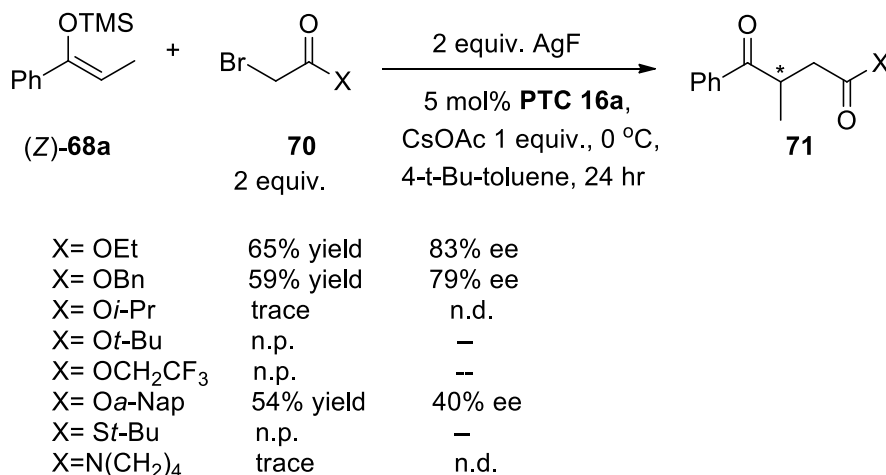
Scheme 2.27. Results of Modification on Ester Part for the Model Reaction.

Results showed that simple extension of aliphatic chain was not useful to improve ee value. While bulky groups and electron withdrawing groups might result in side reaction and no desired product could be obtained. Changing the ester to thioester showed no desired product due to the great changing of electronic effect. We could isolate desired product by using α-bromoamide to replace α-bromoester, but the yield was too low so that we gave it up.

An interesting phenomenon was, although bulky α-bromoester couldn't provide desired product when AgF was contained in the reaction system, it could be used when we simply applied CsF as the fluoride source which indicated that AgF (and the mixture of AgF and CsOAc) might undergo a different pathway compared with CsF.

Further optimization was carried out on the leaving groups shown in Scheme 2.28. We firstly changed the bromide to other halides, only Chloride showed trace amount of product. And once again, the α-iodoester which was not applicable to the mixture of AgF and CsOAc, could be used under the condition that using CsF as fluoride

source which could be explained by the dehalogenation effect of silver cation. When we changed the bromide to some softer leaving groups, such as NO$_3$ and OTs groups, no desired product was formed.

X= NO$_3$, R= Bn   n.p.
X= Cl, R= Et   trace
X= I, R= Et   n.p.
X= F, R= Et   n.p.
X=OTs, R= Et   n.p.
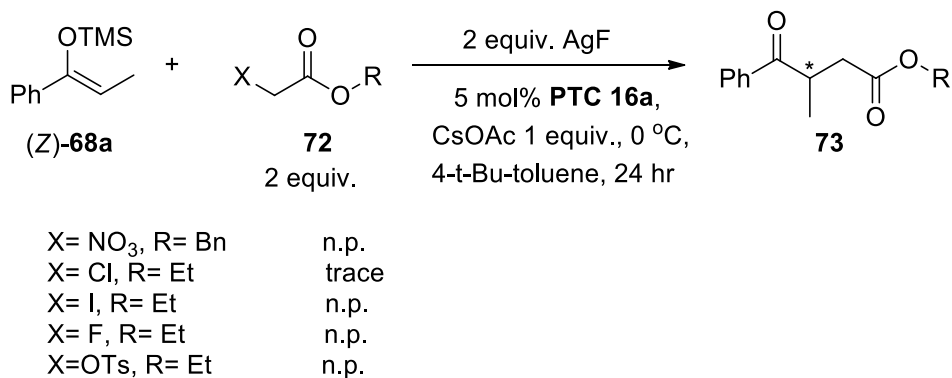
Scheme 2.28. Effects of the Leaving Groups on the Model Reaction.

During the optimization, we accidentally found that if we mixed trace amount of bulky alcohols in the solvent, the ee values could be improved slightly, but too much alcohols could quench the reaction. Further tuning showed that mixing 5 mol% TMSOH into the solvent showed 86% ee (2% ee increased) under standard condition (Scheme 2.29).
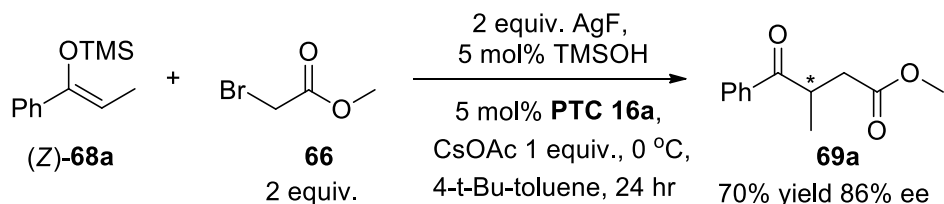
Scheme 2.29. Finalized Reaction Condition to the Model Reaction Using Mixture of AgF and CsOAc as Fluoride Source.
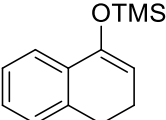
After the optimization, we prepared several different substituted silyl enol ethers and

used them under optimized condition (Table 2.8). The substrate scope was not so satisfying that all other substrates tested showed lower ee than the model **68a**. Entry 2 showed lower yield, since the electron donating group could stabilize its silyl groups. Chloride on phenyl ring could significantly accelerate the reaction, but meta substituted substrate showed lower ee. The cyclic example, which was applicable when CsF was used as fluoride source, showed no desired product when the fluoride source was the mixture of AgF and CsOAc. More substrates could be synthesized, but due to the limited time, broader substrate scope wasn't done.

Table 2.8. Substrate Scope Using Mixture of AgF and CsOAc as Fluoride Source.
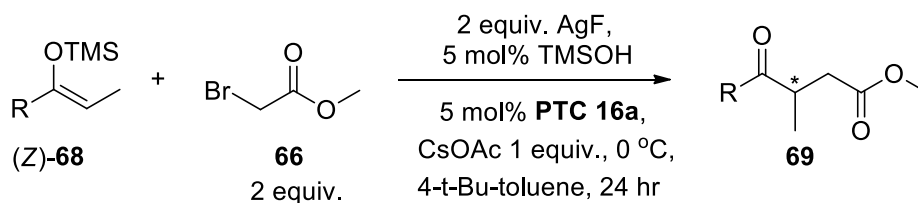
Entry[a]	Silyl enol ethers	yield (%)[b]	Ee (%)[c]
1		70	86
2		40	70
3		75	81
4		72	67

5	OTMS	n.p.	--

[a] Reactions were carried out on a 0.02 mmol scale with 5 mol% PTC in 1.5 mL sealed vials with 150 μL solvents, dark. [b] Isolated yields. [c] Determined by HPLC analysis.

During the optimization, we accidentally found that weak acidic condition was important to enantioselectivity, but too much acid might quench the reaction. Compound **66** could slowly decompose in a hot circumstance and generate HBr so that sometimes **66** with slightly decomposition showed max. 10% ee higher than normal **66**. However, we failed to catch this narrow pH window.

Although the application of AgF could provide the highest ee, lots of unsolved problems were induced by it. Firstly many substrates couldn't be used in AgF system. Secondly, the mechanism was complicated and many other effects were involved into the system which made the optimization lack of direction and the repeatability of reaction was poor. Thirdly, silver fluoride was much more expensive and toxic than other fluoride salts.

For the reasons presented above, we decided to try some new fluoride sources. The reagent attracted us was tetramethyl ammonium fluoride, which is short for TMAF. It can also be a phase-transfer catalyst in polar solvents. But in non-polar solvents, the catalytic ability is depressed due to its bad solubility and strong hydrophilicity. So it is possible to obtain enantiomeric excess if we use catalytic amount of chiral PTC and stoichiometric amount of TMAF in the system (Table 2.9).

Table 2.9. Optimization Using TMAF as Fluoride Source.
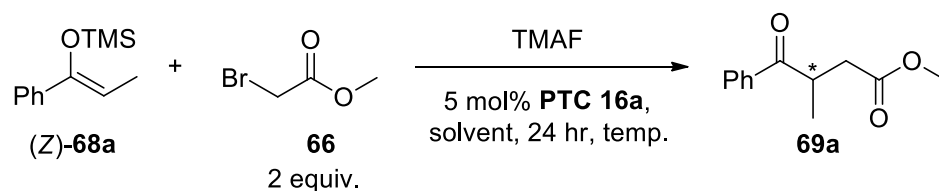
Entry[a]	Equiv. of TMAF	Solvent	Temp.(^{o}C)	Conversion (%)[b]	Ee (%)[c]
1	2	Toluene	-30	100	30
2	2	Toluene	-60	80	48
3	1	Toluene	-60	70	58
4	1	Toluene	-80	70	60
5	1	TBME	-60	n.p.	--
6	1	Ether	-60	90	35
7	1	4-*t*-Bu-toluene	-60	80	40
8	1	DCM	-80	100	0
9	1	n-Hexane	-60	40	18

[a] Reactions were carried out on a 0.02 mmol scale with 5 mol% PTC in 1.5 mL sealed vials with 300 μL solvents. [b] Conversion was based on **68a** determined by TLC. [c] Determined by HPLC analysis.

We firstly set up the reaction at -30 ^{o}C in toluene with 2 equivalents of TMAF. The reaction was so fast that 100% conversion was achieved in 3 hours. Lowering the temperature to -60 ^{o}C could increase the ee value by 18% and the reaction could be finished in 24 hours. No propiophenone was formed at such a low temperature and all consumed starting material **68a** was turned into the desired product. Further decrease of the temperature showed very little increase on ee. Blank reaction (without chiral PTC) under this condition showed strong background reaction so that we decided to reduce the loading of TMAF to 1 equivalent, and further 10% increased ee value was obtained.

Full screening of solvents showed that toluene was the best solvent in this modified system. Concentration of the solution could affect the ee value this time, and 0.07 M (based on **68a**) was the optimized concentration after several careful tests.

With this stronger fluoride salt in hand, we went back to the test of other silyl groups. TBS and TES were tested, and at -30 °C, the results of these two protecting groups were better than that of TMS. But the ee values didn't response to temperature decrease so that at -60 °C, TBS and TES showed lower ee than TMS (Table 2.10).

Table 2.10. Effects of Different Silyl Protecting Groups on the Model Reaction.
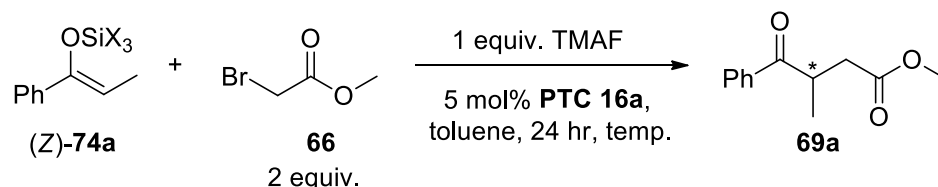
Entry[a]	Silyl compounds	Temp. (°C)	Conv. (%)[b]	Ee (%)[c]
1	OTBS (Ph)	-30	100	50
2	OTES (Ph)	-30	100	49
3	OTBS (Ph)	-80	50	50
4	OTES (Ph)	-80	50	50

[a] Reactions were carried out on a 0.02 mmol scale with 5 mol% PTC in 1.5 mL sealed vials with 300 μL solvents. [b] Conversion was based on **68a** determined by TLC. [c] Determined by HPLC analysis.

Based on this preliminary result, systematic optimization was carried out. Most of the data obeyed the trends obtained from AgF system. When we tested α-bromo

t-butylacetate, the ee value was increased by 10%, but the reaction was quite slow at -60 $^{\circ}$C (Scheme 2.30).
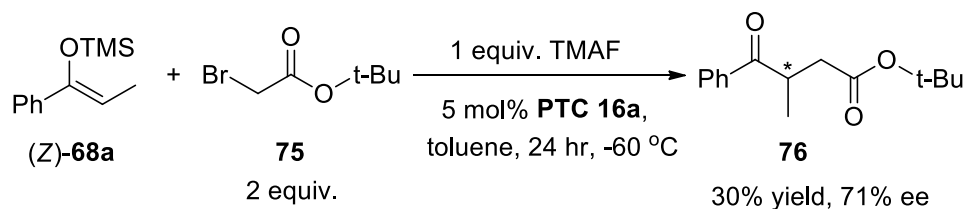
Scheme 2.30. Bis-Guanidium catalyzed Asymmetric Mukaiyama S$_N$2 Alkylation Reaction with α-Bromo *t*-Butylacetate.

Further tuning on catalyst showed that **PTC 16o** showed higher ee than original **PTC 16a** on model reaction (TMAF system). But the reaction rate was so slow that in 24 hours, only 20% to 30% **68a** was consumed due to the higher activation energy of PTC$^+$F$^-$ induced by electron withdrawing substituents. So we decided to add some electron donating substituents on R groups to balance the charge distribution so that **PTC 16u** was synthesized and showed higher ee and yield than **PTC 16o** (Scheme 2.31).
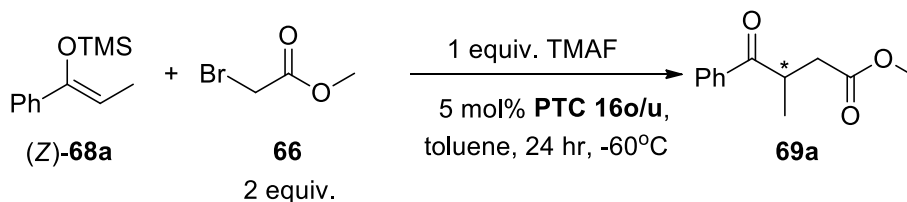
PTC 16o   **PTC 16u**
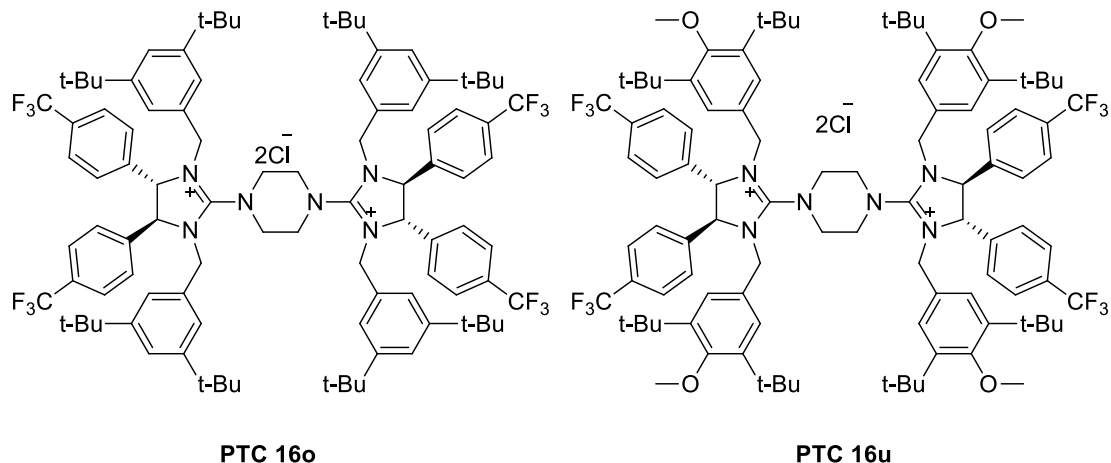
Scheme 2.31. Improvement on Ee Values by Tuning the Catalysts.

Since the reaction rate for **PTC 16u** was still quite low, it need to be further optimized before it was applied to α-Bromo *t*-Butylacetate.

Another direction of optimization was to decrease the loading of TMAF to catalytic amount, which meaned that TMAF should be able to regenerate between the interface of organic layer and solid and another stoichiometric fluoride salt would be needed (Figure 2.3). So the two catalysts form a relay in the system. This part of optimization was not totally finished, but preliminary result was obtained.
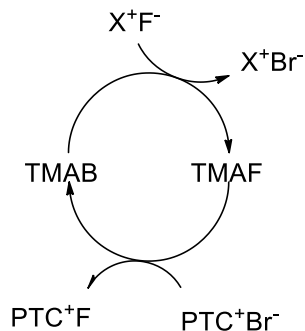
Figure 2.3. Proposed two catalysts relay system.

Under the standard condition, this relay couldn't happen or was extremely slow, so two ideas were raised up to accelerate the anion exchange. One is to use mixed solvents, 90% non-polar solvent with 10% polar solvent, to increase the solubility of stoichiometric amount of inorganic fluoride salts, such as CsF and AgF so that accelerated the anion exchange between tetramethyl ammonium bromide (TMAB) and these inorganic salts. Background reaction could be minimized by lowering the temperature. The other idea was to use stoichiometric amount of ligand to coordinate with AgF and weaken the ionic bond between silver cation and fluoride anion so that the exchange between TMAB and AgF could be easier. Results of these attempts were presented in Table 2.11 and Table 2.12. From the data we could see that both of the idea was possible, but generally low yield was still a problem. Further investigation was needed in this area.

Table 2.11. Effect of Mixed Solvents on the Model Reaction.
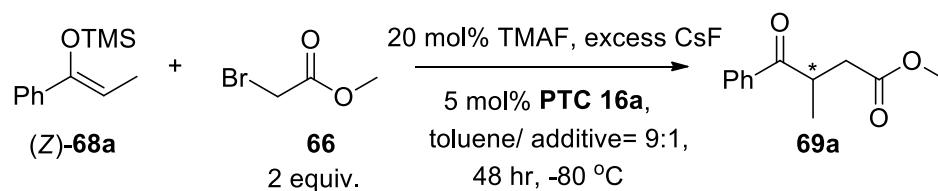
Entry[a]	Additives	Conv. (%)[b]	Ee (%)[c]
1	THF	20	64
2	DCM	30	65
3	MeOH	n.r.	--
4	None	n.r.	--

[a] Reactions were carried out on a 0.02 mmol scale with 5 mol% PTC in 1.5 mL sealed vials with 300 μL solvents (9:1). [b] Conversion was based on **68a** determined by TLC. [c] Determined by HPLC analysis.

Table 2.12. Effects of AgF with Different Ligands on the Model Reaction.
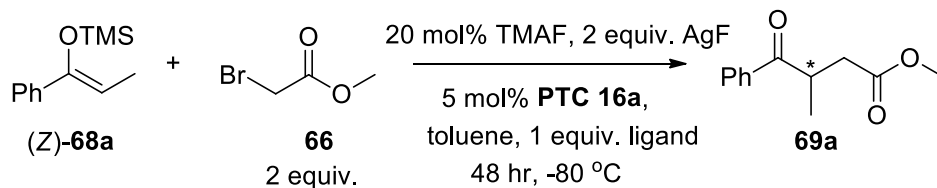
Entry[a]	Ligand	Conv. (%)[b]	Ee (%)[c]
1	PPh_3	30	20
2	—N⌢N—	30	48
3	NEt_3	30	66
4	—NH ... HN—	n.r.	--
5	Pyridine	n.r.	--
6	DMAP	n.r.	--
7	None	n.r.	--

[a] Reactions were carried out on a 0.02 mmol scale with 5 mol% PTC in 1.5 mL sealed vials with 300 μL solvents. [b] Conversion was based on **68a** determined by TLC. [c] Determined by HPLC analysis.

Table 2.13. Full List of Catalysts Used in Chapter 2.

Entry	Structure	Entry	Structure
Code：**PTC 1** MW.[a]: 550.14		Code：**PTC 2** MW.[a]:926.75	

Code：**PTC 3**
MW.^{a}: 1078.95
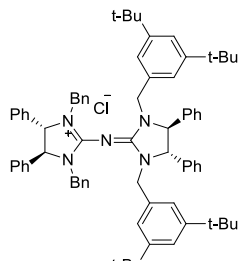
Code：**PTC 4**
MW.^{a}: 1303.37
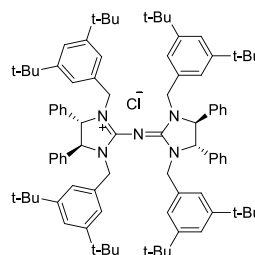
Code：**PTC 5**
MW.^{a}: 954.81
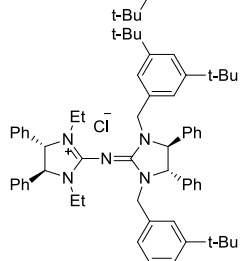
Code：**PTC 6**
MW.^{a}: 1151.18
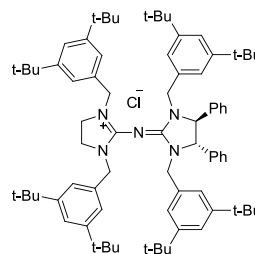
Code：**PTC 7**
MW.^{a}: 774.56
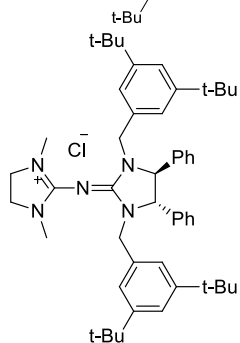
Code：**PTC 8**
MW.^{a}: 610.19
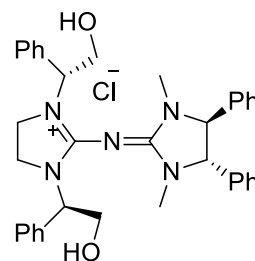
Code：**PTC 9**
MW.^{a}: 1398.50
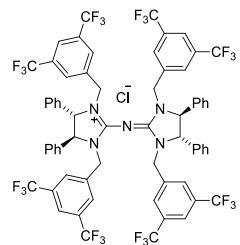
Code：**PTC 10**
MW.^{a}: 732.52
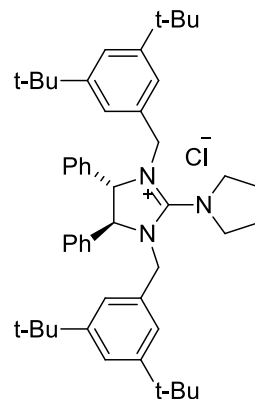
Code：**PTC 11**
MW.^{a}: 351.27
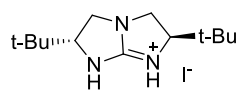
Code：**PTC 12**
MW.^{a}: 795.58
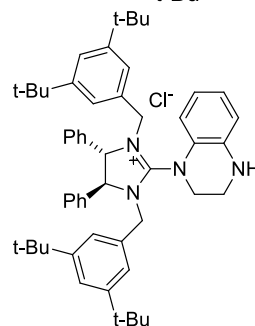
Code：**PTC 13**
MW.[a]: 533.42
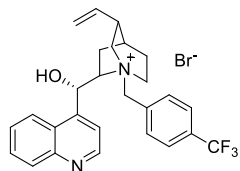
Code：**PTC 14**
MW.[a]: 605.61
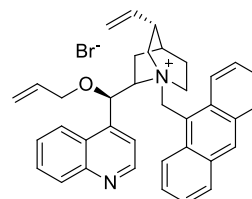
Code：**PTC 15**
MW.[a]: 521.09
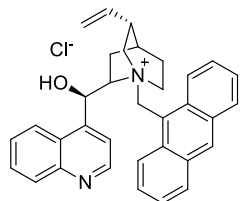
Code：**PTC 16a**
MW.[a]: 1408.94
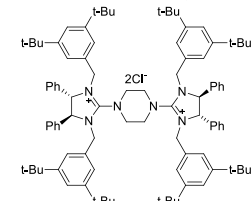
Code：**PTC 16b**
MW.[a]: 655.70
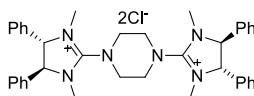
Code：**PTC 16c**
MW.[a]: 1160.32
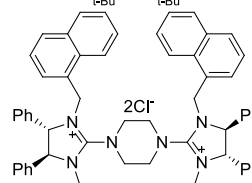
Code：**PTC 16d**
MW.[a]: 962.10
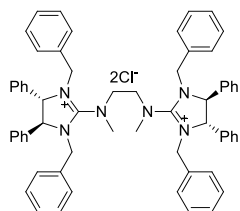
Code：**PTC 16e**
MW.[a]:1160.32
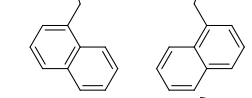
Code：**PTC 16f**
MW.[a]: 1724.52
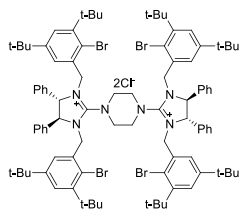
Code：**PTC 16g**
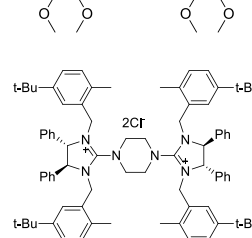MW.[a]: 1320.40
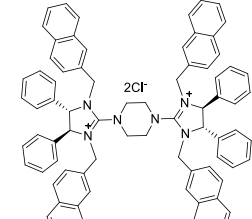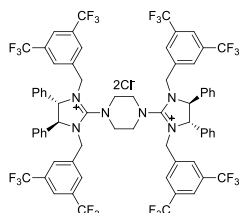
Code：**PTC 16h**
MW.[a]: 1184.51
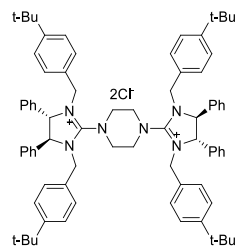
Code：**PTC 16i**
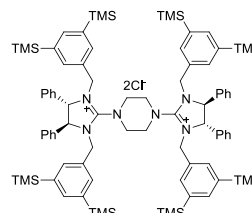MW.[a]: 1240.62
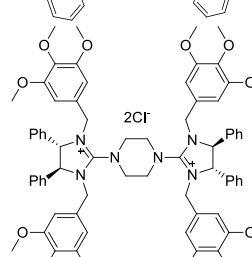
Code：**PTC 16j**
MW.[a]: 1529.04
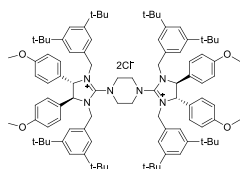
Code：**PTC 16k**
MW.[a]: 1436.99
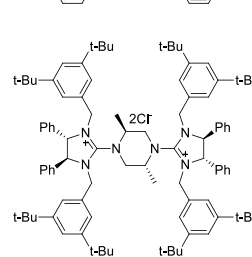
Code：**PTC 16l** MW. ^{a}: 1504.07		Code：**PTC 16m** MW. ^{a}: 1537.54	
Code：**PTC 16n** MW. ^{a}: 1546.72		Code：**PTC 16o** MW. ^{a}: 1680.93	
Code：**PTC 16p** MW. ^{a}: 1609.17		Code：**PTC 16q** MW. ^{a}: 1588.93	
Code：**PTC 16r** MW. ^{a}: 1633.36		Code：**PTC 16s** MW. ^{a}: 1465.04	
Code：**PTC 16t** MW. ^{a}: 1432.96		Code：**PTC 16u** MW. ^{a}: 1801.03	
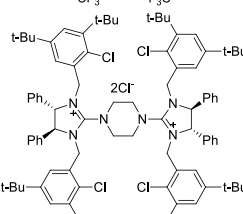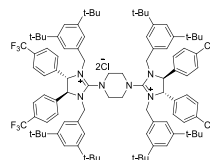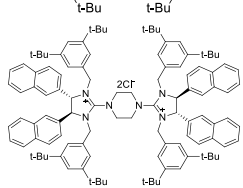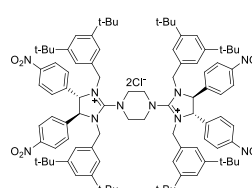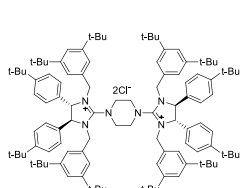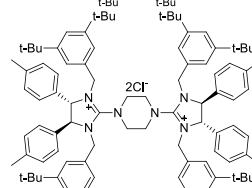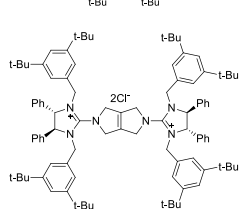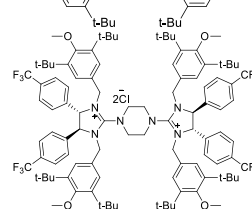
^{a} The molecular weights presented in the table were calculated by BioChemDraw Ultra 12.0.

2.3.3 Conclusion

Asymmetric fluoride anion mediated phase-transfer catalysis was first used to synthesize 1,4-dicarbonyl compounds via Mukaiyama S$_N$2 alkylation reactions. With our original chiral bis-guanidium catalysts, up to 86% ee and 70% yield were achieved. Meanwhile, fundamental problems about fluoride salts and phase-transfer catalysis were studied and discussed in the contents. Two catalytic systems were studied and further optimization is possible and necessary.

References

1   T. Ooi, K. Maruoka, *Acc.Chem.Res.***2004**, *37*, 526-533.

2   S. Colonna, H. Hiemstra, H. Wynberg, *J. Chem. Soc., Chem. Commun.* **1978**, 238-239.

3   T. Ooi, K. Doda, K. Maruoka, *Org. lett.***2001**, *3*, 1273-1276.

4   T. Ooi, H. Sugimoto, K. Doda, K. Maruoka, *Tetrahedron Lett.* **2001**, *42*, 9245-9248.

5   A. Ando, T. Miura, T. Tatematsu, T. Shioiri, *Tetrahedron Lett.* **1993**, *34*, 1507-1510.

6   G. Bluet, J. M. Campagne, *J.Org.Chem.***2001**, *66*, 4293-4298.

7   K. Iseki, T. Nagai, Y. Kobayashi, *Tetrahedron Lett.* **1994**, *35*, 3137-3138.

8   M. D. Drew, N. J. Lawrence, W. Watson, S. A. Bowles, *Tetrahedron Lett.* **1997**, *38*, 5857-5860.

9   M. Horikawa, J. Busch-Petersen, E. J. Corey, *Tetrahedron Lett.* **1999**, *40*, 3843-3846.

10   T. Ooi, K. Doda, K. Maruoka, *J. Am. Chem. Soc.* **2003**, *125*, 2054-2055.

11   T. Ooi, K. Doda, K. Maruoka, *J. Am. Chem. Soc.* **2003**, *125*, 9022-9023.

12   U. Hintermair, G. Francio, W. Leitner, *Chem. Eur. J.* **2013**, *19*, 4538-4547.

13   M. Raynal, F. Portier, P. W. van Leeuwen, L. Bouteiller, *J. Am. Chem. Soc.* **2013**, *135*, 17687-17690.

14   H. Stetter, M. Schreckenberg, *Angew. Chem. Int. Ed.***1973**, *12*, 81.

15   D. Enders, K. Breuer, J. Runsink, J. H. Teles, *Helv. Chem. Acta* **1996**, *79*, 1899-1902.

16   D. Enders, T. Balensiefer, *Acc. Chem. Res.* **2004**, *37*, 534-541.

17   D. Enders, J. Han, A. Henseler, *Chem. Commun.***2008**, 3989-3991.

18   Q. Liu, S. Perreault, T. Rovis, *J. Am. Chem. Soc.* **2008**, *130*, 14066-14067.

19   T. Jousseaume, N. E. Wurz, F. Glorius, *Angew. Chem. Int. Ed.***2011**, *50*, 1410-1414.

20   E. Sanchez-Larios, K. Thai, F. Bilodeau, M. Gravel, *Org. lett.* **2011**, *13*, 4942-4945.

21   X. Fang, X. Chen, H. Lv, Y. R. Chi, *Angew. Chem. Int. Ed.***2011**, *50*, 11782-11785.

22   M. R. Nahm, J. R. Potnick, P. S. White, J. S. Johnson, *J. Am. Chem. Soc.* **2006**, *128*, 2751-2756.

23   H. Y. Jang, J. B. Hong, D. W. MacMillan, *J. Am. Chem. Soc.* **2007**, *129*, 7004-7005.

24   D. A. Nicewicz, D. W. MacMillan, *Science* **2008**, *322*, 77-80.

25   K. Zheng, X. Liu, J. Zhao, Y. Yang, L. Lin, X. Feng, *Chem. Commun.***2010**, *46*, 3771-3773.

26   Z. Jiang, Y. Yang, Y. Pan, Y. Zhao, H. Liu, C. H. Tan, *Chem. Eur. J.***2009**, *15*, 4925-4930.

Chapter 3

The Experimental Procedures

3.1 General Information

^{1}H and ^{13}C NMR spectra were recorded on a Bruker ACF300 (300MHz), Bruker DPX300 (300MHz), 500 MHz Bruker DRX NMR spectrometer or AMX500 (500MHz) spectrometer. Chemical shifts are reported in parts per million (ppm). The residual solvent peak was used as an internal reference. Enantiomeric excess values were determined by chiral HPLC analysis on SHIMADZU HPLC units, including a DGU-20A$_5$ Prominence Degasser, LC-20A7 Prominence Liquid Chromatograph and SPD-M20A Prominence Diode Array Detector. Flash chromatography separations were performed on Merck 60 (0.040 - 0.063 mm) mesh silica gel. Toluene was distilled from sodium/benzophenone and stored under N_2 atmosphere. MeCN was dried by CaH_2. Dichloromethane was distilled from CaH_2. Other reagents and solvents were commercial grade and were used as supplied without further purification, unless otherwise stated. Experiments involving moisture and/or air sensitive components were performed under a positive pressure of nitrogen in oven-dried glassware equipped with a rubber septum inlet. Reactions requiring temperatures 0 ^{o}C, -20 ^{o}C, -30 ^{o}C, -40 ^{o}C, -60 ^{o}C and -80 ^{o}C were stirred in Zhengzhou Great Wall DHJF-8002 Low-Temperature Stirring Reaction Bath. Isopropanol was used as the bath medium. All experiments were monitored by analytical thin layer chromatography (TLC). Instrumentations Proton nuclear magnetic resonance (^{1}H NMR), carbon NMR (^{13}C NMR) were recorded in CDCl$_3$ otherwise stated. ^{1}H (500.1331 MHz), ^{13}C (125.7710 MHz) with complete proton decoupling, All compounds synthesized were stored in a -78 ^{o}C freezer. All silyl protected compounds were synthesized according to published procedures. Chiral diamines were purchased from Chengdu Likai Inc. and

Diaminopharm Inc.. Synthetic procedures for commercial unavailable chiral diamines were based on (*J. Am. Chem. Soc. 130*, 12184). All other purchased chemicals and reagents were of analytical grade, obtained from Sigma Aldrich, TCI or Alfa Acesar and used without further purification unless specified.
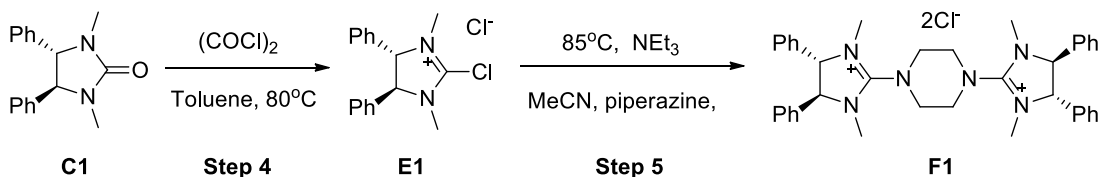
3.2 Syntheses and Characterizations of Chiral Bis-Guanidium Salts

Representative procedure for the synthesis of chiral bis-guanidium salts:

When R is not Me:
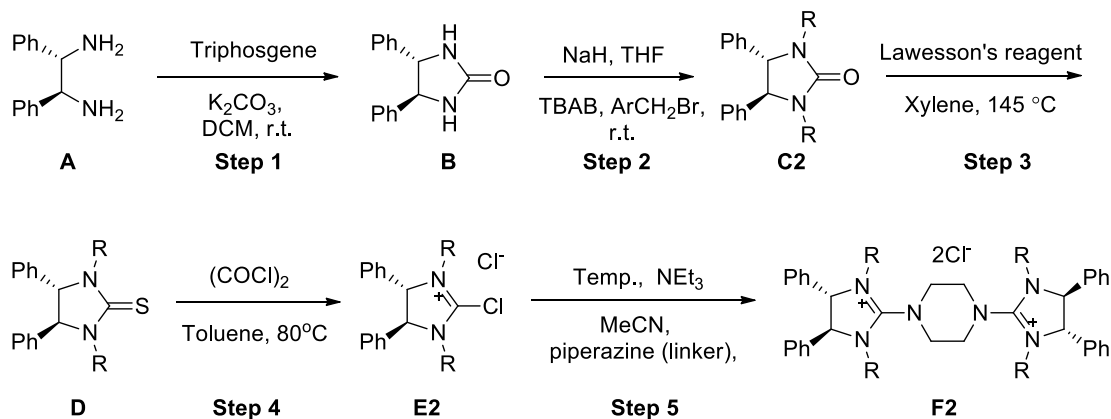
When R is Me:

Step 1: To a vigorously stirred solution of chiral diamine **A** (1.06 g, 5 mmol), K_2CO_3 (2.07 g, 15 mmol, 3 equiv.) in DCM (15 mL), was added the DCM (5 mL) solution of triphosgen (488 mg, 1.67 mmol) dropwise, stir at rt for 6 hours (monitored by TLC). After diamine **A** was completely consumed, reaction was quenched by water (20 mL)

and extracted using DCM 3 times (30 mL x 3). The combined organic layer was washed by brine and dried by Na_2SO_4. Solvent was removed under reduced pressure and **B** was obtained as white to pale yellow needle type solid without further purification.

Step 2: To a suspension of NaH (360 mg, 15 mmol, 3.0 equiv) in THF (10 mL) was added a solution of **B** (from step 1) in THF (10 mL). After 30 minutes, RBr or MeI (2.3 mL, 37 mmol, 3.7 equiv.) was added in one portion. After completion of the reaction (monitored by TLC), the mixture was filtered through a short pad of Celite and the solution was collected and removed under reduced pressure and **C** was obtained by flash chromatography (silica gel, hexane/EA= 15:1), as a white solid, (2 steps, 80 to 90% overall yield).

Step 3: To a solution of **C2** (1mmol, 1 equiv.) in 15 mL xylenes was added lawesson reagent (809 mg, 2 mmol, 2 equiv.) under nitrogen atmosphere. Then the whole solution was heated to 140 $^{\circ}$C for 48 hours and cool to room temperature. Upon the completion of the **C2** on TLC, the whole solution was directly loaded on a column, use gravity to drain all the xylenes and use Hexane/EA= 50:1 to flush out the **D** as pale yellow solid. Further recrystalization in Hexane provided **D** as white solid with 60 to 80% yield.

Step 4: A 100 mL round bottom flask was charged with a solution of **D** or **C1**(1.2 mmol, 1 equiv.) in toluene (10 mL) with a condenser under N_2 atmosphere. $(COCl)_2$ (3.1 mL, 36mmol, 30 equiv.) was added in one portion. The mixture was heated at 80 $^{\circ}$C overnight until **D** or **C1** was mostly reacted. Toluene was removed under reduced pressure and dried under vacuum line. Solid **E1** or **E2** was obtained for the next step

without any further purification.

Step 5: The above solid **E1** or **E2** was dissolved in dry MeCN (10 mL) under nitrogen atmosphere, and then the linker, such aspiperazine (34 mg, 0.4mmol, 0.3 equiv.), was added, followed by the addition of Et$_3$N (0.42 mL, 3 mmol, 2.5 equiv.).

Different substituted bis-guanidiums need different reaction temperature here:

(1) For **PTC 26a** to **PTC 26n** in Chapter 1, the whole solution was heated to reflux for 12hours and cool to room temperature.

(2) For sterically hindered bis-guanidiums, which includes **PTC 26o** to **PTC 26r**, the reaction was set up in a 100 mL sealed tube and heated at 110 $^{\circ}$C for 12 hours and then turned off the heating and left it inside the oil bath for cooling.

(3) For strong electron withdrawing groups substituted bis-guanidiums, the solution was heated at 50 $^{\circ}$C for 8 hours and cool to room temperature.

After cooling to room temperature, MeCN was removed under reduced pressure and 50 mL water was added. The mixture was extracted by DCM times (15 mL x 3). The combined organic layer was dried by Na$_2$SO$_4$. Solvent was removed under reduced pressure and PTC was obtained by flash chromatography (silica gel, DCM/Methanol= 100:1-20:1), as a white solid.
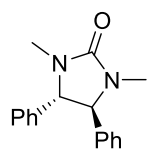
(*S*,*S*)-1,3-Dimethyl-4,5-diphenylimidazolidin-2-one: white solid; 80% yield for 2 steps; ^{1}H NMR (300 MHz, CDCl$_3$): δ 7.34-7.32 (m, 6H), 7.14-7.11 (m, 4H), 4.07 (s, 2H), 2.69 (s, 6H); ^{13}C NMR (126 MHz, CDCl$_3$) δ 161.7, 137.9, 128.7, 128.3, 127.2, 70.2, 29.9.
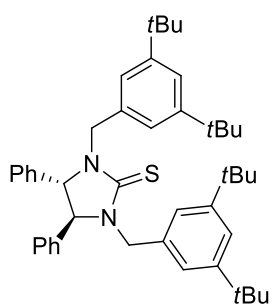
(4*S*,5*S*)-1,3-bis(3,5-di-tert-butylbenzyl)-4,5-diphenylimidaz olidine-2-thione: white solid, 89% yield; ^{1}H NMR (500 MHz, CDCl$_3$) δ 7.28 (tdd, *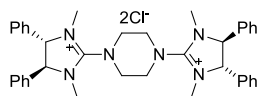J* = 10.0, 7.4, 2.4 Hz, 4H), 7.02 (d, *J* = 1.5 Hz, 2H), 7.00 − 6.94 (m, 2H), 5.89 (d, *J* = 14.6 Hz, 1H), 4.25 (s, 1H), 3.75 (d, *J* = 14.6 Hz, 1H), 1.28 (s, 19H); ^{13}C NMR (126 MHz, CDCl$_3$) δ 182.1, 151.0, 139.2, 135.1, 129.0, 128.5, 127.0, 122.9, 121.4, 77.2, 77.0, 76.8, 68.7, 49.7, 34.7, 31.4.

(4*S*,4'*S*,5*S*,5'*S*)-2,2'-(piperazine-1,4-diyl)bis(1,3-dimethyl-4,5-diphenyl-4,5-dihy dro-1*H*-imidazol-3-ium) chloride (PTC 26a): white solid, 70% yield; ^{1}H NMR (500 MHz, CDCl$_3$) δ 7.41 (q, *J* = 5.2 Hz, 12H), 7.32 − 7.18 (m, 8H), 4.65 (d, *J* = 9.4 Hz, 4H), 4.53 (s, 4H), 4.15 (d, *J* = 9.4 Hz, 4H), 3.25 (s, 12H).
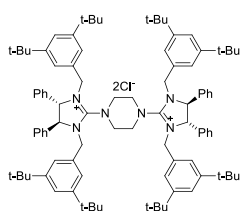
(4*S*,4'*S*,5*S*,5'*S*)-2,2'-(piperazine-1,4-diyl)bis(1,3-bis(3,5-di-tert- butylbenzyl)-4,5-diphenyl-4,5-dihydro-1*H*-imidazol-3-ium) chloride (PTC 26b): white s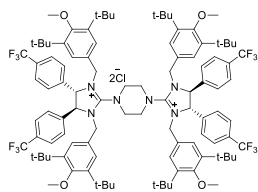olid, 40% yield; ^{1}H NMR (500 MHz, CDCl$_3$) δ 7.35 − 7.27 (m, 12H), 7.21 (s, 4H), 7.09 − 6.99 (m, 8H), 6.96 (d, *J* = 1.2 Hz, 8H), 5.20 (d, *J* = 14.6 Hz, 4H), 4.79 (d, *J* = 14.6 Hz, 4H), 4.70 (d, *J* = 9.3 Hz, 4H), 4.48 (d, *J* = 9.5 Hz, 4H), 4.31 (s, 4H), 1.14 (s, 72H).^{13}C NMR (126 MHz, CDCl$_3$) δ 162.71, 151.37, 137.78, 131.97, 129.61, 129.19, 126.56, 123.48, 122.33, 70.35, 54.48, 49.07, 34.73, 31.32.
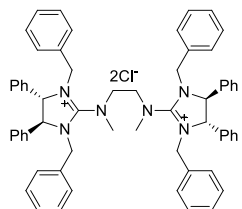
(4*S*,4'*S*,5*S*,5'*S*)-2,2'-(piperazine-1,4-diyl)bis(1,3-bis(3,5-di-ter t-butyl-4-methoxybenzyl)-4,5-bis(4-(trifluoromethyl)phenyl)-4,5-dihydro-1*H*-imidazol-3-ium) chloride (PTC 26c): white solid, 33% yield; ^{1}H NMR (500 MHz, CDCl$_3$) δ 7.56 (d, *J* = 8.0 Hz, 8H), 7.23 (d, *J* = 8.0 Hz, 8H), 6.93 (s, 8H), 5.18 (d, *J* = 14.3 Hz, 4H), 4.98 (d, *J* = 9.0 Hz, 4H), 4.76 (d, *J* = 14.3 Hz, 4H), 4.56 (d, *J* = 9.5 Hz, 4H), 4.38 (s, 4H), 3.50 (s, 12H), 1.21 (s, 72H).^{13}C NMR (126 MHz, CDCl$_3$) δ 163.13, 159.93, 144.53, 141.34, 131.72, 127.66, 127.03, 126.64, 125.96, 124.59, 122.42, 69.94, 64.25, 54.90, 49.04, 35.63, 31.82.
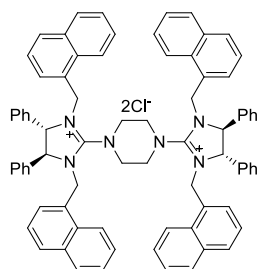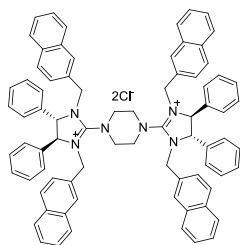

(4*S*,4'*S*,5*S*,5'*S*)-2,2'-(piperazine-1,4-diyl)bis(1,3-bis(naphthal en-1-ylmethyl)-4,5-diphenyl-4,5-dihydro-1*H*-imidazol-3-ium) chloride (PTC 26d): white solid, 41% yield; ^{1}H NMR (500 MHz, CDCl$_3$) δ 7.75 (d, *J* = 7.9 Hz, 4H), 7.66 (dd, *J* = 17.4, 7.6 Hz, 8H), 7.39 (dt, *J* = 14.4, 6.9 Hz, 8H), 7.28 (s, 8H), 7.14 (dt, *J* = 14.4, 7.1 Hz, 12H), 6.94 (d, *J* = 7.2 Hz, 8H), 5.42 (d, *J* = 16.0 Hz, 4H), 5.04 (d, *J* = 16.1 Hz, 4H), 4.41 (d, *J* = 33.6 Hz, 12H), 2.37 (s, 8H).

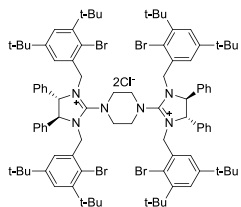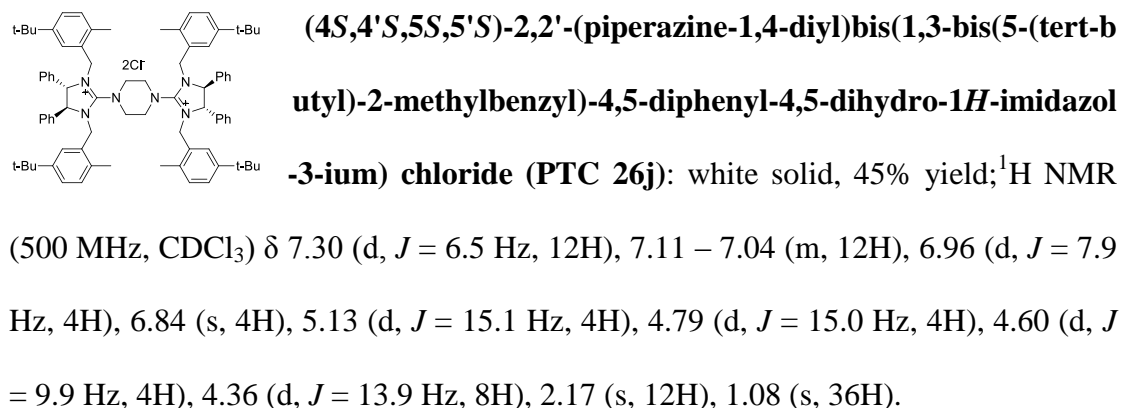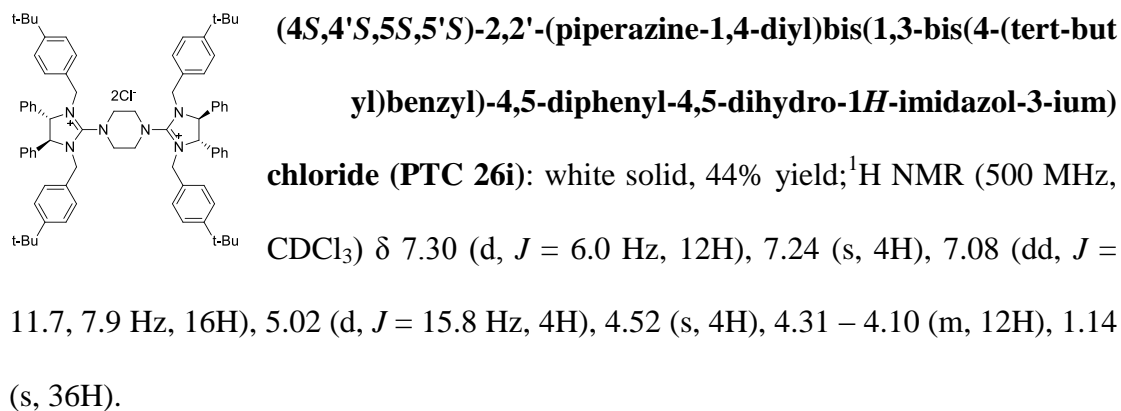**(4S,4'S,5S,5'S)-2,2'-(ethane-1,2-diylbis(methylazanediyl))bis(1,3-dibenzyl-4,5-diphenyl-4,5-dihydro-1H-imidazol-3-ium) chloride (PTC 26e)**: white solid, 45% yield; ¹H NMR (500 MHz, CDCl₃) δ 7.31 – 7.02 (m, 20H), 4.86 (d, *J* = 15.9 Hz, 2H), 4.61 (s, 2H), 4.46 – 4.39 (m, 3H), 3.33 (s, 4H).
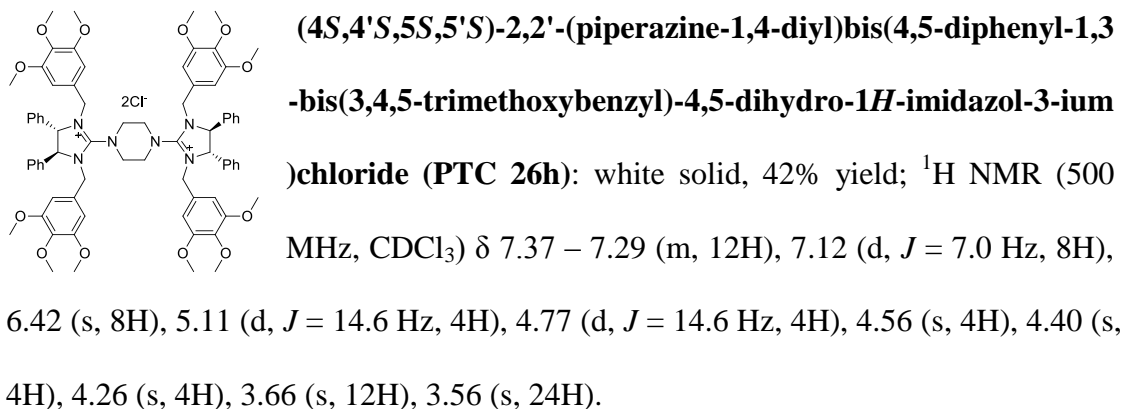
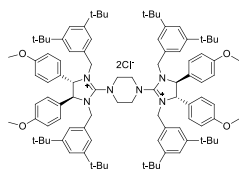**(4S,4'S,5S,5'S)-2,2'-(piperazine-1,4-diyl)bis(1,3-bis(naphthalen-2-ylmethyl)-4,5-diphenyl-4,5-dihydro-1H-imidazol-3-ium) chloride (PTC 26f)**: white solid, 28% yield; ¹H NMR (500 MHz, CDCl₃) δ 7.70 – 7.56 (m, 16H), 7.40 – 7.26 (m, 24H), 7.18 – 7.08 (m, 8H), 5.21 (d, *J* = 15.8 Hz, 4H), 4.68 (d, *J* = 15.8 Hz, 4H), 4.59 (s, 4H), 4.38 (d, *J* = 9.6 Hz, 4H), 4.28 (d, *J* = 9.4 Hz, 4H).

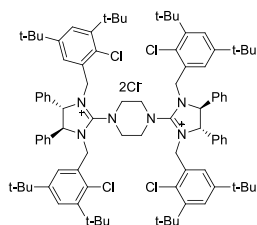**(4S,4'S,5S,5'S)-2,2'-(piperazine-1,4-diyl)bis(1,3-bis(2-bromo-3,5-di-tert-butylbenzyl)-4,5-diphenyl-4,5-dihydro-1H-imidazol-3-ium)chloride (PTC 26g)**: white solid, 32% yield; ¹H NMR (500 MHz, CDCl₃) δ 7.35 (d, *J* = 2.0 Hz, 4H), 7.32 – 7.27 (m, 12H), 7.05 – 6.98 (m, 8H), 6.49 (d, *J* = 2.2 Hz, 4H), 5.29 (d, *J* = 13.5 Hz, 4H), 4.84 (d, *J* = 13.5 Hz, 4H), 4.77 (s, 8H), 3.85 (s, 4H), 1.43 (s, 36H), 0.99 (s, 36H).

(4*S*,4'*S*,5*S*,5'*S*)-2,2'-(piperazine-1,4-diyl)bis(4,5-diphenyl-1,3-bis(3,4,5-trimethoxybenzyl)-4,5-dihydro-1*H*-imidazol-3-ium)chloride (PTC 26h): white solid, 42% yield; ^{1}H NMR (500 MHz, CDCl$_3$) δ 7.37 − 7.29 (m, 12H), 7.12 (d, *J* = 7.0 Hz, 8H), 6.42 (s, 8H), 5.11 (d, *J* = 14.6 Hz, 4H), 4.77 (d, *J* = 14.6 Hz, 4H), 4.56 (s, 4H), 4.40 (s, 4H), 4.26 (s, 4H), 3.66 (s, 12H), 3.56 (s, 24H).

(4*S*,4'*S*,5*S*,5'*S*)-2,2'-(piperazine-1,4-diyl)bis(1,3-bis(4-(tert-butyl)benzyl)-4,5-diphenyl-4,5-dihydro-1*H*-imidazol-3-ium)chloride (PTC 26i): white solid, 44% yield; ^{1}H NMR (500 MHz, CDCl$_3$) δ 7.30 (d, *J* = 6.0 Hz, 12H), 7.24 (s, 4H), 7.08 (dd, *J* = 11.7, 7.9 Hz, 16H), 5.02 (d, *J* = 15.8 Hz, 4H), 4.52 (s, 4H), 4.31 − 4.10 (m, 12H), 1.14 (s, 36H).

(4*S*,4'*S*,5*S*,5'*S*)-2,2'-(piperazine-1,4-diyl)bis(1,3-bis(5-(tert-butyl)-2-methylbenzyl)-4,5-diphenyl-4,5-dihydro-1*H*-imidazol-3-ium) chloride (PTC 26j): white solid, 45% yield; ^{1}H NMR (500 MHz, CDCl$_3$) δ 7.30 (d, *J* = 6.5 Hz, 12H), 7.11 − 7.04 (m, 12H), 6.96 (d, *J* = 7.9 Hz, 4H), 6.84 (s, 4H), 5.13 (d, *J* = 15.1 Hz, 4H), 4.79 (d, *J* = 15.0 Hz, 4H), 4.60 (d, *J* = 9.9 Hz, 4H), 4.36 (d, *J* = 13.9 Hz, 8H), 2.17 (s, 12H), 1.08 (s, 36H).
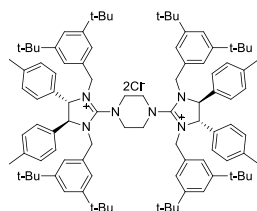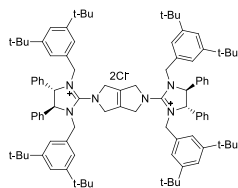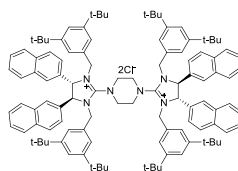
(4*S*,4'*S*,5*S*,5'*S*)-2,2'-(piperazine-1,4-diyl)bis(1,3-bis(3,5-di-tert-butylbenzyl)-4,5-bis(4-methoxyphenyl)-4,5-dihydro-1*H*-imidazol-3-ium) chloride (PTC 26k): white solid, 42% yield; ^{1}H NMR (500 MHz, CDCl$_3$) δ 7.23 (s, 2H), 7.02 – 6.95 (m, 8H), 6.81 (d, *J* = 8.6 Hz, 4H), 5.12 (d, *J* = 14.7 Hz, 2H), 4.73 (d, *J* = 14.9 Hz, 2H), 4.53 (s, 2H), 4.37 (d, *J* = 10.5 Hz, 2H), 4.31 (s, 2H), 3.76 (s, 6H), 1.17 (s, 36H).

(4*S*,4'*S*,5*S*,5'*S*)-2,2'-(piperazine-1,4-diyl)bis(1,3-bis(3,5-di-tert-butyl-2-chlorobenzyl)-4,5-diphenyl-4,5-dihydro-1*H*-imidazol-3-ium) chloride (PTC 26l): white solid, 31% yield; ^{1}H NMR (500 MHz, CDCl$_3$) δ 7.37 (d, *J* = 2.2 Hz, 4H), 7.32 – 7.28 (m, 12H), 7.01 – 6.93 (m, 8H), 6.56 (d, *J* = 2.1 Hz, 4H), 5.28 (d, *J* = 13.6 Hz, 4H), 4.71 (d, *J* = 16.8 Hz, 12H), 3.89 (s, 4H), 1.42 (s, 36H), 1.04 (s, 36H).

(4*S*,4'*S*,5*S*,5'*S*)-2,2'-(piperazine-1,4-diyl)bis(1,3-bis(3,5-di-tert-butylbenzyl)-4,5-di-p-tolyl-4,5-dihydro-1*H*-imidazol-3-ium) chloride (PTC 26m): white solid, 29% yield; ^{1}H NMR (500 MHz, CDCl$_3$) δ 7.19 (s, 4H), 7.08 (d, *J* = 7.6 Hz, 8H), 6.92 (d, *J* = 10.1 Hz, 16H), 5.11 (d, *J* = 14.7 Hz, 4H), 4.78 (d, *J* = 14.8 Hz, 4H), 4.62 (d, *J* = 8.5 Hz, 4H), 4.39 (d, *J* = 9.4 Hz, 4H), 4.27 (s, 4H), 2.27 (s, 12H), 1.13 (s, 72H).
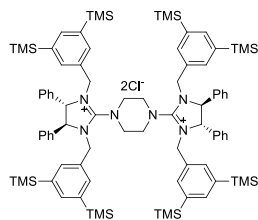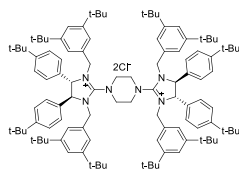
(4*S*,4'*S*,5*S*,5'*S*)-2,2'-(pyrrolo[3,4-c]pyrrole-2,5(1*H*,3*H*,4*H*,6*H*)-diyl)bis(1,3-bis(3,5-di-tert-butylbenzyl)-4,5-diphenyl-4,5-dihydro-1*H*-imidazol-3-ium) chloride (PTC 26n): white solid, 45% yield;^{1}H NMR (500 MHz, CDCl₃) δ 7.30 (dd, *J* = 5.0, 1.6 Hz, 12H), 7.24 (s, 4H), 7.01 (dd, *J* = 6.8, 2.2 Hz, 8H), 6.87 (d, *J* = 1.4 Hz, 8H), 5.41 (d, *J* = 10.3 Hz, 4H), 5.08 (dd, *J* = 27.3, 12.4 Hz, 8H), 4.67 (d, *J* = 14.5 Hz, 4H), 4.24 (s, 4H), 1.12 (d, *J* = 5.8 Hz, 72H).

(4*S*,4'*S*,5*S*,5'*S*)-2,2'-(piperazine-1,4-diyl)bis(1,3-bis(3,5-di-tert-butylbenzyl)-4,5-di(naphthalen-2-yl)-4,5-dihydro-1*H*-imidazol-3-ium) chloride (PTC 26o): white solid, 18% yield; ^{1}H NMR (500 MHz, CDCl₃) δ 7.87 (d, *J* = 8.5 Hz, 4H), 7.80 (d, *J* = 7.5 Hz, 4H), 7.76 (d, *J* = 7.5 Hz, 4H), 7.52 – 7.42 (m, 12H), 7.36 (d, *J* = 8.5 Hz, 4H), 7.16 (s, 4H), 6.99 (d, *J* = 1.1 Hz, 8H), 5.28 (d, *J* = 15.2 Hz, 4H), 4.93 (d, *J* = 14.8 Hz, 4H), 4.84 (d, *J* = 8.7 Hz, 4H), 4.65 (s, 4H), 4.59 (d, *J* = 9.5 Hz, 4H), 1.06 (s, 72H).

(4*S*,4'*S*,5*S*,5'*S*)-2,2'-(piperazine-1,4-diyl)bis(1,3-bis(3,5-bis(trimethylsilyl)benzyl)-4,5-diphenyl-4,5-dihydro-1*H*-imidazol-3-ium) chloride (PTC 26p): pale yellow to white solid, 15% yield; ^{1}H NMR (500 MHz, CDCl₃) δ 7.44 (s, 4H), 7.29 (dd, *J* = 14.0, 12.5 Hz, 20H), 7.07 – 6.96 (m, 8H), 5.30 – 5.19 (m, 4H), 4.82 (dd, *J* = 26.7, 12.0 Hz, 8H), 4.49 (d, *J* = 9.5 Hz, 4H), 4.28 (s, 4H), 0.14 (s, 72H).^{13}C NMR (126 MHz, CDCl₃) δ 162.68,

156.39, 140.23, 138.23, 137.72, 134.69, 131.05, 129.69, 129.27, 126.42, 70.51, 54.43, 48.99, 29.59, -1.11.

(4*S*,4'*S*,5*S*,5'*S*)-2,2'-(piperazine-1,4-diyl)bis(4,5-bis(4-(tert-butyl)phenyl)-1,3-bis(3,5-di-tert-butylbenzyl)-4,5-dihydro-1*H*-imidazol-3-ium) chloride (PTC 26q): white solid, 9% yield; ^{1}H NMR (500 MHz, CDCl₃) δ 6.82-7.35 (m, 28H), 4.21-5.18 (m, 20H), 1.28 (s, 36H), 1.12 (s, 72H).
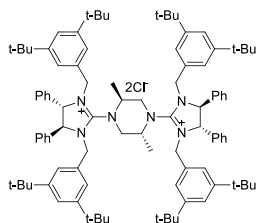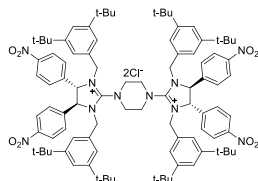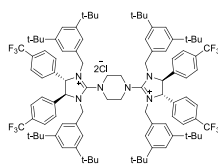

(4*S*,4'*S*,5*S*,5'*S*)-2,2'-((2*S*,5*R*)-2,5-dimethylpiperazine-1,4-diyl)bis(1,3-bis(3,5-di-tert-butylbenzyl)-4,5-diphenyl-4,5-dihydro-1*H*-imidazol-3-ium) chloride (PTC 26r): white solid, 14% yield; ^{1}H NMR (500 MHz, CDCl₃) δ 7.24-7.30(m, 20H), 6.94 (s, 2H), 6.85 (s, 4H), 4.31-5.13 (m, 18H),1.85 (d, *J* = 6.3 Hz, 3H), 1.62 (d, *J* = 6.2 Hz, 3H), 1.18 (d, *J* = 6.6 Hz, 72H).
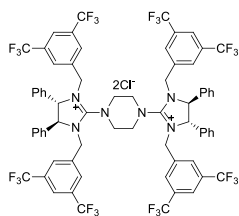
(4*S*,4'*S*,5*S*,5'*S*)-2,2'-(piperazine-1,4-diyl)bis(1,3-bis(3,5-bis(trifluoromethyl)benzyl)-4,5-diphenyl-4,5-dihydro-1*H*-imidazol-3-ium) chloride (PTC 26s): white solid, 7% yield; ^{1}H NMR (400

MHz, CDCl$_3$) δ 7.68 (s, 12H), 7.35 (d, *J* = 6.9 Hz, 12H), 7.15 – 7.08 (m, 8H), 5.58 (d,

J = 16.3 Hz, 4H), 5.22 (d, *J* = 16.4 Hz, 4H), 4.93 (d, *J* = 9.1 Hz, 4H), 4.45 (s, 4H),

4.12 (d, *J* = 8.8 Hz, 4H).

(4*S*,4'*S*,5*S*,5'*S*)-2,2'-(piperazine-1,4-diyl)bis(1,3-bis(3,5-di-ter t-butylbenzyl)-4,5-bis(4-nitrophenyl)-4,5-dihydro-1*H*-imidaz ol-3-ium) chloride (PTC 26t): yellow solid, 14% yield;[1]H

NMR (500 MHz, CDCl$_3$) δ 8.13 (dd, *J* = 8.2, 1.4 Hz, 4H), 8.07 (d, *J* = 7.2 Hz, 4H),

7.60 (dd, *J* = 19.2, 11.2 Hz, 8H), 7.24 (s, 4H), 6.90 (d, *J* = 1.3 Hz, 8H), 5.21 (d, *J* =

14.9 Hz, 4H), 4.74 (dd, *J* = 30.7, 15.7 Hz, 12H), 4.47 (d, *J* = 9.5 Hz, 4H), 1.14 (s,

72H).

(4*S*,4'*S*,5*S*,5'*S*)-2,2'-(piperazine-1,4-diyl)bis(1,3-bis(3,5-di-tert-b utylbenzyl)-4,5-bis(4-(trifluoromethyl)phenyl)-4,5-dihydro-1*H*-i midazol-3-ium) chloride (PTC 26u): white solid, 16% yield; [1]H

NMR (400 MHz, CDCl$_3$) δ 7.58 (d, *J* = 8.1 Hz, 8H), 7.24 (dd, *J* = 5.9, 3.9 Hz, 12H),

6.91 (d, *J* = 1.4 Hz, 8H), 5.21 (d, *J* = 14.5 Hz, 4H), 4.81 (dd, *J* = 21.8, 12.0 Hz, 8H),

4.51 (d, *J* = 9.5 Hz, 4H), 4.38 (s, 4H), 1.13 (s, 72H).
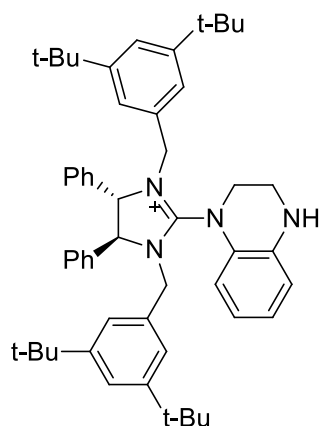
(4S,5S)-1,3-bis(3,5-di-tert-butylbenzyl)-2-(3,4-dihydroquinoxalin-1(2H)-yl)-4,5-diphenyl-4,5-dihydro-1H-imidazol-3-ium chloride (PTC 26v): white to pale yellow solid, 50% yield; ^{1}H NMR (500 MHz, CDCl$_3$) δ 6.66-7.48 (m, 20H), 3.84-5,17 (m, 10H), 1.27 (s, 18H), 1.19 (s, 18H).

## 3.3 Representative Procedure for Asymmetric Mukaiyama Type S$_N$2 Alkylation Reactions of Silyl Compounds and α-Bromoesters
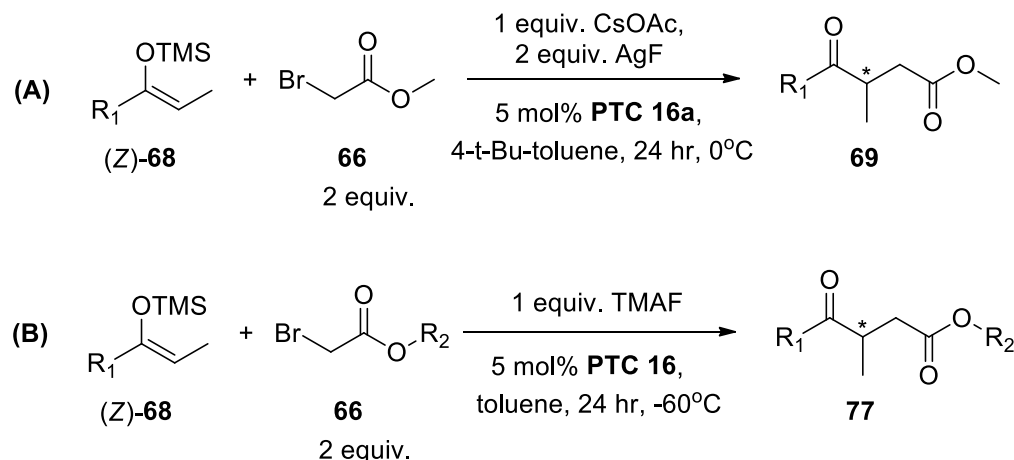

Method A: To a 1.5 mL vial added AgF (5 mg, 0.04 mmol), CsOAc (2.8 mg, 0.02 mmol) and PTC 16a (1.4 mg, 5 mol%). Then filled the vial with 0.15 mL 4-t-Bu-toluene and α-bromo methylacetate (4 μL, 0.04 mmol) and cool it to 0 oC, and stirred for 15 minutes. (Z)-68 (0.02 mmol) was added into the solution in one portion. The reaction mixture was stirred at 0 oC for another 24 hours and monitored by TLC.

All the processes above were carried out in dark. When the reaction finished, all the solution was add to silica flash column and flushed with EA/hexane= 50:1. The product was colorless oil, 68% yield.

Method B: To a 1.5 mL vial added TMAF (1.8 mg, 0.02 mmol) and **PTC 16a** (5 mol%). Then filled the vial with 0.3 mL toluene and α-bromo ester (0.04 mmol) and cool it to -60 °C, and stirred for 15 minutes. (*Z*)-**68** (0.02 mmol) was added into the solution in one portion. The reaction mixture was stirred at -60 °C until the reaction was finished and monitored by TLC. When the reaction finished, all the solution was add to silica flash column and flushed with EA/hexane= 50:1. The product was colorless oil, 30~ 80% yield.
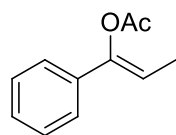
(*Z*)-1-phenylprop-1-en-1-yl acetate: pale yellow liquid, prepared according to published procedures;^{1}H NMR (500 MHz, CDCl$_3$) δ 7.43 − 7.23 (m, 5H), 5.90 (q, *J* = 7.0 Hz, 1H), 2.31 (s, 3H), 1.72 (d, *J* = 7.0 Hz, 3H). Z/E =8:2.
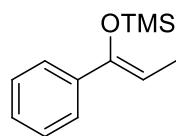
**(*Z*)-trimethyl((1-phenylprop-1-en-1-yl)oxy)silane**: colorless liquid, prepared according to published procedures;^{1}H NMR (500 MHz, CDCl$_3$) δ 7.49 (d, *J* = 7.4 Hz, 2H), 7.31 (t, *J* = 7.5 Hz, 2H), 7.25 (t, *J* = 7.2 Hz, 1H), 5.36 (q, *J* = 6.8 Hz, 1H), 1.77 (d, *J* = 6.9 Hz, 3H), 0.11 (s, 9H).^{13}C NMR (126 MHz, CDCl$_3$) δ 149.91, 139.24, 128.03, 127.30, 125.22, 105.33, 11.69, 0.59.
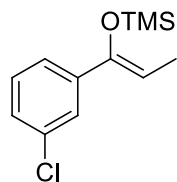
(Z)-((1-(3-chlorophenyl)prop-1-en-1-yl)oxy)trimethylsilane: colorless liquid, prepared according to published procedures;^{1}H NMR (500 MHz, CDCl$_3$) δ 7.45 (s, 1H), 7.34 (dt, *J* = 7.0, 1.7 Hz, 1H), 7.26 – 7.17 (m, 2H), 5.36 (q, *J* = 6.9 Hz, 1H), 1.74 (d, *J* = 6.9 Hz, 3H), 0.16 (s, 9H).
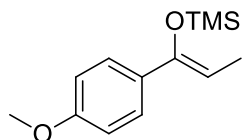
(Z)-((1-(4-methoxyphenyl)prop-1-en-1-yl)oxy)trimethylsilane: colorless liquid, prepared according to published procedures;^{1}H NMR (500 MHz, CDCl$_3$) δ 7.42 – 7.37 (m, 2H), 6.85 – 6.79 (m, 2H), 5.21 (q, *J* = 6.8 Hz, 1H), 3.81 (s, 3H), 1.72 (d, *J* = 6.8 Hz, 3H), 0.14 (s, 9H). Z/E =10:1.
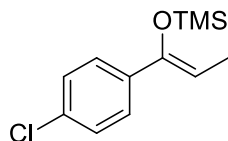
(Z)-((1-(4-chlorophenyl)prop-1-en-1-yl)oxy)trimethylsilane: colorless liquid, prepared according to published procedures;^{1}H NMR (500 MHz, CDCl$_3$) δ 7.38 (d, *J* = 8.5 Hz, 2H), 7.26 (d, *J* = 8.5 Hz, 2H), 5.32 (q, *J* = 6.8 Hz, 1H), 1.73 (d, *J* = 6.9 Hz, 3H), 0.14 (s, 9H).
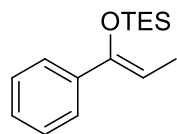
(Z)-triethyl((1-phenylprop-1-en-1-yl)oxy)silane: colorless liquid, prepared according to published procedures;^{1}H NMR (500 MHz, CDCl$_3$) δ 7.49 – 7.42 (m, 2H), 7.27 (dt, *J* = 20.8, 7.1 Hz, 3H), 5.22 (q, *J* = 6.8 Hz, 1H), 1.76 (d, *J* = 6.8 Hz, 3H), 0.94 (t, *J* = 7.9 Hz, 9H), 0.62 (q, *J* = 7.9 Hz, 6H).
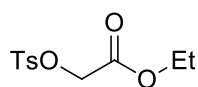
**Ethyl 2-(tosyloxy)acetate**: colorless liquid, prepared according to

106

published procedures; ^{1}H NMR (500 MHz, CDCl$_3$) δ 7.84 (d, J = 8.3 Hz, 2H), 7.36 (d, J = 8.0 Hz, 2H), 4.58 (s, 2H), 4.19 (q, J = 7.1 Hz, 2H), 2.45 (s, 3H), 1.24 (t, J = 7.1 Hz, 3H).
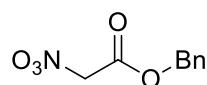
Benzyl 2-(nitrooxy)acetate: colorless liquid, prepared according to published procedures; ^{1}H NMR (500 MHz, CDCl$_3$) δ 7.50 – 7.28 (m, 5H), 5.25 (s, 2H), 4.93 (s, 2H).
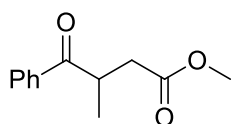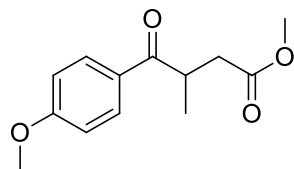
Methyl 3-methyl-4-oxo-4-phenylbutanoate: colorless liquid; ^{1}H NMR (500 MHz, CDCl$_3$) δ 8.01 – 7.93 (m, 2H), 7.55 (ddd, J = 8.5, 2.4, 1.2 Hz, 1H), 7.46 (dd, J = 10.6, 4.7 Hz, 2H), 3.63 (s, 3H), 2.95 (dd, J = 16.8, 8.4 Hz, 1H), 2.45 (dd, J = 16.8, 5.8 Hz, 1H), 1.22 (d, J = 7.2 Hz, 3H). ^{13}C NMR (126 MHz, CDCl$_3$) δ 202.70, 172.79, 135.88, 133.06, 128.68, 128.44, 51.68, 37.23, 17.85. HPLC analysis: DAICEL OD-H 0.46x 25 cm (Hexane/IPA = 95:5, 0.5 mL/min, 254 nm, 25 ℃), 16.0 min, 23.1 min.
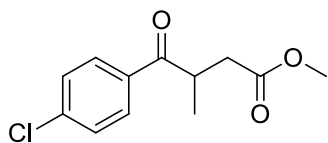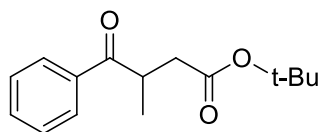
Methyl 4-(4-chlorophenyl)-3-methyl-4-oxobutanoate: colorless liquid; ^{1}H NMR (500 MHz, CDCl$_3$) δ 7.90 (d, J = 8.6 Hz, 2H), 7.42 (d, J = 8.6 Hz, 2H), 3.86 (ddd, J = 8.4, 7.1, 5.6 Hz, 1H), 3.61 (s, 3H), 2.93 (dd, J = 16.9, 8.6 Hz, 1H), 2.43 (dd, J = 16.9, 5.5 Hz, 1H), 1.18 (d, J = 7.2 Hz, 3H). HPLC analysis: DAICEL OD-H 0.46x 25 cm (Hexane/IPA = 95:5, 0.5 mL/min, 260 nm, 25 ℃), 14.4 min, 31.0 min.
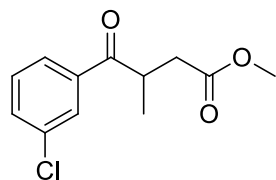
Methyl 4-(3-chlorophenyl)-3-methyl-4-oxobutanoate: colorless liquid; ^{1}H NMR (500 MHz, CDCl$_3$) δ 7.98 – 7.88 (m, 1H), 7.84 (d, J = 7.8 Hz, 1H), 7.59 – 7.47 (m, 1H), 7.40 (t, J = 7.9 Hz, 1H), 3.86 (ddd, J = 8.6, 7.2, 5.5 Hz, 1H), 3.62 (s, 3H), 2.95 (dd, J = 16.9, 8.7 Hz, 1H), 2.45 (dd, J = 16.9, 5.4 Hz, 1H), 1.19 (d, J = 7.2 Hz, 3H). HPLC analysis: DAICEL OD-H 0.46x 25 cm (Hexane/IPA = 95:5, 0.5 mL/min, 272 nm, 25 ℃), 13.1 min, 21.5 min.

Methyl 4-(4-methoxyphenyl)-3-methyl-4-oxobutanoate: colorless liquid; ^{1}H NMR (500 MHz, CDCl$_3$) δ 7.98 (d, J = 8.9 Hz, 2H), 6.95 (d, J = 8.9 Hz, 2H), 3.94 – 3.82 (m, 4H), 3.64 (s, 3H), 2.94 (dd, J = 16.7, 8.2 Hz, 1H), 2.44 (dd, J = 16.7, 5.9 Hz, 1H), 1.22 (d, J = 7.2 Hz, 3H). HPLC analysis: DAICEL AD-H 0.46x 25 cm (Hexane/IPA = 90:10, 1.0 mL/min, 290 nm, 25 ℃), 9.4 min, 11.1 min.

Tert-butyl 3-methyl-4-oxo-4-phenylbutanoate: colorless liquid; ^{1}H NMR (400 MHz, CDCl$_3$) δ 7.68 (s, 12H), 7.35 (d, J = 6.9 Hz, 12H), 7.15 – 7.08 (m, 8H), 5.58 (d, J = 16.3 Hz, 4H), 5.22 (d, J = 16.4 Hz, 4H), 4.93 (d, J = 9.1 Hz, 4H), 4.45 (s, 4H), 4.12 (d, J = 8.8 Hz, 4H). HPLC analysis: Phenomenex Lux 5μ 0.46x 25 cm (Hexane/IPA = 95:5, 0.5 mL/min, 190 nm, 25 ℃), 13.5 min, 15.8 min.

Appendices

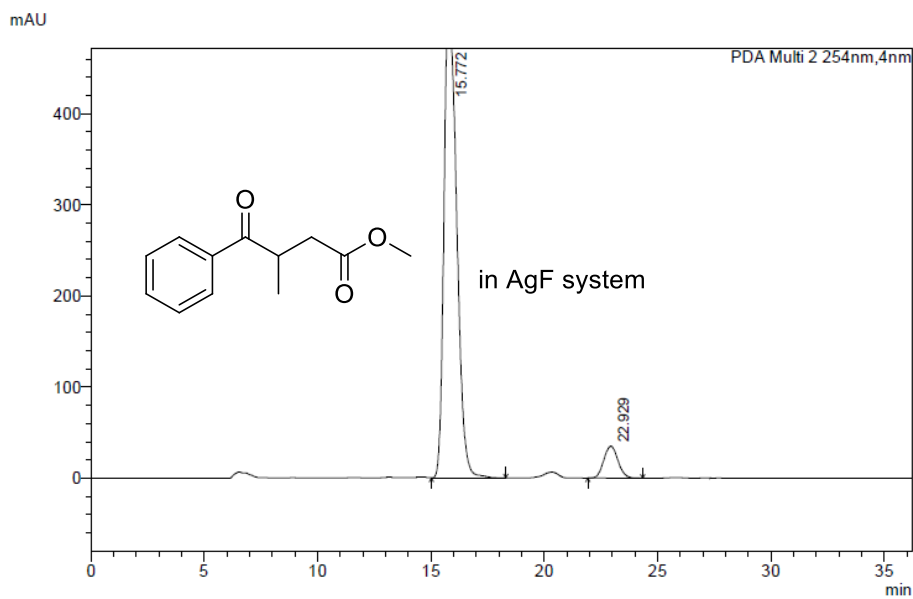## ==== Shimadzu LabSolutions Multi-Chromatogram ====
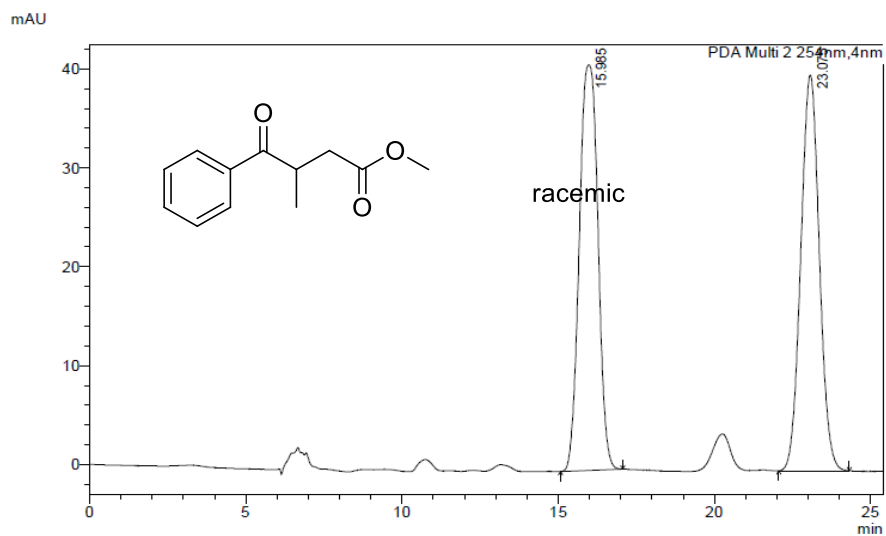
Peak#	Ret. Time	Peak Start	Peak End	Area%
1	15.985	15.083	17.067	50.740
2	23.075	22.059	24.331	49.260
Total				100.000

==== Shimadzu LabSolutions Multi-Chromatogram ====

Peak#	Ret. Time	Peak Start	Peak End	Area%
1	15.772	15.008	18.283	92.873
2	22.929	21.920	24.331	7.127
Total				100.000

109

==== Shimadzu LabSolutions Multi-Chromatogram ====

mAU

PDA Multi 2 260nm,4nm

racemic
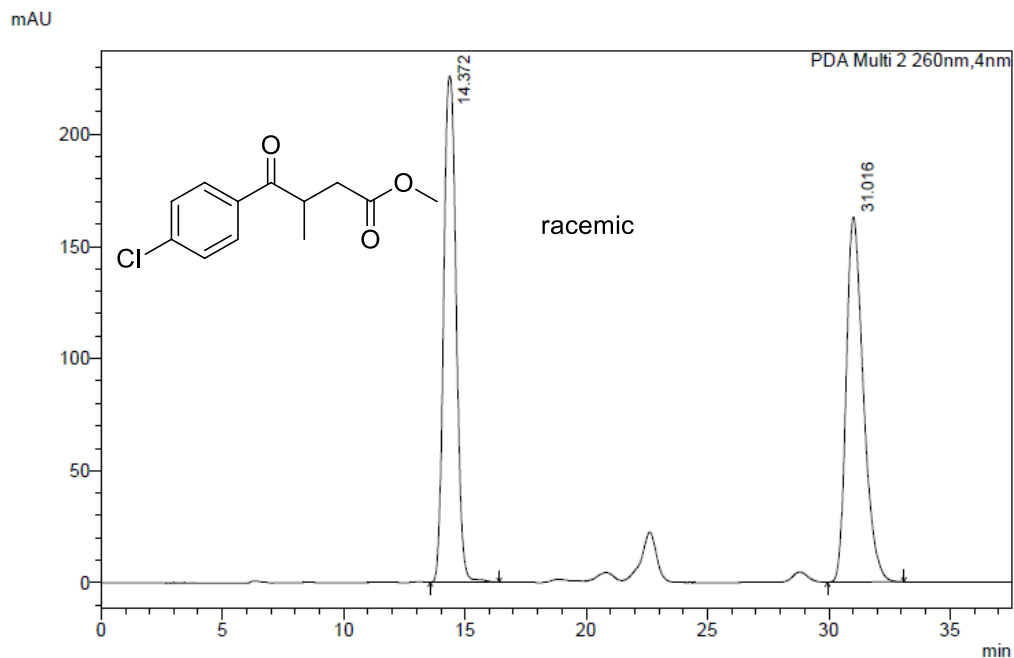
Peak#	Ret. Time	Peak Start	Peak End	Area%
1	14.372	13.579	16.405	50.103
2	31.016	29.941	33.099	49.897
Total				100.000

PDA Ch2 260nm

==== Shimadzu LabSolutions Multi-Chromatogram ====

mAU

PDA Multi 3 260nm,4nm

in AgF system
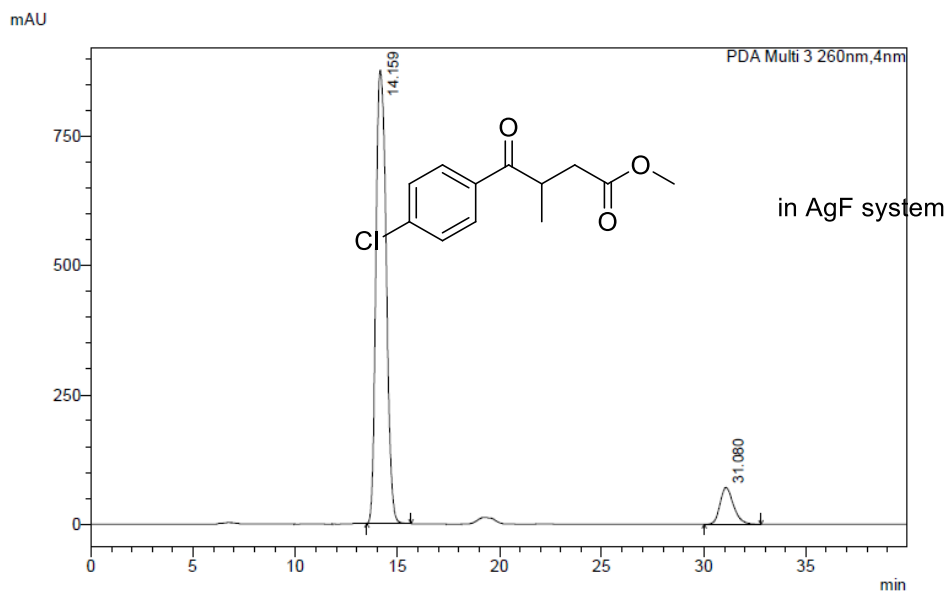
Peak#	Ret. Time	Peak Start	Peak End	Area%
1	14.159	13.504	15.659	90.439
2	31.080	30.027	32.800	9.561
Total				100.000

PDA Ch3 260nm

110

==== Shimadzu LabSolutions Multi-Chromatogram ====

Peak Table

PDA Ch2 290nm
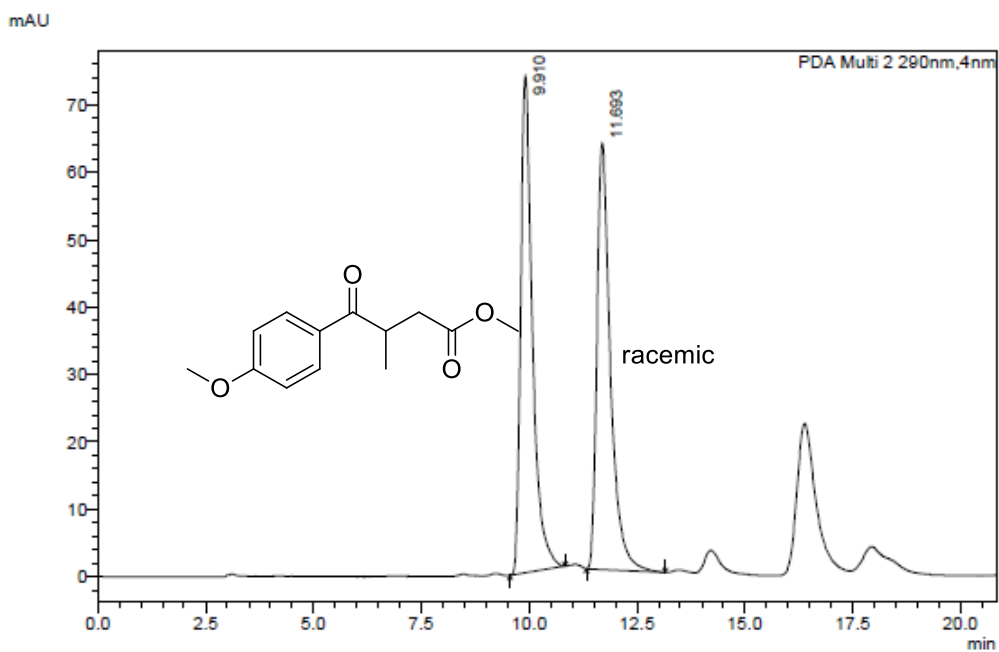
Peak#	Ret. Time	Peak Start	Peak End	Area%
1	9.910	9.557	10.827	50.459
2	11.693	11.328	13.152	49.541
Total				100.000

==== Shimadzu LabSolutions Multi-Chromatogram ====

Peak Table

PDA Ch4 290nm
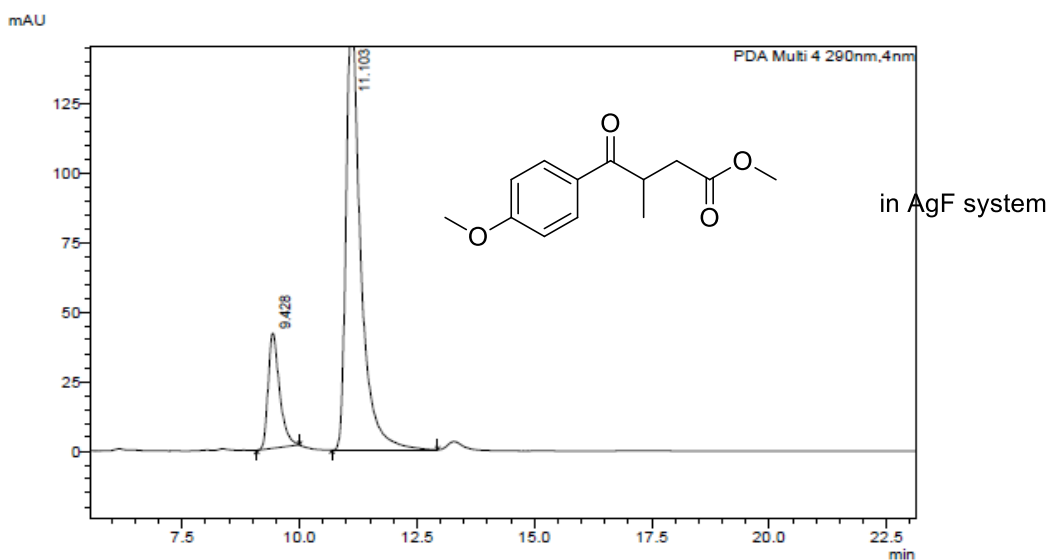
Peak#	Ret. Time	Peak Start	Peak End	Area%
1	9.428	9.088	9.995	17.076
2	11.103	10.688	12.939	82.924
Total				100.000

==== Shimadzu LabSolutions Multi-Chromatogram ====

racemic
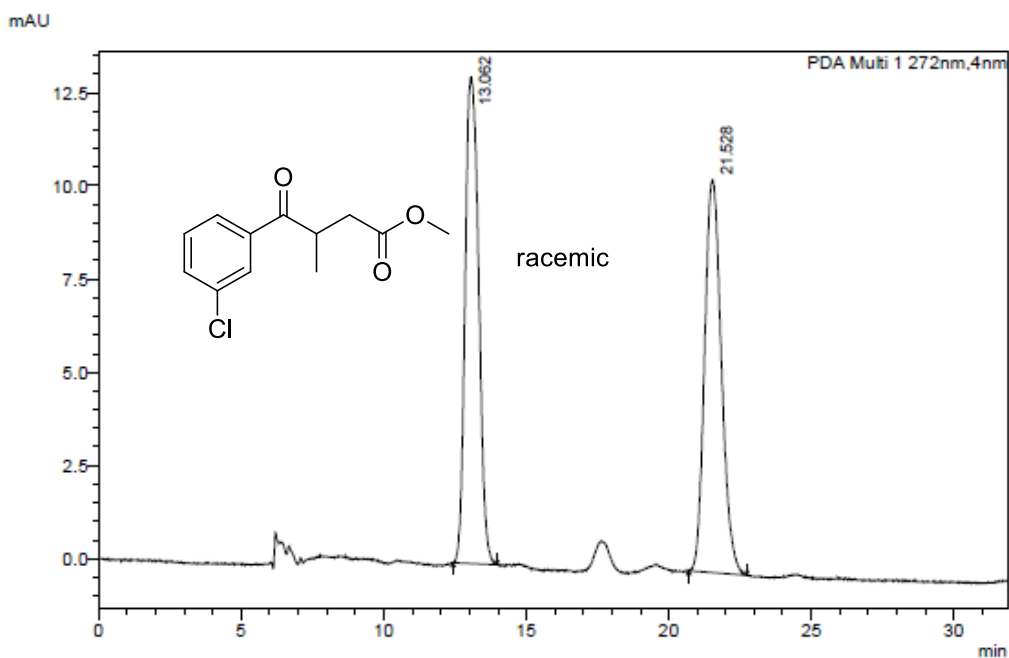
Peak#	Ret. Time	Peak Start	Peak End	Area%
1	13.062	12.427	13.952	49.950
2	21.528	20.704	22.720	50.050
Total				100.000

==== Shimadzu LabSolutions Multi-Chromatogram ====

in AgF system
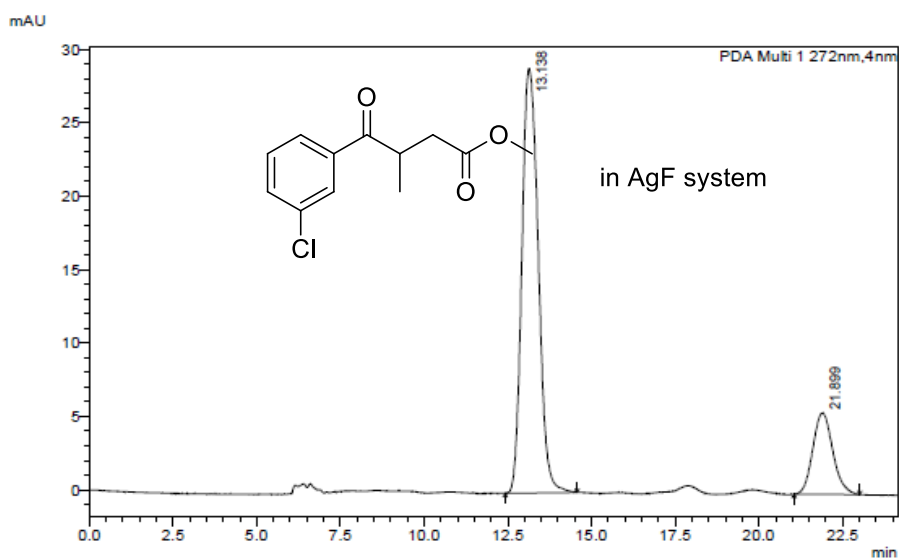
Peak#	Ret. Time	Peak Start	Peak End	Area%
1	13.138	12.427	14.571	81.018
2	21.899	21.045	23.008	18.982
Total				100.000

==== Shimadzu LabSolutions Multi-Chromatogram ====

racemic

PDA Extracted 190nm,4nm

Peak Table

PDA Ch1 272nm
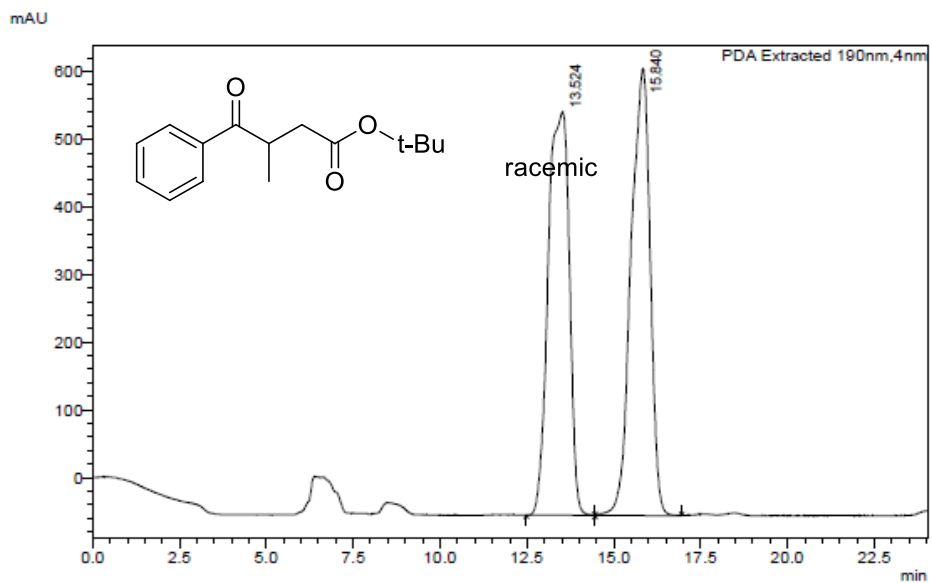
Peak#	Ret. Time	Peak Start	Peak End	Area%
1	13.524	12.533	14.357	50.130
2	15.840	14.581	16.768	49.870
Total				100.000

==== Shimadzu LabSolutions Multi-Chromatogram ====

in TMAF system

PDA Multi 1 272nm,4nm

Peak Table

PDA Ch1 272nm
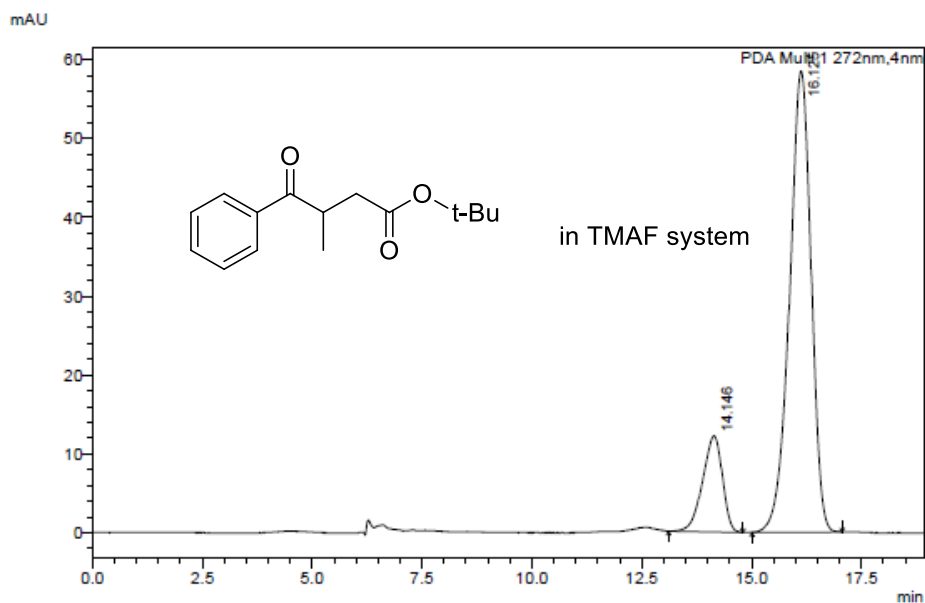
Peak#	Ret. Time	Peak Start	Peak End	Area%
1	14.146	13.109	14.805	16.053
2	16.125	15.008	17.056	83.947
Total				100.000

113